2017

EXPANDING MONOAMINE TRANSPORTERS PHARMACOLOGY USING CALCIUM CHANNELS

Iwona Ruchala
Virginia Commonwealth University

EXPANDING MONOAMINE TRANSPORTERS PHARMACOLOGY USING CALCIUM

CHANNELS

A dissertation submitted in partial fulfillment of the requirements for the degree of

Doctor of Philosophy at Virginia Commonwealth University School of Medicine.

by

Iwona Ruchala

MS, Virginia Commonwealth University, 2011

Director: Jose M. Eltit, PhD

Assistant Professor of Physiology and Biophysics

Virginia Commonwealth University

Richmond, Virginia

August 2017

Acknowledgment

Firstly, I would like to express my sincere gratitude to my advisor Dr. Jose M. Eltit for the continuous support of my work, for his patience, motivation, and immense knowledge. His guidance helped me in all the time of research and writing of this dissertation. I could not have imagined having a better advisor and mentor for my Ph.D. study.

I would like to offer special thanks to Dr. Louis DeFelice, who, although no longer with us, continues to encourage me by his example and dedication to the students he served over the course of his career. He was the reason I joined the department and started Ph.D. program, he was truly an inspiration for me.

Next, I would like to thank my dissertation committee: Dr. Steve Negus, Dr. Adam McQuiston, Dr. Diomedes Logothetis and Dr. Carlos Escalante for their insightful comments and encouragement, but also for the hard question which incented me to widen my research from various perspectives.

I would also like to thank everyone that I met in the Department of Physiology and Biophysics during my years of studies, especially Krasnodara Cameron, Ernesto Solis Jr., Tyler Steele, Guoqing Xiang as well as all faculty, staff and other students for advice, support and friendship.

I am also indebted to Cal & George Jennison and Michelle & Mark Davis and their wonderful families for endless love and support for me over the time of my studies.

Last but not the least, I would like to express my gratitude to my family: my amazing parents Danuta and Pawel and my sisters Kinia and Monia for their constant support throughout the writing process as well as in life in general. I would not be able achieve my goals without your unconditional love! Also, my dear friends: Marta Squadrito, Sanja Lukovic-Yomby and Dagusia Paetz, thank you so much for your love and friendship!

Jezu Ufam Tobie! Dziękuję!

Table of Contents

ABSTRACT

EXPANDING MONOAMINE TRANSPORTERS PHARMACOLOGY USING CALCIUM CHANNELS

By Iwona Ruchala, Ph.D.

A dissertation submitted in partial fulfillment of the requirements for the degree of Doctor of Philosophy at Virginia Commonwealth University School of Medicine.

Virginia Commonwealth University, 2017

Dissertation Director: Jose M. Eltit, Ph.D.

Assistant Professor of Physiology and Biophysics

Research in drug development meets many challenges including lengthy, complex and costly procedures to identify novel pharmacotherapies. In our lab, we developed a method for fast screening of small molecules that interact with monoamine transports – dopamine and serotonin (DAT, SERT). These membrane proteins play important roles in brain neurotransmission responsible for cognition, motion and pleasure. Dysfunction in dopaminergic and serotonergic systems result in neurological disorders such as depression, Attention Deficit Hyperactivity Disorder (ADHD), schizophrenia and addiction.

DAT and SERT are responsible for uptake of dopamine (DA) or serotonin (5HT) into the synapse and they limit neurotransmitter signaling. Drugs that mimic or antagonize actions of endogenous neurotransmitters (DA and 5HT) increase the concentrations of DA and/or 5HT

either by blocking the transporter (blockers) or by competing uptake with neurotransmitter (substrate). The uptake of substrates is associated to an inward current that depolarizes the cell membrane. Voltage-gated calcium channels (CaV) can respond to small changes in membrane potential. In our method, we combined permanent cell line expressing the human dopamine transporter (hDAT) or the human serotonin transporter (hSERT) (FlpIn TREx expression system) with transient transfection of CaV. This system works as a tightly electrically coupled system. Cells challenged with substrate of the transports produce detectable Ca^{2+} signal while monoamine transporter blockers can inhibit these Ca^{2+} signals. The novelty of this method relies on the ability to discriminate between substrate and blockers of monoamine transporters. Preliminary experiments measuring our optimized cell system in a Flex Station 3 plate reader suggest that the co-expression of a voltage-gated Ca^{2+} channel, a monoamine transporter and a genetically encoded Ca^{2+} sensor constitute a rapid screening biosensor to identify active drugs at monoamine transporters.

Our novel methodology can rapidly assess drug-effect profile on monoamine transporters and benefit development of new psychotherapeutics for treatment of mental illnesses. It can also be used to characterize mechanism of action of emerging drug of abuse, as well as to discover small molecules with novel drug-effect profile useful in basic neuroscience research.

1. Chapter one: Introduction

1.1 Psychoactive drugs history of use

Psychoactive substances are all chemical compounds that can alter homeostasis of the central nervous system. They have been used throughout the centuries to influence mood, perception, consciousness and behavior. [1] Traditionally, mind-altering plants were used in ritual ceremonies, cults and early medicine. Usage of such substances played less entertaining roles than nowadays, instead they played the important role of making the tribe coherent thus implicated in the survival of the tribe. [2] The archaeological evidence shows use of psychoactive drug plants already in the prehistoric times – in prepottery Neolithic times, i.e. 8000BC. [3] The earliest use of psychotropic substances was *Amanita muscaria* which caused hallucination, hypersensation and a perception of time standing still. [4] Although *Amanita* is no longer used as a psychoactive drug there are other psychoactive substances that were known in the ancient time and are still used nowadays – opium, cannabis, alcohol, nicotine and cocaine.

Through the centuries, psychoactive substances were used in a number of ways, including the military, during rituals and spirituals, for anesthesia and pain management and to threat mental disorders. Nowadays, the substance misuse or abuse is a major public health problem and a huge burden to societies throughout the world. [1] In the scale developed to determine harmful effects of the drugs Nutt et al. [5] show three categories of harm. Category one consist of acute toxic effect of drugs as well as chronic physical harm, which results as consequence of repeated usage – e.g. drug like heroin can cause sudden death from respiratory depression [6] or repeated stimulant intake causes psychosis [7]. The second category is predisposition of the drug to induce dependence and the third category is drug effect on the whole society. The scale goes from 0-3

where 3 represents "extreme risk". This scale shows some differences in comparison to the current "Class in Misuse of Drug Act" (Figure 1.1).

Figure 1.1: (Left) Mean harm scores for 20 substances, (right) classes in Misuse of Drug Act [5].
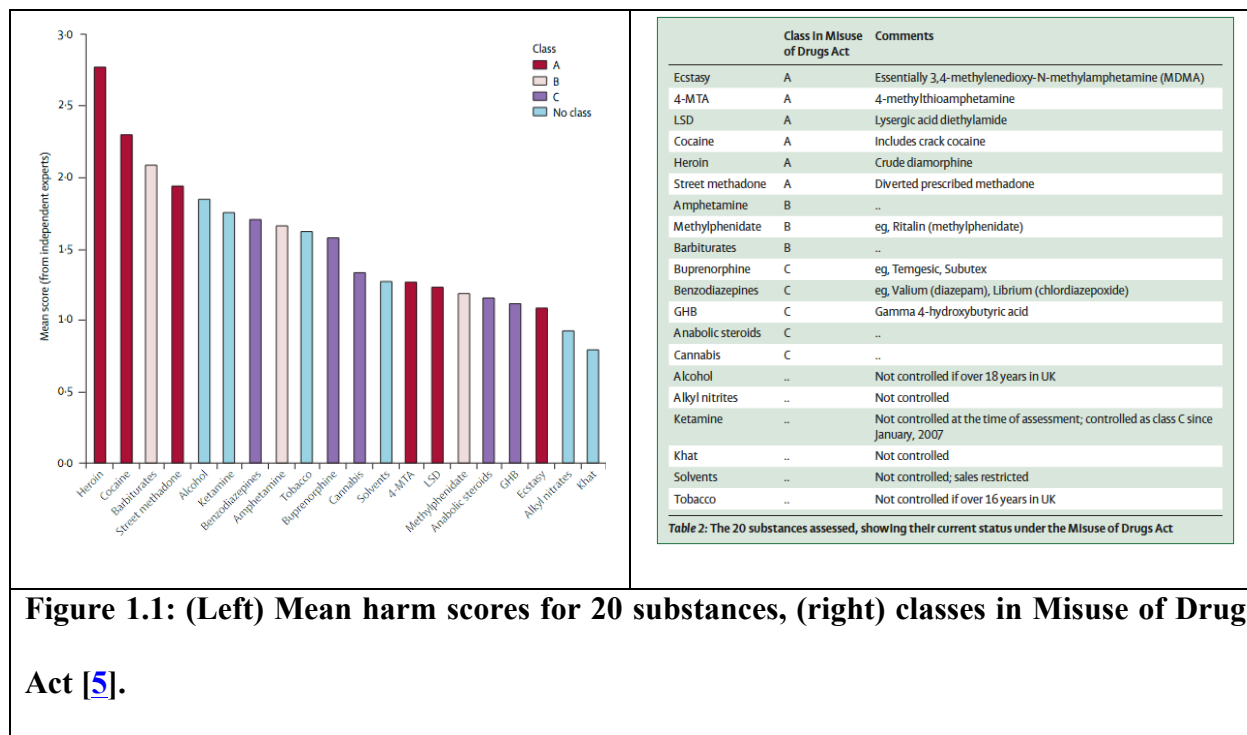
Harm scale determined that cocaine is the second most harmful drug and most commonly used illicit substrates (after Cannabis) are Amphetamine-type stimulants (Amphetamine, Ecstasy) and cocaine according to United Nations Office on Drugs and Crime (UNODC) [8]. Why such harmful drugs are so commonly used (about 200 million people make illicit use of some type illicit substance) [8] can be explained by their enhancing effects in the brain.

1.2   Psychostimulants

Psychostimulants are a diverse class of drugs that produce increase locomotion, cognition-enhancement, wakefulness and attention, sense of power and confidence as well as euphoria [9].

The strong reinforcing effect of the drugs is also responsible for its addictive effect [10]. On the molecular level psychostimulants activate mesocorticolimbic dopaminergic system in the Central Nervous System (CNS) [11]. Mesocortical dopaminergic pathways propagate from the Ventral Tegmental Area (VTA) to the prefrontal cortex and are associated with psychophysiological responses like motivation, cognitive control, and emotions [12]. Mesolimbic system originate in the VTA and project dopaminergic neurons into the ventral striatum, which include nucleus accumbens (NAc) and olfactory tubercle [13]. This system is particularly involved in the development of addiction [14].
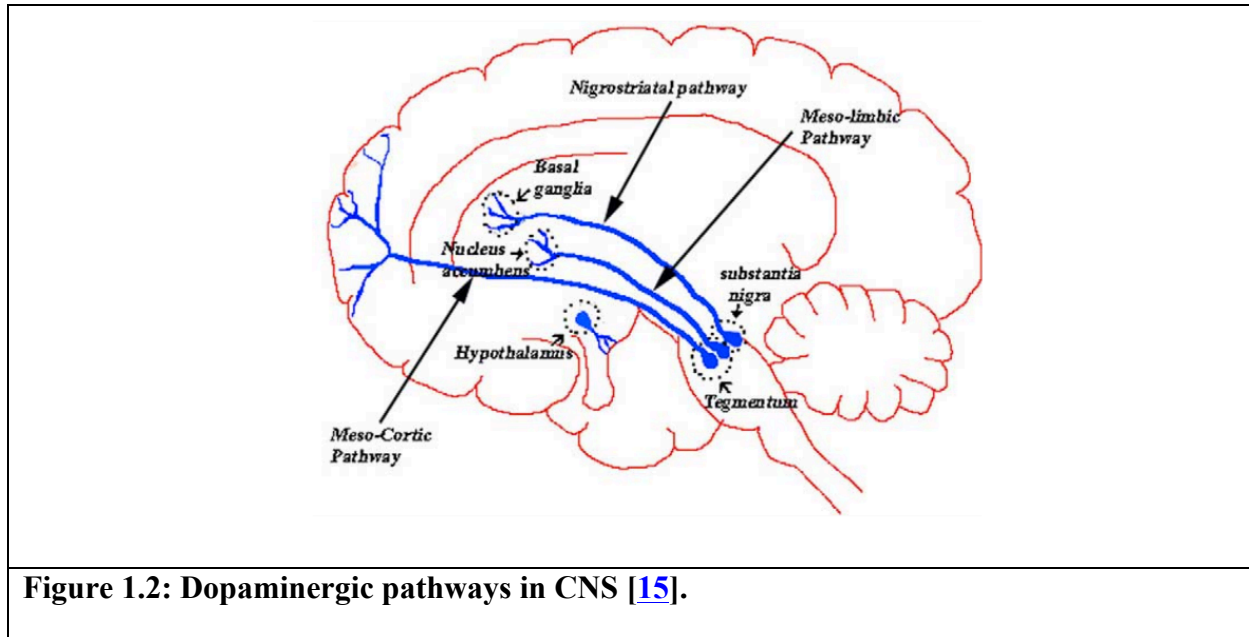
Figure 1.2: Dopaminergic pathways in CNS [15].

Stimulants increase few important neurotransmitters in the brain - dopamine, serotonin and norepinephrine [16] [17]. The sharp increase of dopamine triggers associative (reward) learning and conditioning [18] (two very important aspects in developing addiction). Serotonin (5-hydroxytryptamine 5HT) is important in the sleep cycle, mood and appetite regulation [19]. Raphe nuclei are the primary site from where 5HT-neurons project to the cortex, thalamus, basal ganglia and hippocampus [20]. Norepinephrine (NE) neurons project from the locus coeruleus

(LC) towards everywhere in the brain, playing an important role in the working memory formation, enhancing attention [21] as well as in arousal and wakefulness. Psychostimulants interfere with monoamine transporters function and elevate the extracellular concentration of monoamines, potentiating the monoaminergic neurotransmission [22].

1.3   Monoamine transporters

Monoamine transporters are important membrane proteins that belong to the solute carrier 6(SLC6) neurotransmitter transporters gene family. The norepinephrine transporter (NET), dopamine transporter (DAT) and serotonin transporter (SERT) are all part of this gene family. They share similar primary sequences and all have the same overall secondary structure consisting of 12 transmembrane domains. As mentioned above, the main function of these transporters is to regulate neurotransmitters concentration in extracellular space by reuptake them to the synapse [23] (Figure 1.3).
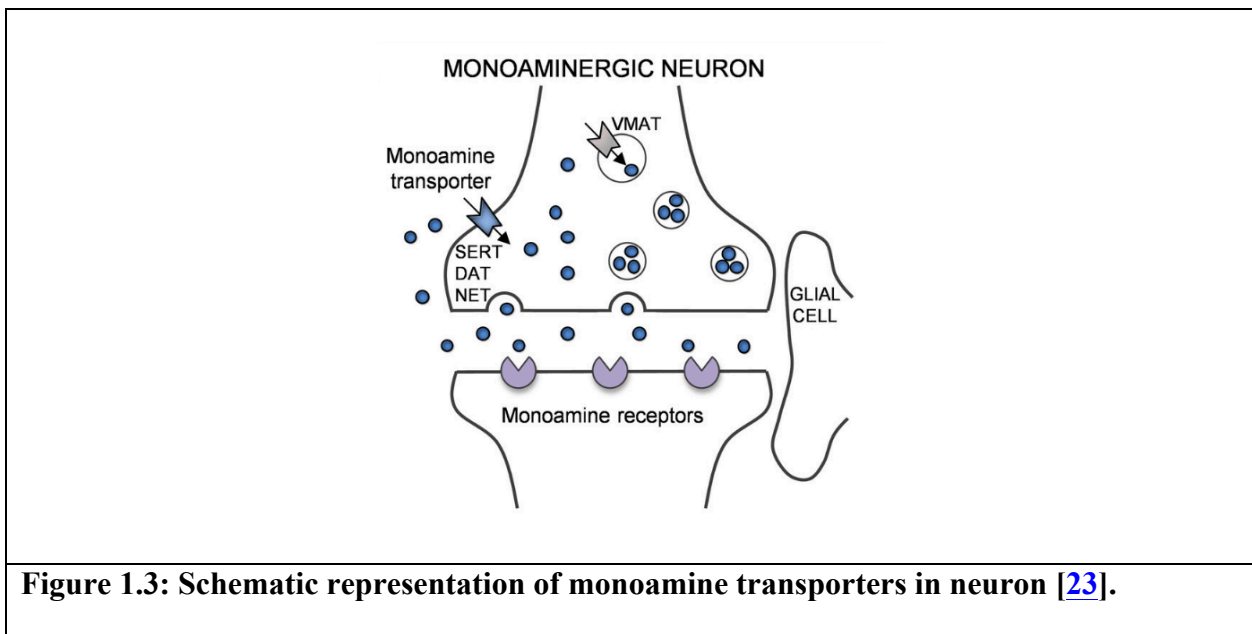
Figure 1.3: Schematic representation of monoamine transporters in neuron [23].

Neurotransmitter uptake was first described in 1967 by Julius Axerlod [24] where he explained how norepinephrine is reuptake into the sympathetic nerve terminal. In 1971, Iverson [25] proposed a similar uptake process for other neurotransmitters – glycine, dopamine, GABA and 5HT. He also pointed out that some drugs like imipramine and cocaine can inhibit uptake of NE. Since then, many research groups had been involved in describing drugs that modulate the reuptake of neurotransmitters. Such pharmacological modulation of neurotransmitters can regulate neuronal activity. Indeed, neurotransmitter transporters (NTT) have become essential therapeutic drug targets for treatment of many brain diseases like anxiety disorder, depression, Attention Deficit Hyperactivity Disorder (ADHD), obesity, bipolar disorder and schizophrenia [26] [27] [28] [29]. More than 30 compounds working as substrate or as non-transportable inhibitors of monoamine transporters are currently used in clinical trials [23].

Drugs can interact with monoamine transporters in two different ways, either as a substrates or blockers; substrates are small organic molecules or synthetic compounds that bind to the transporter and are physically transported to the intracellular space; blockers of monoamine transporter are not transporters inside the cell but rather bind to the transporter and inhibit its function. Classical examples of these two groups are Amphetamine (Amph) and cocaine. The former acts as substrate when interacting with transporters, whereas the latter acts as a blocker in all three transporters. In the brain cocaine works as a reuptake inhibitor by blocking the reuptake thus allowing more neurotransmitters to stay active in the synapse. Amphetamine, one the other hand, is taken up by the transporter in exchange for neurotransmitter release into the synapse [30]. Converging evidence suggests that Amph enters the cell through monoamine transporters, and once inside the cell, it disrupt intracellular stores of neurotransmitters. All this triggers reverse transport of neurotransmitters through the transporters and leads to a large release of transmitter to the cytosol [31], which is why substrates are often called releasers [32].
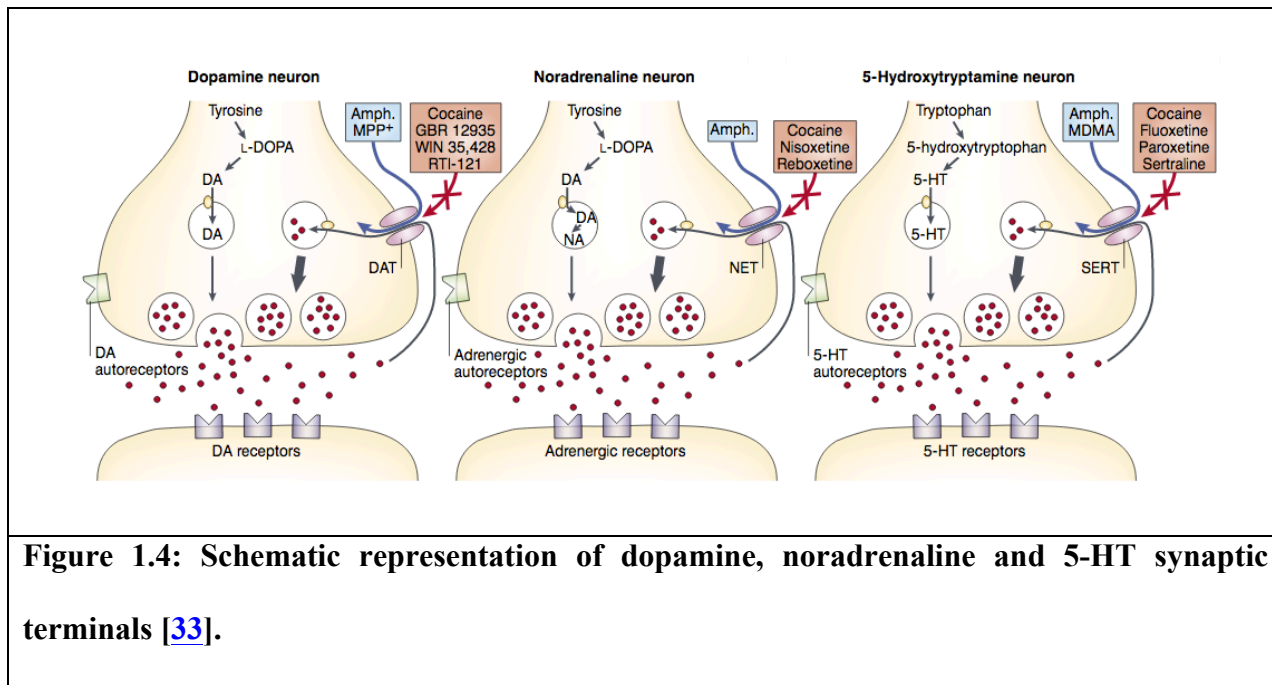
Figure 1.4: Schematic representation of dopamine, noradrenaline and 5-HT synaptic terminals [33].

Examples of the blockers of monoamine transporters that are used therapeutically are the following:

Tricyclic antidepressants (TCAs): Imipramine, Desipramine, Nortriptiline, Doxepin, Amitriptyline. TCA primarily inhibits NET and SERT (14). First widely used as an antipsychotic in a Paris hospital in 1955, few years later, it was found to be effective antidepressant [34]. It was used as treatment for major depressive disorder (MDD), dysthymia (persistent depressive disorder), but also social phobia, panic disorder and Post Traumatic Stress Disorder (PTSD). Since TCAs have many other targets, they have several side effects including fatal overdose. **Fluoxetine (Prozac)** first approved in 1980 [35], was one of the first Selective Serotonin Reuptake Inhibitors (SSRI) [36]. All SSRIs have similar efficacy as TCAs [37] but a much lower tendency to cause severe cardiovascular effects. [38] It is used to treat depression, obsessive-compulsive disorder (OCD), bulimia nervosa and panic disorder. Prozac has low physical and psychological dependence liability; accordingly, it is not a controlled substance. **Methylphenidate (Ritalin)** is a potent blocker of DAT and NET and used for treatment of

ADHD and narcolepsy. [39] According to the Food and Drug Administration (FDA), Ritalin is a federally controlled substance (CII) because it can be abused or lead to dependence.

There are also monoamine transporters substrates that are used therapeutically such as **Amphetamine (Adderall) and Methamphetamine**. They have higher affinities on DAT and NET rather than SERT and are used as a treatment for ADHD, narcolepsy and obesity [40]. They are in Schedule II controlled substance for their high potential of abuse.

Many other drugs that interact with monoamine transporters are well recognized due to their high abuse potential. The most infamous is cocaine, which is placed in Schedule II due to its local anesthetic usage. It has high abuse potential with loss of contact with reality, an intense feeling of happiness, or agitation in people that abuse it. Cocaine is a powerful vasoconstrictor and can cause vascular toxicity [41]. Other physical symptoms may include sweating, enlarged pupils or even stroke. [42] High doses can result in very high blood pressure or body temperature. It has high psychological and addiction liability. **MDMA (Esctasy)** it is a Schedule I in the USA but in November 2016 the FDA granted permission for large-scale Phase 3 clinical trials, the final set of human trials required before the FDA will consider a new drug useful in treatment of PTSD. Its dependence liability is moderate to low-moderate. In the official FDA report, it is stated, there is conflicting evidence about wherever MDMA is addictive.

At the cellular level, the adverse effect of psychostimulants includes cytotoxicity [43], mitochondrial dysfunction, [44] formation of highly reactive free radicals [45], neuroinflammation and damage of the blood-brain barrier [46]. These effects of psychostimulants contribute to long-term degradation of dopaminergic and serotonergic systems in the brain, including attenuation in monoamine transporter activity, decrease tyrosine and tryptophan hydroxylase function as we as deprivation of nerve terminal markers [47] [48] [49] [50].

1.4   Drugs pharmacology on transporters

1.4.1   Abuse potential of drugs and their affinities to MAT

It is important to define which pharmacological properties of a drug define its abuse liability. An important related question is why some drugs that interact with MAT can be used therapeutically and others represent a high risk of abuse. It is well established that drugs that increase dopamine level in NAc have direct positive correlation with its abuse potential, whereas compounds that potentiate the serotonergic neurotransmission have low risk of abuse. In this regard, the relative DAT over SERT selectivity of drugs could work as an indicator of its abuse potential, thus, in general drugs that show higher DAT over SERT potency would probably be abused.

Other important properties of drugs that would help to foresee its abuse potential are whether they are substrate or blockers of the transporters. As mentioned above monoamine transporters' substrates potentiate neurotransmission in a more profound way than the blockers. This is because substrates, in addition to competing the uptake of the natural substrate, they also can induce the release of neurotransmitters. On the other hand, blockers only interfere with the uptake, thus the increase of neurotransmitters ultimately relies only on the electrical activity of the neuron.

1.4.2   Drug-profiling on monoamine transporters

In general, drugs that are highly selective to DAT over SERT show high abuse liability whether or not they work as substrates or blockers on transporters; good examples are

methylphenidate (blocker), and amphetamine (substrate) (Figure 1.5). When compounds are not selective, their abuse liability would depend on whether they are blockers or substrates on transporters. Experimental evidence strongly suggests that blockers like cocaine, that are not selective among the three transporters, show high abuse liability; whereas a non-specific substrate like MDMA produces moderate to low abuse potential. In the case of blockers, the modest increase of 5HT is not strong enough to counteract the effect of the increased extracellular DA, and the abuse potential of DA will dominate. On the contrary, the strong release of 5HT produced, a non-specific releaser (like MDMA) would counteract the abuse effect of DA. Thus, blockers that are not selective still will show positive abuse potential, whereas substrates that are not selective will have reduced abuse potential. In summary, drug profiling – which distinguishes the efficacy of the drug on monoamine transporters as well as characterizing substrate or blocker interactions – is crucial in predicting the abuse liability of the drugs.

	DAT Ki (nM) Uptake	NET Ki (nM) Uptake	SERT Ki (nM) Uptake	SERT/ DAT	Abuse potential
Methylphenidate	84	514	>50,000	595	high
MDPV	4.1	26	3349	837	high
Cocaine	478	779	304	0.6	high
Fluoxetine	>5000	600	10	0.002	Low
	Release via DAT	Release via NET	Release via SERT		
MDMA	125	78	55	0.96	Low-moderate
Methamphetamine	9	14	1291	143	high

Figure 1.5: Relative potencies in uptake studies predict abuse potential, modified from [51].

Drug-profiling can be also useful in searching for potential candidate medications that can be used in normalization therapy of stimulant dependence [22]. Few studies show that amphetamine-type clinically available appetite suppressants (like phentermine, diethylpropion and phendimetrazine) decrease cocaine and methamphetamine self-administration. It was suggested that reduction of cocaine reinforcement could be achieved partially using serotonergic drugs (fluoxetine, phentermine and fenfluramine) [52]. A combination of low doses of fenfluramine with phentermine can be used in cocaine addiction [53]. Fenfluramine (5HT releaser), that is much more potent than phentermine (DA and NE releaser and weak 5HT releaser [54]) decreases methamphetamine self-administration [55].

1.5 Monoamine transporters drug-profiling methods

1.5.1 In vitro:

1.5.1.1 Competition assays – binding assay, uptake of radiolabeled compound

One method broadly used to test the effect of psychostimulants on monoamine transporters is the uptake competition assay. In this method, a traceable monoamine transporter substrate ($[^3H]$ DA, $[^3H]$ 5HT or $[^3H]$ NE) is co-applied with increasing concentrations of a test compound. This method is used to determine the potency of compounds to inhibit transport of the tracer. Usually these experiments are carried out either in brain synaptosomes or cells transfected with monoamine transporters. Uptake inhibition assays cannot discriminate between test drugs that work as substrates or blockers of the monoamine transporter.

Another method to study the monoamine transporters interaction with test drugs is the radioligand-binding assay. This method is also a   competition   assay   but   uses   high-affinity

radiolabeled MAT blockers as a tracer (e.g. $[^{125}I]$ RTI-55, $[^{3}H]$ CFT). The assay includes competing the binding of these high-affinity radiolabeled ligands with different concentrations of the test drugs. It was proposed that the comparison of potencies (Ki) of a test drug obtained using the uptake- vs. the binding- inhibition assays could distinguish between substrates and blockers [59]. Monoamine transporters inhibitors that are already well established in the literature, like cocaine or fluoxetine, produce a low binding-to-uptake ratio (0.7 and 2.2 respectively), while established substrates like Amph or DA yield high binding-to-uptake ratios (582 and 1621 respectively) [59]. The explanation for these differences can rely on pharmacological aspects of the blockers and substrates. It is proposed that blockers and substrates bind to the different sites of transporters that could account for the differences in the binding-to-uptake ratio [60] [61]. Unfortunately, some drugs tested later with a more direct method to classify drugs as substrates or blockers revealed weaknesses in using binding-to-uptake ratios as a discrimination tool to identify substrates over blockers on MATs [59].

1.5.1.2 Synaptosome

As mentioned above, just describing whether a new molecule is a ligand of monoamine transporters without describing if it works as a substrate or blocker, would limit the prediction that can be made about its possible biological function. Since DAT and SERT play a crucial role in the action of abused drugs, the profile that a particular drug has in these transporters, would essentially define its abuse liability.

One of the techniques commonly used to distinguish between substrates (or releaser) and blockers of MAT is the synaptosome release assay. This *in vitro* assay measures the release of radiolabeled $[^{3}H]$ MPP^{+} (used as more stable a dopamine surrogate) or $[^{3}H]$ 5-HT from

synaptosomes [57]. Synaptosomes are nerve-ending vesicles usually isolated from the brain [62]. The name derives from its structural homogeneity and similarity to the membranes and organelles that conform the synapse [62]. They are prepared from neuronal tissues after mild homogenization and density gradient centrifugation (Figure 1.6) and contain all necessary machinery for neurotransmitters uptake and release.
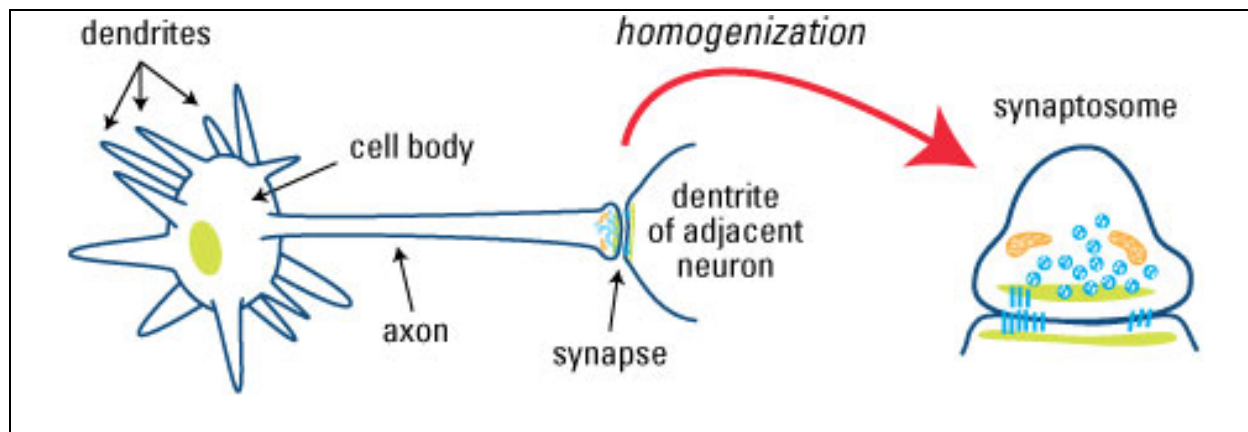
Figure 1.6: Schematic representation of preparation of synaptosomes. From Thermo Fisher Scientific "Enrich neuronal synaptic proteins while maintaining phosphoprotein integrity" *by* Hai-Yan Wu, Kay Opperman and Barbara Kaboord.

For studying particular transporters, different parts of the brain are dissected. For SERT and NET assay, whole brain minus cerebellum is used, while for DAT assay only striatum is used [22]. Part of the brain is homogenized and incubated with 1uM reserpine that irreversibly blocks the vesicular monoamine transporter (VMAT) and then is incubated with $[^3H]$ neurotransmitters until a steady state is achieved. Usually $[^3H]$ 5-HT is used as the radiolabeled substrate for SERT and $[^3H]$ MPP$^+$ (or $[^3H]$ DA) as the radiolabeled substrate for NET and DAT [22]. After the steady state is achieved, preloaded synaptosomes are added to a tube containing the test drug. Substrates evoke non-exocytotic release of titrated neurotransmitters via reverse transport. The decrease in the remaining amount of tritium (^3H) will demonstrate that tested drug was a releaser

[22]. Blockers such as nonselective uptake inhibitor Indatraline (Figure 1.7) show a very weak release of neurotransmitter, while transports substrate, METH display dose-dependent release on all three transporters with high affinity on DAT and NET and low affinity on SERT [63].

Figure 1.7: Effects of the reuptake blocker Indatraline (left) and the transporter substrate methamphetamine (right) on the release of [³H] dopamine, [³H] norepinephrine and [³H] 5-HT in synaptosomes, taken from [22].
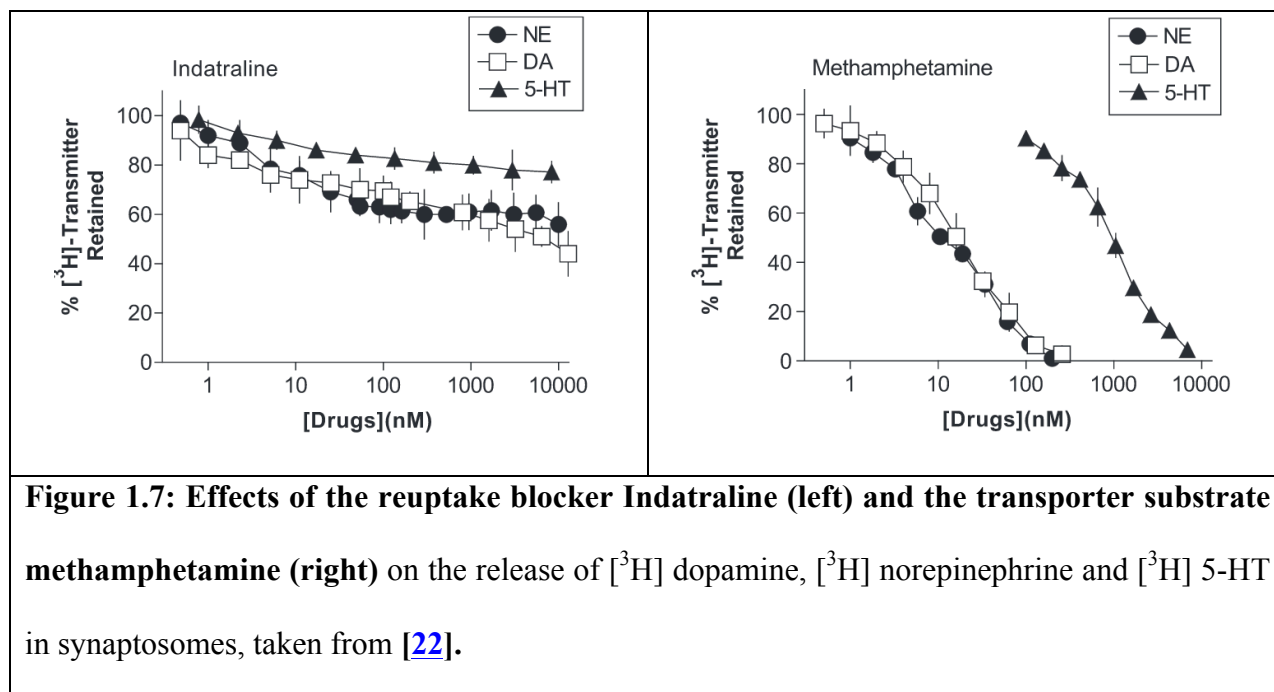
1.5.2   In vivo:

1.5.2.1 ICSS intracranial self stimulation

Intracranial self-stimulation (ICSS) is a method to study drug effects where rodents can self-administer rewarding electrical stimuli. [64] Subjects are trained to press a lever to deliver pulses via microelectrode's implanted in the brain regions such as the medial forebrain bundle (MFB). This region of the brain allows for stimulation of the "first stage" neurons that later project and activate "second stage" mesolimbic dopaminergic neurons in ventral tegmental area and promotes release of DA in NAc [65].

13

Different frequencies or intensities of brain stimulations maintain different rates of lever pressing. When the rodent is exposed to a psychostimulant, the amount of stimulation required to get a response is smaller than when the rodents is exposed to the vehicle alone. This "facilitation" of the ICSS is depicted as a leftward shift in the rate-frequency graph (see example of Methamphetamine in Figure 1.8) [64]. ICSS facilitation (increase %MCR in low rates) is interpreted as an abuse-related drug normally correlated with an exacerbated dopaminergic tone. In addition, drugs that potentiate extracellular serotonin levels produce a depression ICSS response at higher frequencies. This particular preclinical abuse testing method has a great advantage of discriminating drugs increasing 5HT release, so called "abuse-limiting drugs" [66].
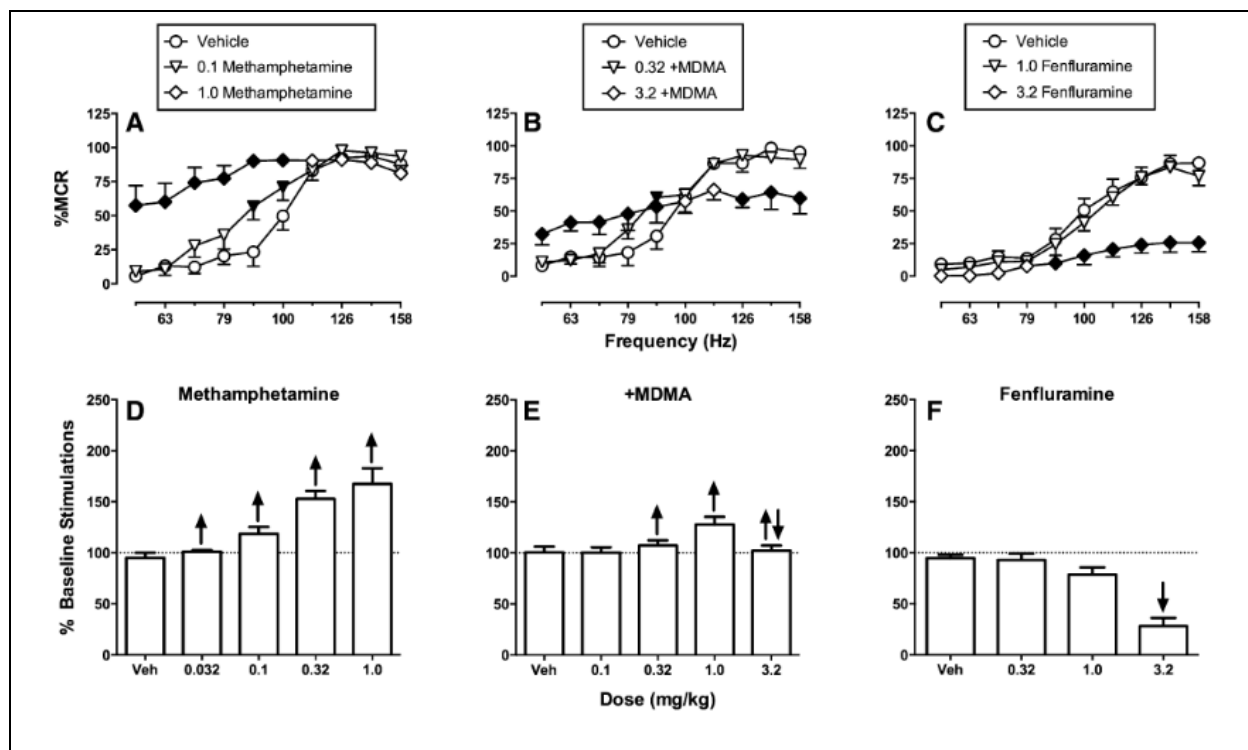
Figure 1.8: Effects of Methamphetamine, MDMA, Fenfluramine on full ICSS frequency-rate curves. Abscissae: frequency of electrical brain stimulation in log Hz. Ordinates: percent maximum control reinforcement rate (%MCR), modified from [67].

2. Chapter two: Electrical properties of monoamine transporters and calcium channel

2.1 Monoamine transporters as channels

2.1.1 Inward current in oocytes

Monoamine transporters are proteins mainly responsible for transport cargo across the membrane, but they contain other interesting features that characterize them as channels. Transporters require binding and co-transport of Na^+ and Cl^- ions as well as the ion concentration gradient preserved in the long term by the membrane Na^+/K^+ ATPase (Figure 2.1) [68] [33].

Figure 2.1: Schematic representation of monoamine transporters transport, modified from [23].
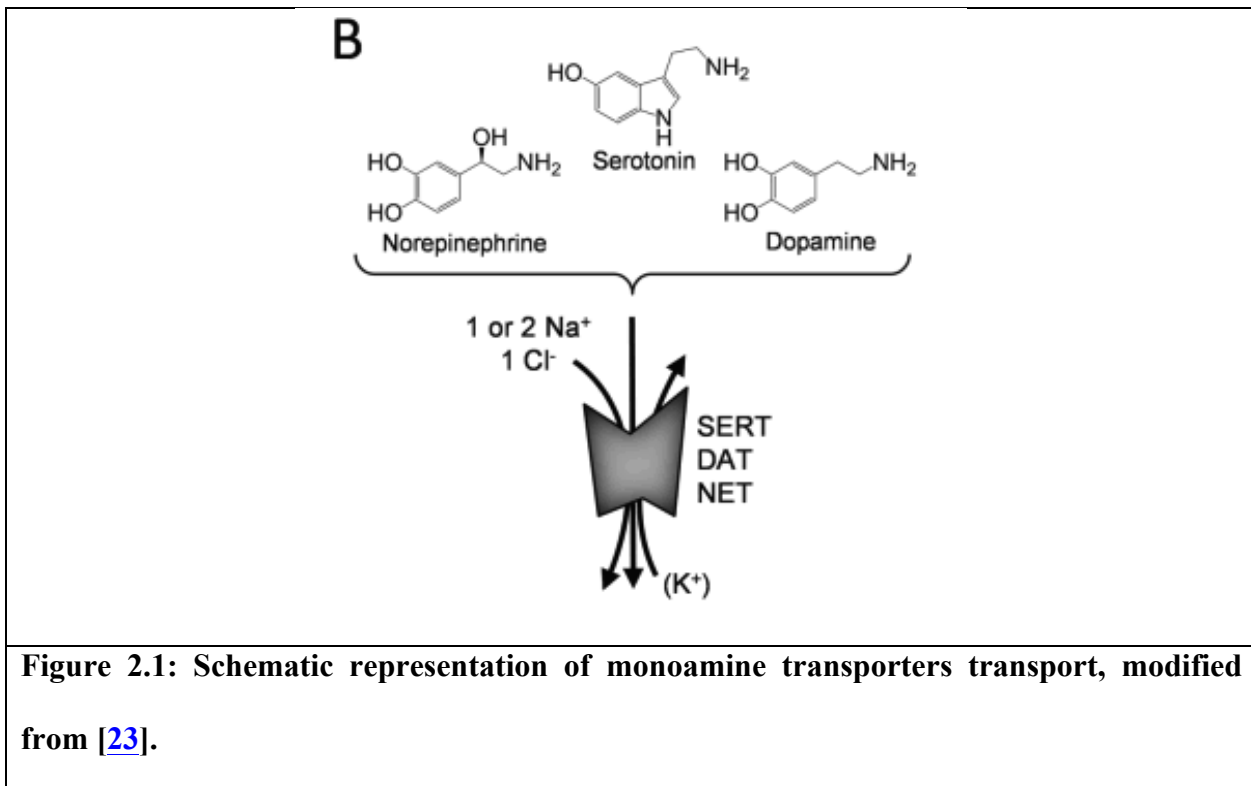
For each transporter we can find a net charge (stoichiometry) that is translocated during that process generally by measuring kinetic determinants of transport rate (concentration of substrate K_m and maximal velocity V_{max}) on Na^+, Cl^- or K^+ concentrations [32]. DAT requires two Na^+ and one Cl^- per 1 transported DA while NET and SERT require only one Na^+ and one Cl^- per one NE or 5HT, but it is worth to mentioning that SERT during one translocation cycle translocates one K^+ out of the cell (Figure 2.2). Based on the stoichiometry of SERT, transport appears to be electroneutral [69].

Figure 2.2: Transport of 5HT (S) in SERT coupled to Na^+, Cl^- and K^+ co-transport [32].
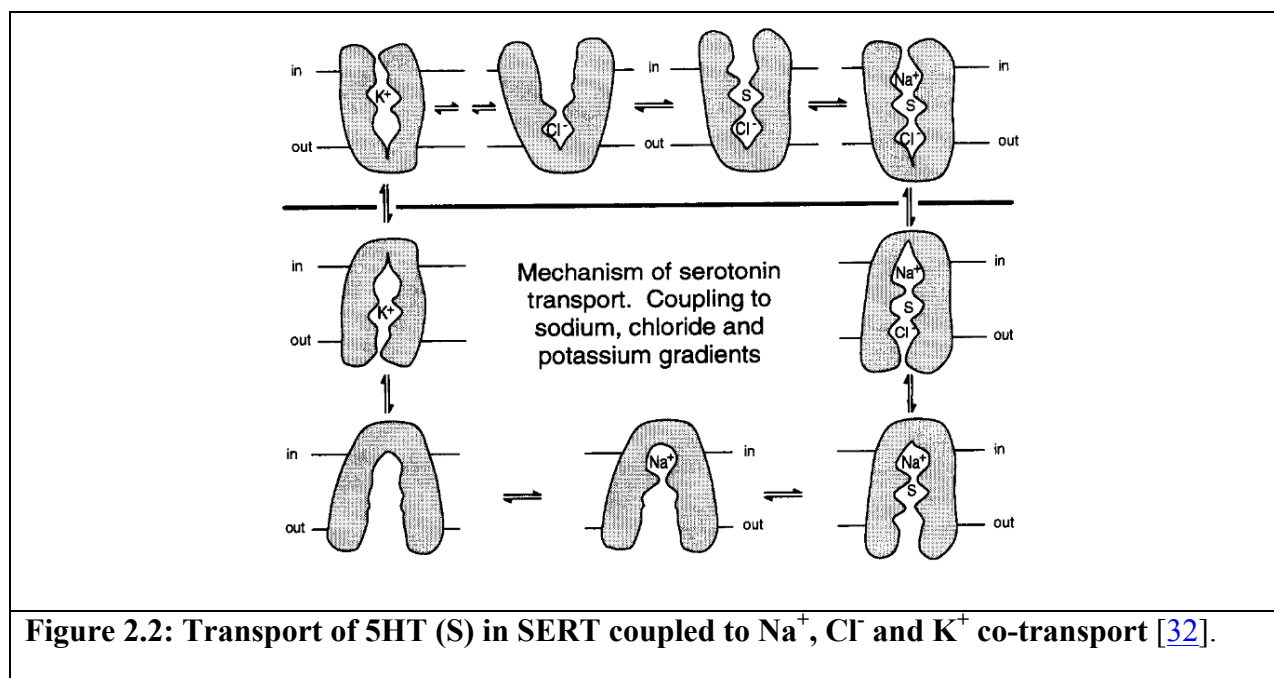
It is surprising to find that oocytes expressing SERT induce an inward current when exposed to 5HT [70]. In fact, three conductances (currents) associated with SERT have been recognized. The first conductance (mentioned in the beginning) is induced by application of substrate (5HT). It shows voltage rectification, and although it is activated by the substrate, it is presumably uncoupled to the uptake mechanism.
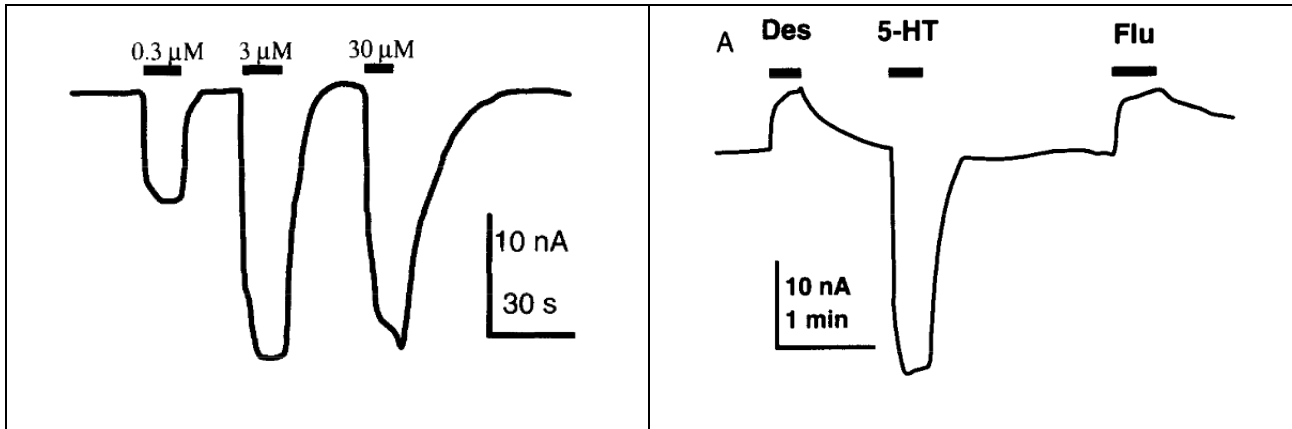
Figure 2.3: (Left) 5HT induced current with varied concentration of 5HT. (Right) Inhibition of leak current by desipramine (3uM) and fluoxetine (3uM) in oocytes injected with 5HT transporter cRNA [70].

Two other currents are transport–independent and occur in the absence of 5HT. One is the inward current found as a consequence of a rapid change to negative potential (transient current), and the second one is a small (size of several nanoampers) inward current called leak current; it is constitutive to SERT expression, thus visible when transporter is inhibited by a blocker revealed as an outward deflection in the current measurement (Figure 2.3) [70].

NET and DAT also exhibit these currents (Figure 2.4) [71] [72]. As it is mentioned before, presumed fixed stoichiometry for NET (one NE^+, one Na^+, one Cl^-) assumes one positive net charge transported per cycle. The number of transporters expression vary from 10^6 in a HEK293 cell [71] to 10^{11} in Xenopus oocytes [70]. Knowing the uptake velocity for NE that was estimated to be one NE per second, we could presume that the current evoked would be less than 0.2pA while the patch-clamp experiment in HEK293 cells expressing hNET show currents of the order of 100pA when cells were exposed to 30uM NE [73].

Figure 2.4: hDAT expressing oocytes induce inward current when 10uM DA is applied and outward during application of 10uM cocaine. No responses were elicited in control water-injected oocyte [72].
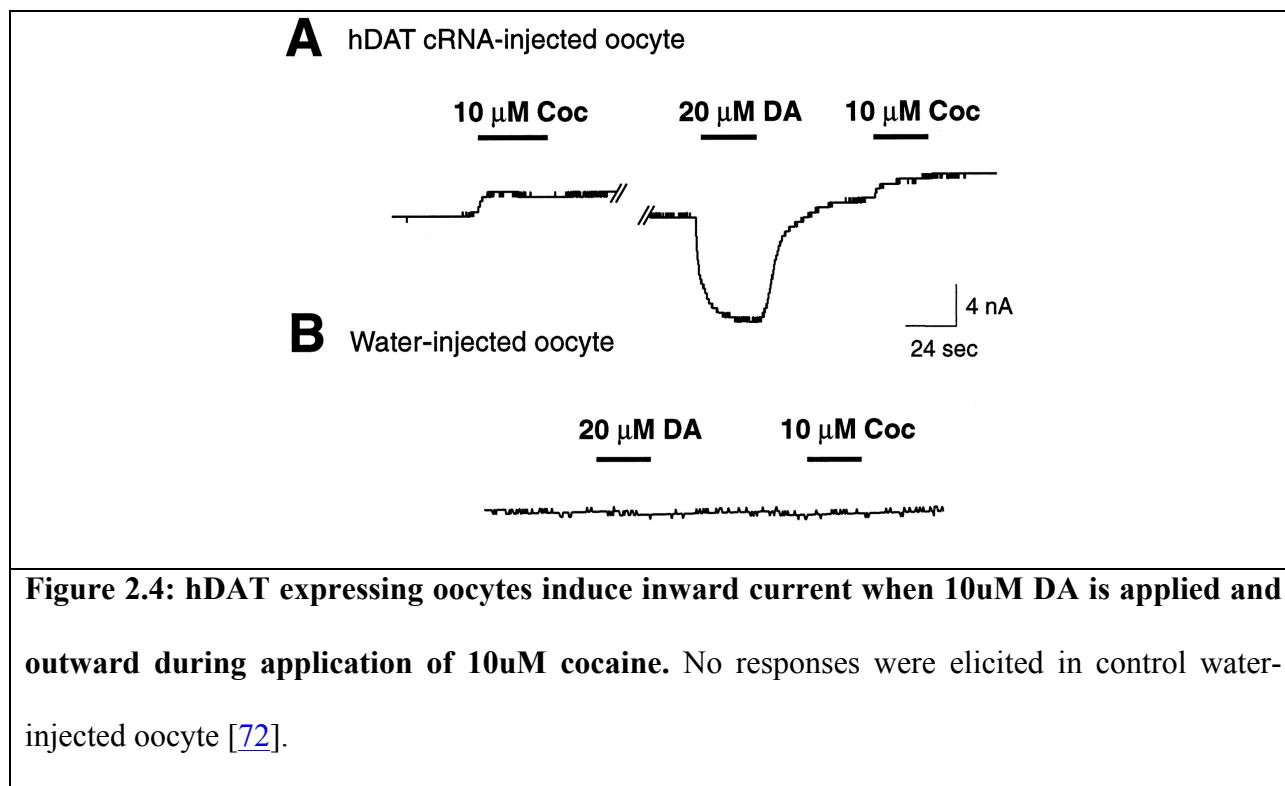
Along with the substrate transport, transporters elicit currents in the presence of substrate that exceeds the prediction that can be made by the fixed-coupling stoichiometry, turnover rate and transporter density. [74] Examination of the time course of transport of 5HT in HEK293 expressing hSERT indicates that SERT functions more as a channel than a cargo-carrier. [75] A definite experiment that describes the channel-like activity arises from direct measurements done by Carvelli et al [74]. They described direct single-channels events that occur in *Caenorhabditis elegans* DA neurons. Dopamine transporter (DAT-1) inhibitor could block DA-induced channel activity and were absent in *dat-1* KO DA neurons. All patch-clamp experiments were performed in the presence of butaclamol and spiperone – inhibitors of DA receptor - to exclude the possibility of currents evoked by the activation of ion channels downstream those receptors. When the holding potential stepped from -40 to -100mV DA or AMPH, perfusion generated significant transport-associated inward current that was abolished when Na^+ was replaced with $NMDG^+$ (Na^+ free solution) [74]. Thus, providing evidence that transporters during the transport

cycle should adopt a conformation that constitute an ion conduction pathway that can modulate the membrane potential in neurons from C. elegans.

2.1.2 Excitability in neurons

The functional role of the currents associated with transport of the substrate is not fully understood. It was suggested that those currents might depolarize the membrane in dopamine neurons since carried by Na^+ ions. Ingram et *al*. demonstrated that DA modulates excitability in dopaminergic neurons in the *substantia nigra* [76]. Extracellular DA activates D2 autoreceptors, which are coupled to K^+ channels, hyperpolarize membranes, and inhibit the electrical activity of dopaminergic neurons [77]. However, by adding a D2 receptor antagonist, neurons experienced rebound excitation in the presence of DA. Inhibiting a transporter, either by cocaine or a selective DAT inhibitor in the presence of DA and D2 receptor antagonists will decrease the firing rates. Thus, DAT is essential for substrate-induced excitation (e.g., DA or AMPH). It is proposed that Cl^- ions is the current carrier in DA neurons- a surprising and unexplained result since the inward current carries negative charges yet elicits excitability. Therefore, another important feature associated with DAT current is modulating excitability.

Another group showed similar effects of methamphetamine. [78] Low concentrations of METH modulate dopamine neurotransmission by increasing dopamine-firing neurons. METH and most amphetamine-type substrates are used to treat attention deficit disorder by enhancing cognition. All substituted amphetamines increase DA levels in extracellular space at cell body and axon terminal fields and lead to hyperpolarization because of autoreceptors activation. However, low dose of METH does not generate enough D2 receptor activation to counteract the increase in pacemaker firing rate produced by the DAT- mediated excitatory conductance and in fact

significantly increases firing rate.

If substrate-induced currents alter excitability, they might be also associated with activation of voltage-gated channels that are involved in excitability. One example can be activation of voltage-gated calcium channels. Vaarmann et *al.* [79] presented that dopamine can alter cytosolic calcium. This experiment was done using neurons from hippocampal, cortical or midbrain areas. Dopamine applied in the range 0.1 to 100uM elicited significant Ca^{2+} changes in the cell body and dendrites. The calcium responses were repeated using cortical hippocampal explant cultures where in vivo tissue properties were "well retained" to eliminate any concerns of possible culture conditions depending properties. It was reported that changes of Ca^{2+} could be increased by receptor dependent Ca^{2+} flow through voltage-gated calcium channels (VDCC) [80]. DA-induced Ca^{2+} response was receptor independent since calcium changes were not altered while applying D1/D5 receptor antagonist. Source of the increased Ca^{2+} was only extracellular because the results were replicated even when Ca^{2+} was depleted from ER. Moreover, the intracellular calcium changes were completely abolished when verapamil was used, which is a VDCC inhibitor. Interestingly, more potent VDCC blocker – nifedipine – just reduced the amplitude of DA-induced $[Ca^{2+}]_c$ signal but it never abolished it. Nifedipine, inhibit VGCC in the voltage-dependent manner [81] and in the range of DA-induced depolarization probably was not totally blocked. The activity of DAT, in particular the substrate-induced current depolarizes the plasma membrane and this depolarization is what activates the VDCC. This provides evidence that DA uptake through DAT depolarizes neuronal membrane and allows calcium influx by opening VDCC.

2.2 Voltage-gated calcium channel

2.2.1 Type of Ca_V and expression:

Voltage-dependent calcium channels are localized in the membrane of all excitable cells - muscle, neuroendocrine cells, and neurons, and regulate the permeability to Ca^{2+} as a function of membrane potential. Ca^{2+} channels are formed by at least 3 subunits, the main α1 subunit, and the auxiliary β and $α_2δ$ subunits. The $α_1$ subunit forms the ion conducting pore, whereas the associated subunits have several functions including modulation of gating [82]. The cytosolic β subunit is very important in stabilizing the final $α_1$ subunit conformation and delivering it to the cell membrane by its ability to mask an endoplasmic reticulum retention signal in the $α_1$ subunit. The endoplasmic retention brake is contained in the I–II loop in the $α_1$ subunit that becomes masked when the β subunit binds [83]. Therefore, the β subunit functions initially to regulate the current density by controlling the amount of $α_1$ subunit expressed at the cell membrane. In addition to this trafficking role, the β subunit plays an important function in regulating the activation and inactivation kinetics. Ca_V inactivates in voltage- and Ca^{2+}-dependent manner [84] and this process can be modulated by β by generally shifting voltage-dependence of inactivation to more negative voltages, usually about 10-20mV. The most profound increase in channel probability produce $β_{2A}$ [85] while $β_{2e}$ decelerate inactivation [84].

Voltage-gated Ca^{2+} channels might be defined by having different α1 subunit as - Ca_V1, Ca_V2, and Ca_V3. The first group, Ca_V1 are called L-type calcium channels. The currents through those channels are distinguished by large single channel conductance, slow voltage-dependent inactivation and high voltage activation with one exception, $Ca_V1.3$ L-type Ca^{2+} channel that is not high voltage activated [86]. Ca_V3, also known as T-type (transient opening) is characterized by low voltage activation, rapid inactivated, slow deactivated and small channel conductance

[87]. Ca$_V$2 family of Ca^{2+} channel has more negative and faster voltage dependence but more positive and slower than T-type. Neuronal presynaptic Ca^{2+} channels, P/Q, N and R –type, require strong depolarization and are coupled to neurotransmitters release [88].

Dopaminergic neurons that demonstrate two predominant activity patterns termed tonic and phasic [22]. It was shown that in mouse VTA, firing activity is regulated by L-type Ca^{2+} channel, in particular Ca$_V$1.2 and Ca$_V$1.3 [23]. Ca$_V$1.3 activation is necessary for basal single-spike firing, while burst firing is supported by activation of both subtypes. Since Ca$_V$ channels play important roles in neuronal excitation, some studies pointed out the possibility that substrate-induced monoamine transporter currents can regulate membrane excitability through activation of Ca$_V$ channels.

3.   Chapter three: Hypothesis and Aims:

3.1   HYPOTHESIS 1: Monoamine transporters substrates indirectly activates voltage-gated calcium channels

3.1.1   AIM1: Expression of monoamine transporters and calcium channels in heterologous expression system

3.1.2   AIM2: Identification of the substrate-induced current at monoamine transporter

3.1.3   AIM3: Opening of voltage-gated calcium channels due to depolarization induced by monoamine transporter activation
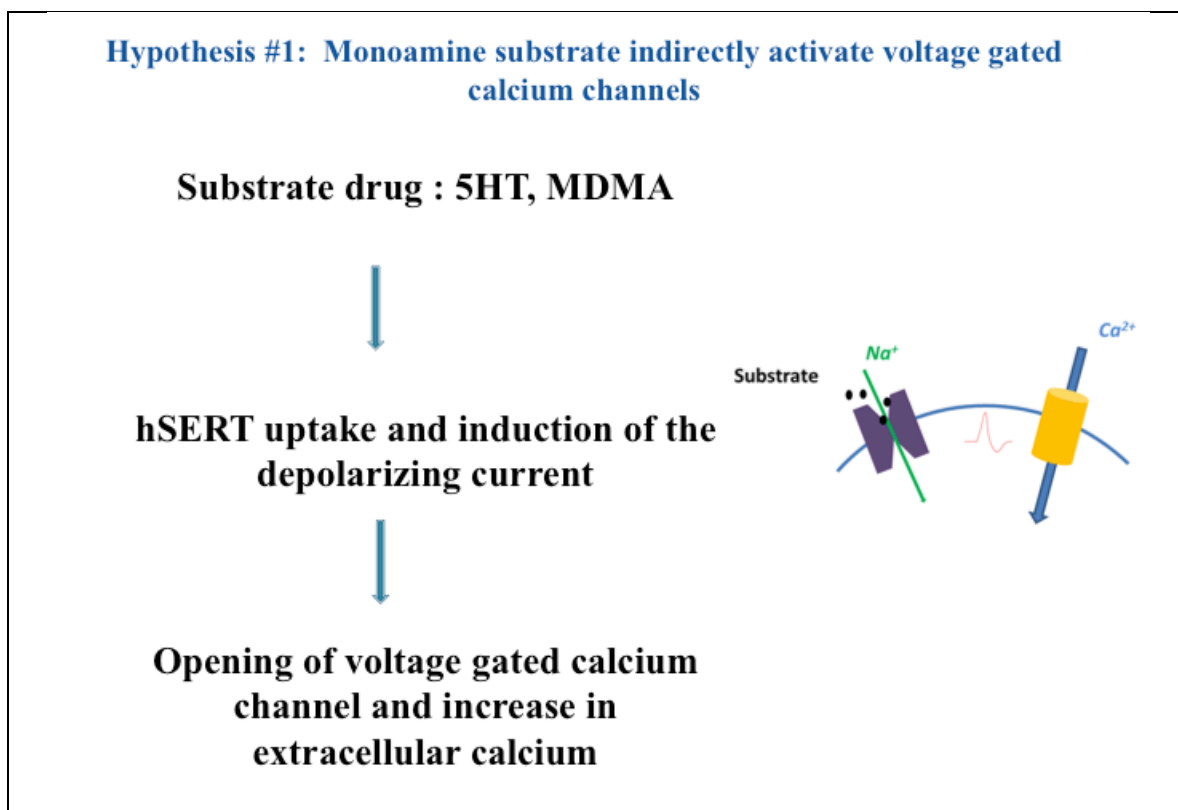
3.2   HYPOTHESIS 2: Electrical coupling between calcium channels and monoamine transports can discriminate substrates and blockers of the transporters

3.2.1   AIM1: Developing protocols for identification of substrates and blockers

3.2.2   AIM2: Characterization of calcium sensors

3.2.3   AIM3: Optimization of calcium channels subunits in hDAT and hSERT

3.2.4   AIM4: FlexStation as calcium mobilization assay technique in first approach for High Throughput Screening (HTS)

3.2.4.1 Optimization: testing sensitivity of known drugs in FlexStation

3.2.4.2 Testing set of newly synthesized drugs

3.2.4.3 Secondary post screening: detailed analysis using epifluorescence microscopy
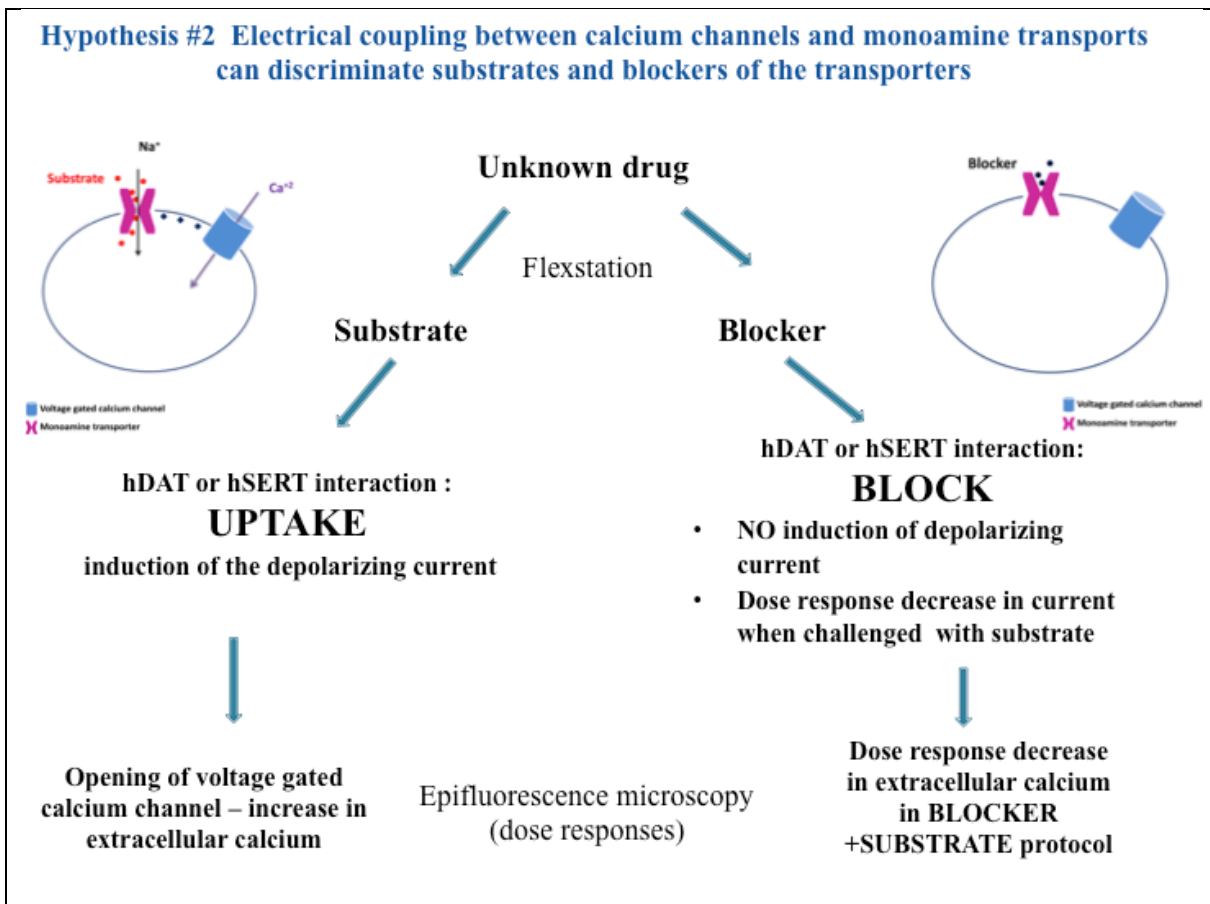
4. Chapter four: materials and methods

4.1 Culture of HEK293

HEK293 cells were prepared in Dulbecco's modified Eagle's medium (DMEM) supplemented with 10% fetal bovine serum (FBS), penicillin (100units/ml) and streptomycin (100g/ml) and were incubated at 37°C to reach 80% confluence. Subsequent splitting was done using PBS/Trypsin solution. DMEM with FBS was used to stop trypsin activity. 10% of cells were plated in new culture dish for subsequent grow.

4.2 Generation of Flp-In Trex cells and permanently expression of MOT

To generate inducible cell lines that permanently express one of the monoamine transporter of interest (hDAT or hSERT) cells undergo Flp-In^{TM}T-REx^{TM}293 (Flp) (Invitrogen) expression system. Flp-In^{TM} T-REx^{TM} cell lines are HEK cells that contain FRT recombination site and Tet repressor gene. To generate cells expressing hSERT, Flp cells were co-transfected with pcDNA5/hSERT-IRES-DsRED/FRT/TP (that was previously created by subcloning hSERT-IRES-DsRED DNA fragment with pcDNA5/FRT/TP vector) and plasmid encoding the Flp recombines pOG44 plasmid. Clones that have inserted a single copy of the gene of interest into the recombination site acquire a hygromycin resistance. hDAT expressing cells undergo very similar process, the only difference is hDAT cDNA (accession number : NM_001044) do not have IRES_DsRED sequence.

25

4.3 Experimental solutions

Imagine solution IS (all values in mM): 130 NaCl, 4 KCl, 2 $CaCl_2$, 1 Mg Cl_2, 10 Hepes, 10 glucose, with pH adjusted to 7.4.

High K^+ solution: 134 KCl, 2 $CaCl_2$, 1 Mg Cl_2, 10 Hepes, 10 glucose, with pH adjusted to 7.4.

Internal solution (for patch clamp): 135 mM CsCl, 10 mM Cs2-EGTA, 1 mM CaCl2,4 mM MgCl2, and 10 mM Hepes, pH 7.4 with CsOH.

External solution (for patch clamp): 155 mM tetraethylammonium (TEA)-Cl, 5 mM CaCl2and 10 mM Hepes, pH 7.4, with TEA-OH.

4.4 Transient transfection

For epifluorescence experiment Fln-hMAT were cultured in 96 well imaging plate at about 30% confluence at day one. On second day cells, undergo transfection using Fugene 6 (Promega) as transfection reagent. The CaV2.2 (α_{1B}), CaV1.3 (α_{1D}), β_3 and $\alpha_2\delta$ expression plasmids were obtained from Addgene (cat# 26570, 26571, 26574 and 26575, respectively) and were kindly provided by Dr. Diane Lipscombe (Department of Neuroscience, Brown University, Providence, Rhode Island, USA). The CaV1.2 ($\alpha1C$ accession number: NM 001136522) was kindly provided by Dr. Manfred Grabner (Department of Medical Genetics, Molecular, and Clinical Pharmacology, Innsbruck Medical University, Innsbruck, Austria). Cells were transfected with calcium channels subunits in ratio $\alpha_1:\beta_3:\alpha_2\delta:EGFP=1:1:1:0.2$, where EGPF expression vector was a transfection marker. Lipofectamine was used in the cells co-transfecting hSERT-IRES-DsRED with calcium channels.

4.5   Intracellular Ca^{2+} determination

Intracellular calcium was measured using Ca^{2+} sensitive dyes Fluo-4AM or Fura-2AM (Life Technologies). Dyes vials were dissolved in DMSO pluronic F-127 20% and stored at -20C until used.   Prior to experiment dyes/DMSO were diluted in imagine solution IS for final concentration 5.5uM. 50ul of either dye were loaded into the cells and placed into 37°C for 12 min (Fluo-4AM) or for 25 min (Fura-2). After incubation time dye solution was replaced with IS and cells were kept at RT for about 25 min. Visualization of calcium signal was done using epifluorescence microscope following the method described previously. [89] Measurements were done under constant perfusion at RT or at 35°C using an excitation wavelength of 490/10nm, a dichroic mirror and an emission wavelength of 535/50nm for Fluo-4. The Fura-2 signals were acquired by switching the excitation wavelength between 340/10nm and 380/10nm at 6Hz and the emission wavelength was 510/40nm. Transfected cells were identified by visualization of DsRed (excitation 510/10nm, emission 620/60nm) or EGFP (excitation 490/10nm, emission 535/50nm). The reported values are the fluorescence values divided by the basal level of each cell and reported as $\Delta F/F_o$ forFluo-4 and $\Delta F_{(340/380)}/F_o$ for Fura-2. All signals were background subtracted. The Ca^{2+} signal was acquired at 50 or 100 Hz as indicated in the figure legends for Fluo-4 or 3 Hz (ratio image) for Fura-2.

The dose-response relationships for Ca^{2+} and [^{3}H]-5HT uptake experiments were fit by the equation: (1)

$$Y(X) = \frac{Y_{max}}{[1+10\exp(\{\log EC_{50} - \log X\}*n)]} \qquad (1)$$

where X is the concentration of 5HT or S(+)MDMA applied, Y(X) is the response measured,

27

Y_{max} is the maximal response, EC50 is the concentration that produces half-maximal response, and n is the Hill slope parameter.

4.5.1 APP$^+$ uptake assay

To monitor hSERT uptake we used previously described APP$^+$ (4-(4-(Dimethylamino) phenyl)-1-methylpyridinium). APP$^+$ is fluorescent substrate transported by hSERT used to monitor hSERT activity by fluorescence microscopy as previously described [90]. It does not exhibit fluorescence while outside cells, nor during interaction with transporter. APP$^+$ can fluoresce only after changing confirmation from "twisted" intermolecular charge transfer state-forming compound (TICT) to co-planar confirmation (ref). This co-planar confirmation is energetically more favorable when APP$^+$ binds to intracellular molecules such as proteins, DNA or RNA. When APP$^+$ is transported, it diffuses in the cytosol and later on is accumulated in mitochondria and nuclei. Cells grown on imaging plates were placed on the stage of the fluorescence microscope describe above. The wavelengths used to detect the APP$^+$ signal were 460/10 nm for excitation and 535/50 nm for emission.

4.6 Radiolabeled uptake studies

Flp-In cells expressing hSERT were counted and 2×10^6 cells were exposed to different concentrations of 5HT where 3% of a given concentration consisted of [^{3}H]-5HT. The 5HT uptake was carried out for 10 min at 37◦C in IS (see composition above). Non-specific uptake was measured adding 5µM fluoxetine to the radioactive mixture. Then the cells were centrifuged, washed once with cold 1X PBS, centrifuged again, cell pellets were resuspended in Ecoscint H

(National Diagnostics, Atlanta, GA, USA), and the radioactivity counted using a liquid scintillation counter. The mean ± S.E.M. of 5 independent experiments done in duplicates are reported.

4.7   Whole cell patch clamp

Macroscopic Ca^{2+} currents (I_{Ca}) were measured as previously described [91]. External solution and the patch pipette internal solution compositions are described above. The whole-cell patch-clamp parameters of the recordings were: cell capacitance = 27 ± 3 pF, access resistance = 5.5 ± 0.5 MΩ, τ= 153 ± 26 µs (n = 14). The effective series resistance was compensated and corrected by 80% using the Axopatch circuit. In these conditions, the remaining voltage error is <1.5 mV. The leak current was subtracted using a −P/6 protocol before each sweep. The pipettes were fire polished, Sylgard coated and had a resistance of ∼2.5 MΩ when filled with the internal solution. The liquid-junction potential was not corrected. The recorded signals were acquired at 10 kHz and filtered at 5 kHz. The voltage dependence of the I_{Ca} was fit to the following equation:

$$I_{Ca} = \frac{G_{max}(V - V_r)}{1 + \exp((V_{1/2} - V)/k)} \qquad (2)$$

where G_{max} is the maximal conductance, V is the test potential, $V_{1/2}$ is the potential at which G = 1/2 G_{max}, k represents a slope parameter and V_r is the reversal potential.

4.8   Flexstation calcium mobilization assay

Cells that permanently express hDAT or hSERT were co-transfected with $Ca_V1.2$ (auxiliary subunits were used when indicated on the graphs) and GCamp6s coding plasmids, and plated in a 96 well-imaging plates. After 3 days of transfection, growing media was replaced with 50ul of IS and cells settled for 25min.

Time-lapse of the fluorescent signal was acquired in a Flex Station 3 that allows for simultaneous reading of 8 wells (one column in 96 well-plate). Data were acquired using SoftMAx Pro software with following settings: fluorescence read mode with excitation and emission wavelength: 488nm and 525nm; PMT sensitivity: high; run time: 180sec with interval length 1.69sec; total number of reads 107. Maximal pipette height is 50ul with a total volume of 80ul and rate of injection 3 (~47ul/sec). Time point (which is the time after drug was injected) was 30sec.

4.9   Statistics and data analysis

All data are presented as mean ± S.E.M. unless indicated in the figure legend. Comparisons were made by unpaired, two-tailed t-test, with $p < 0.05$ considered significant.

5.   Chapter five- results: Monoamine substrate indirectly activate voltage gated calcium channels

5.1   Expression of hSERT in HEK293 cells

Expression of hSERT after transfecting HEK293 cells with hSERT-IRES-DsRed plasmid was evaluated by immunostaining and epifluorescence microscopy. The hSERT signal is shown in green and the DAPI nuclear staining is shown in blue (Figure 5.1) Cells not transfected with hSERT did not show green immunofluorescence as is shown in Figure 5.1B (Scale bar = 100 μm). Using confocal microscopy we could depict hSERT membrane localization in transfected cells subjected to immunostaining (Figure 5.1C) (Scale bar = 10 μm). Further evidence of hSERT expression is the detection of a specific band of ~80 kDa by Western blot analysis in samples transfected with hSERT-IRES-DsRed plasmid (Figure 5.1D). Cells transfected with the hSERT-IRES-DsRed plasmid were exposed to APP^+ for 1 min and APP^+ uptake was evaluated by live fluorescence microscopy. To demonstrate that hSERT expressed by the cells is a functional transporter we subjected the cells to fluorescence APP^+ substrate, the APP^+ signal is shown in green in Figure 5.1E. Merging of the green (APP^+) and red (DsRed) channels show only cells expressing hSERT uptake APP^+ (Figure 5.1F). Other cells (not transfected) depicted in DIC image (Figure 5.1G) do not uptake APP^+. Representative traces of the kinetics of APP^+ uptake is shown in Figure 5.1H. Time-lapse experiments show that APP^+ uptake is completely abolished by fluoxetine (selective hSERT inhibitor) in DsRed positive cells (Figure 5.1I).

31
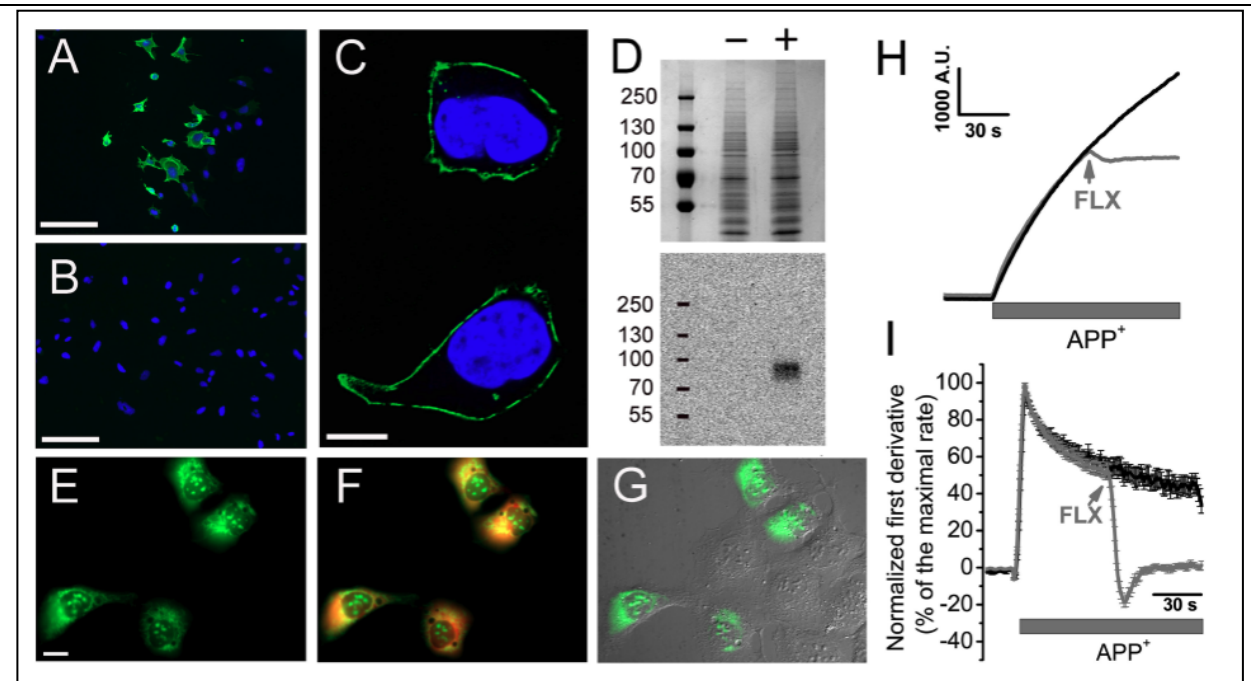
Figure 5.1: Expression of hSERT in HEK293 cells. Cells were transfected with the hSERT-IRES-DsRed plasmid. (A) hSERT expression was evaluated by immune-staining and epifluorescence microscopy. The hSERT signal is shown in green and the DAPI nuclear staining is shown in blue. (B) Immunofluorescence of non-transfected cells. Scale bar = 100μm. (C) Confocal image showing the membrane localization of hSERT in transfected cells subjected to immunostaining. Scale bar = 10 μm. (D) The lower image is a western blot showing the expression of hSERT only in samples from cells transfected with hSERT-IRES-DsRed plasmid (+) but not from cells transfected with the empty vector (-). The upper image shows the total protein content as a loading control for the same samples evaluated by SDS-PAGE and Coomassie blue staining (standards in kDa). (E) Cells transfected with the hSERT-IRES-DsRed plasmid were exposed to APP$^+$ (fluorescent hSERT substrate [90]) for 1 min and APP$^+$ uptake was evaluated by live fluorescence microscopy. The APP$^+$ signal is shown in green. (F) Merging of the green (APP$^+$) and red (DsRed) channel. (G) Merging of the green channel (APP$^+$) and the DIC image. (H) Representative traces of the kinetics of APP$^+$ uptake for several minutes. The black trace shows the control condition and the grey trace shows the effect of fluoxetine (FLX). (I) The first derivative (rate) of the APP$^+$ uptake plotted as a function of time.

32

5.2   The intracellular Na$^+$ concentration induced by SERT substrates

Since 5HT induces inward current that consist partly of Na$^+$ ions [92] we wanted to study intracellular Na$^+$ in hSERT expressing cells. Cells exposed to SERT substrates (5HT or S(+)MDMA) increase intracellular Na$^+$ concentration which is shown in Figure 5.2 A and B. Although both hSERT substrates showed potencies in a similar range, S(+)MDMA is more efficacious than 5HT at elevating internal Na$^+$. Raising the temperature from 23ºC to 35ºC significantly increased the Na$^+$ permeability induced by both substrates (Figure 5.2 C). Using whole-cell voltage clamp ionic current was measured at a holding potential of -60 mV. Transfected cells were exposed to 10 µM S(+)MDMA for 50 s and after a 2 min wash the cells were exposed to 10 µM 5HT also for 50 s and then washed again for 1 min. The experiments were done under constant perfusion at 35°C. Ionic currents induced by 5HT (I$_{5HT}$) or S(+)MDMA (I$_{MDMA}$) showed identical initial peaks followed by a slow decay (Figure 5.2 D). It is possible that some blocking mechanism 5HT induced some blocking mechanism, which inhibit in part the current after longer exposure.
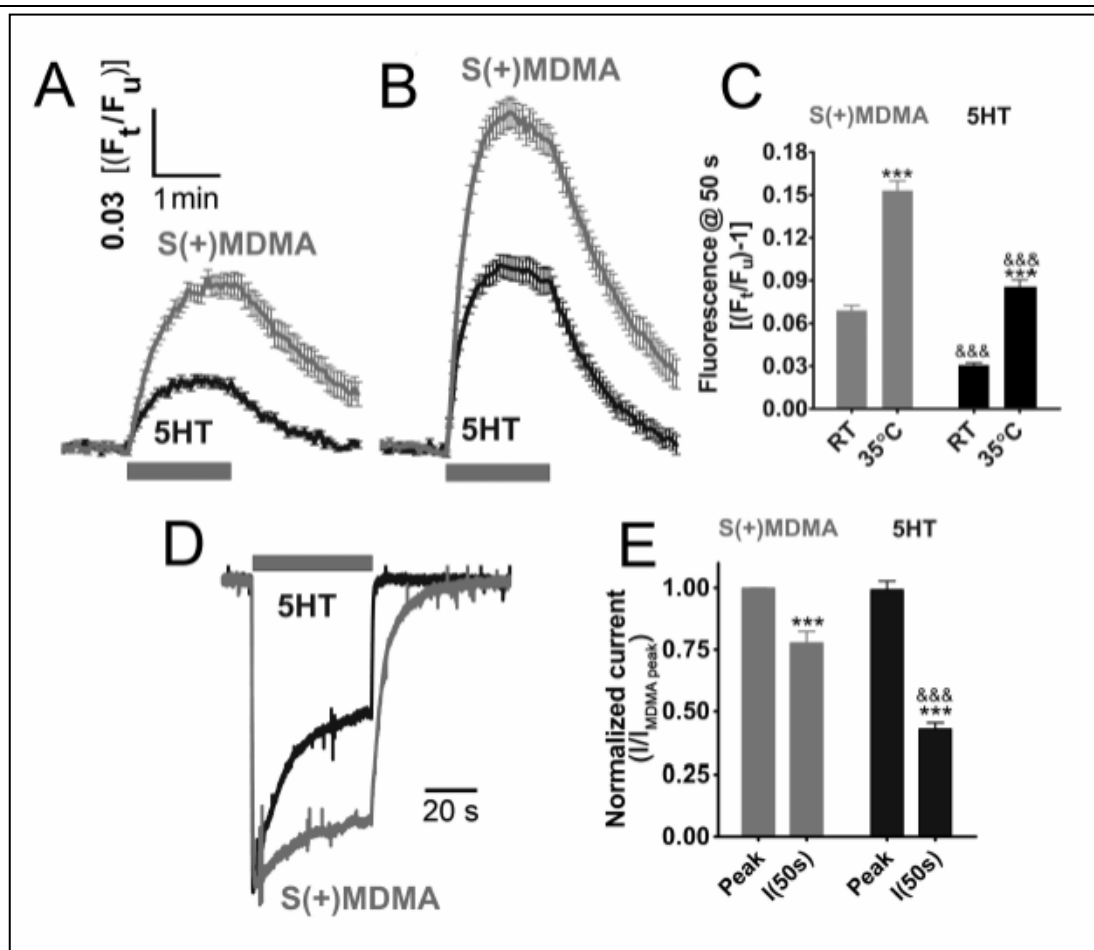
Figure 5.2: S(+)MDMA and 5HT show increase in intracellular Na$^+$ in hSERT expressing cells. HEK293 cells transfected with the hSERT-IRES-DsRed plasmid were loaded with the permeable Na$^+$ sensitive dye Asante NaTRIUM Green-2 AM. (A) Intracellular Na$^+$ increase induced by 5HT (black trace) or S(+)MDMA (grey trace), both 10 μM and at room temperature (23 °C) or (B) at 35°C. (C) The intensity of the Na$^+$ signal after 50 s exposure to S(+)MDMA (grey bars) or 5HT (black bars) either at room temperature (RT) or at 35°C. (D) Ionic currents measured by whole-cell voltage-clamp technique at a holding potential of -60 mV. Transfected cells were exposed to 10 μM S(+)MDMA for 50 s and after a 2 min wash the cells were exposed to 10 μM 5HT also for 50 s and then washed again for 1 min. The experiments were done under constant perfusion at 35°C. (E) Normalized current intensities at the peak or after 50 s exposure (I50s) to S(+)MDMA (grey bars) or 5HT (black bars).

5.3 Voltage-dependence of CaV1.3- and CaV2.2- mediated Ca2+ currents.

To test the hypothesis that either I_{5HT}- or I_{MDMA}- induced depolarization can activate LVA Ca^{2+} channels, the $Ca_V1.3$ (LVA) - or as a control, $Ca_V2.2$ (HVA) Ca^{2+} channels - were co-expressed with hSERT in HEK293T cells. As shown by others [93] and confirmed here, the Ca^{2+} current (I_{Ca}) of $Ca_V1.3$ has a 34 mV left shift in its voltage dependence curve compared to the I_{Ca} of $Ca_V2.2$. Therefore, the activation threshold of I_{Ca} is ~-35 mV and ~0 mV for $Ca_V1.3$ and $Ca_V2.2$, respectively (Figure 5.3).
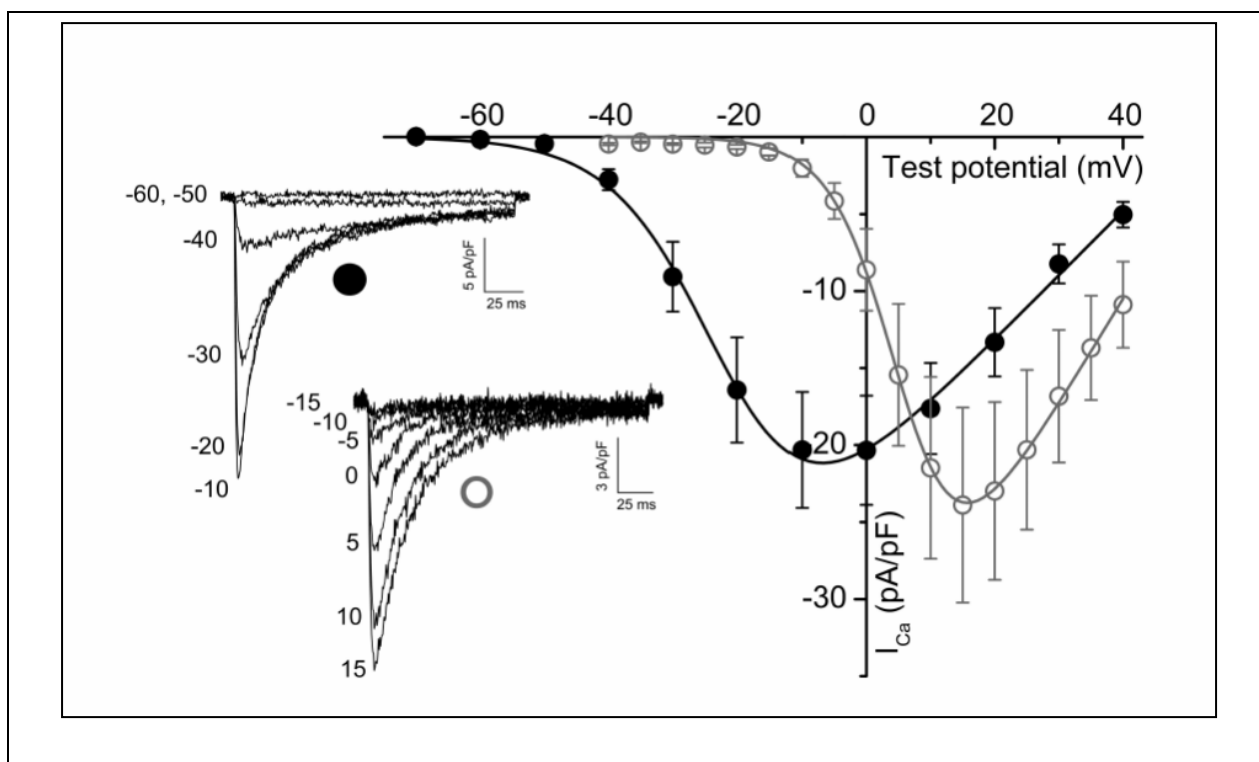
Figure 5.3: Voltage-dependence of CaV1.3- and CaV2.2- mediated Ca2+ currents.

HEK293T cells were co-transfected with hSERT-IRES-DsRed, β_3, $\alpha_2\delta_1$ and alternatively Ca$_V$1.3 (closed black circles) or Ca$_V$2.2 (open gray circles) plasmids. The experiments were done under constant perfusion at 35°C. The currents were evoked by a trend of pulses starting at a holding potential of -60 mV in steps of 10 mV. Representative family of responses for Ca$_V$1.3 and Ca$_V$2.2 are shown in A and B, respectively. C, The current-voltage dependence of the peak current densities was fit according to Eq.1 (Materials and Methods) for Ca$_V$1.3 (black trace) and Ca$_V$2.2 (grey trace). The data are expressed as mean ± SEM. The fitting parameters are the following: G_{max}, 2,394 ± 312 and 2,336 ± 251 (pS/pF); $V_{1/2}$, -17 ± 1.5 and 16*** ± 1.0 (mV); k, 3.9 ± 0.43 and 3.1 ± 0.33 (mV) for Ca$_V$1.3 (n = 7) and Ca$_V$2.2 (n = 5) respectively. *** = p < 0.0001, t-test.

5.4 The depolarization induced by hSERT activation is electrically coupled to CaV1.3 opening

To study the electrical coupling between hSERT and these Ca^{2+} channels, the co-transfected cells were subjected to intracellular Ca^{2+} determination by fluorescence microscopy as described in Materials and Methods. When hSERT was expressed without either Ca$_V$ channel, the cells did not respond to hSERT substrates or to high K$^+$-depolarization (Figure 5.4 A). In contrast, 5HT and S(+)MDMA evoked fast Ca^{2+} transients when Ca$_V$1.3 (but not Ca$_V$2.2) was co-expressed with hSERT. Nevertheless, high K$^+$ depolarization evoked Ca^{2+} transients when either Ca^{2+} channel was expressed (Figure 5.4 B and C), demonstrating that hSERT-mediated depolarization activates Ca$_V$1.3 but not Ca$_V$2.2. Finally, cells transfected with Ca$_V$1.3 in the absence of hSERT only have a positive response to high K$^+$ depolarization, whereas S(+)MDMA or 5HT show no

effect (Figure 5.4 D).
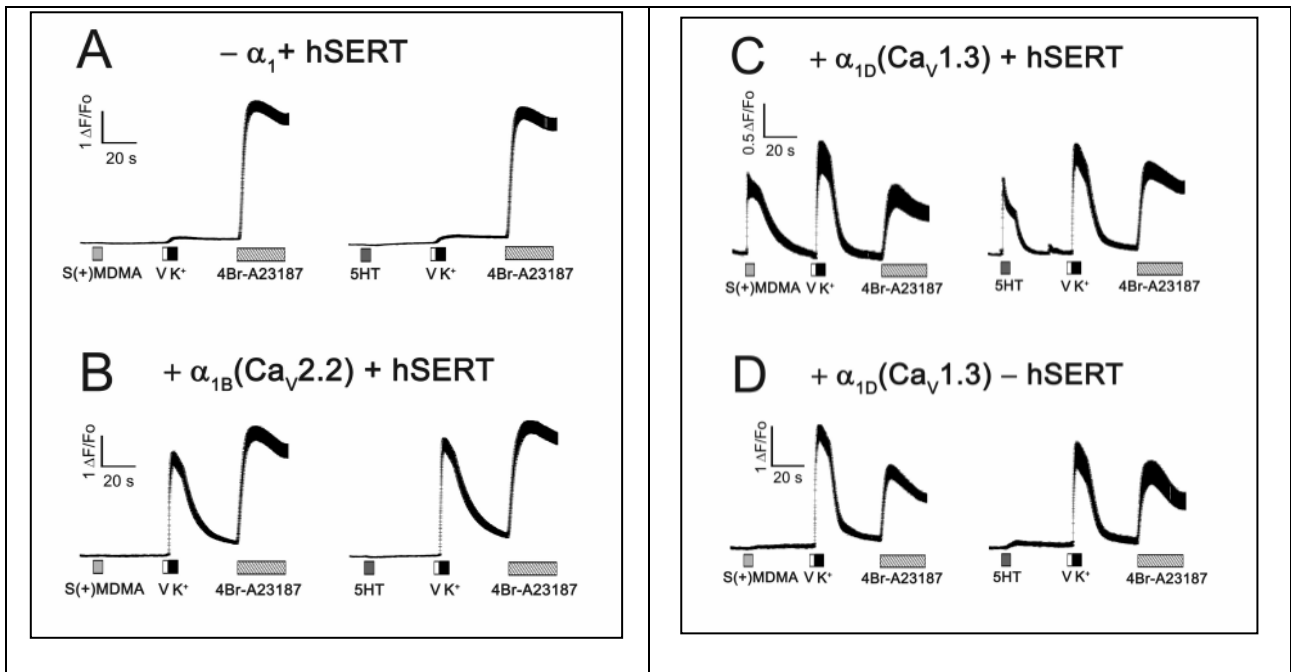
Figure 5.4: HEK293T cells were loaded with the permeable Ca^{2+} sensitive dye Fluo-4AM and the intracellular Ca2+ concentration was measured by fluorescence microscopy at an acquisition rate of 50 Hz. The tested ells were transfected with the following plasmids: (A) hSERT-IRES-DsRed (without CaV channel); (B) α1B (CaV2.2) and hSERT-IRES-DsRed; (C) α1D (CaV1.3) and hSERT--IRES- DsRed; (D) α1D (CaV1.3) and DsRed (without transporter). (A-D) As indicated in each trace, the cells were exposed to 10 μM S(+)MDMA (light grey box) or 10 μM 5HT (dark grey box) for 5 s. After wash the cells were exposed to 200 nM valinomycin (V, white box) for 2s to increase the K+ permeability and were immediately exposed to 130 mM K^{+} solution for 5s (K^{+}, black box) to depolarize the cells toward positive potentials, then after wash the cells were exposed to 3μM 4Br-A23187 - Ca^{2+} ionophore. The traces shown are mean ± s.e.m. of n ≥ 20 cells.

5.5 5HT shows higher potency activating hSERT/CaV1.3-mediated Ca^{2+} signals than inducing its transport.

The over-expression of hSERT in transient transfection experiments would lead to non-physiological levels of depolarization upon challenging the cells to hSERT substrates. To address this concern, a stable cell line expressing the hSERT–IRES–DsRED construct was generated using the Flp-InTMT-RexTM expression system as described in Materials and Methods. Since these cells are restricted to a single copy of the gene of interest, the expression level of the inserted gene is lower than in transient tranfection experiments. Using the APP^+ assay, the Flp-In cells showed 60% less hSERT maximal activity than HEK cells subjected to transient transfection with the hSERT–IRES–DsRED plasmid, both the transient transfection of HEK cells and the induction of Flp-In cells were carried out 3days prior to the experiment (Figure 5.5 A). Similarly, the DsRed signal was reduced 93% in Flp-In cells (Figure 5.5 A). Although hSERT activity is reduced in Flp-In cells, when they were transfected with $Ca_V1.3$, 5HT induced Ca^{2+} signals in a dose-dependent manner (Figure 5.5 B) whereas un-transfected Flp-In cells (no Ca^{2+} channel but expressing SERT) are refractory to 5HT treatment (not shown). Interestingly, dose-response experiments for $[^3H]$-5HT uptake done in Flp-In cells showed an EC_{50} of 1.68 ± 0.38 µM (n = 5, Figure 5.5 C), whereas the EC_{50} for the Ca^{2+} signal induced by 5HT in these cells was 0.90 ± 0.08 µM (n > 57, Figure 5.5 C) (p < 0.01, t-test). The comparable potency of both actions of 5HT, as a substrate of hSERT, and driving hSERT-mediated depolarization toward $Ca_V1.3$ activation, suggests that the coupling between hSERT-mediated depolarization and Ca_V channel opening is significant in the physiological range of 5HT concentration.
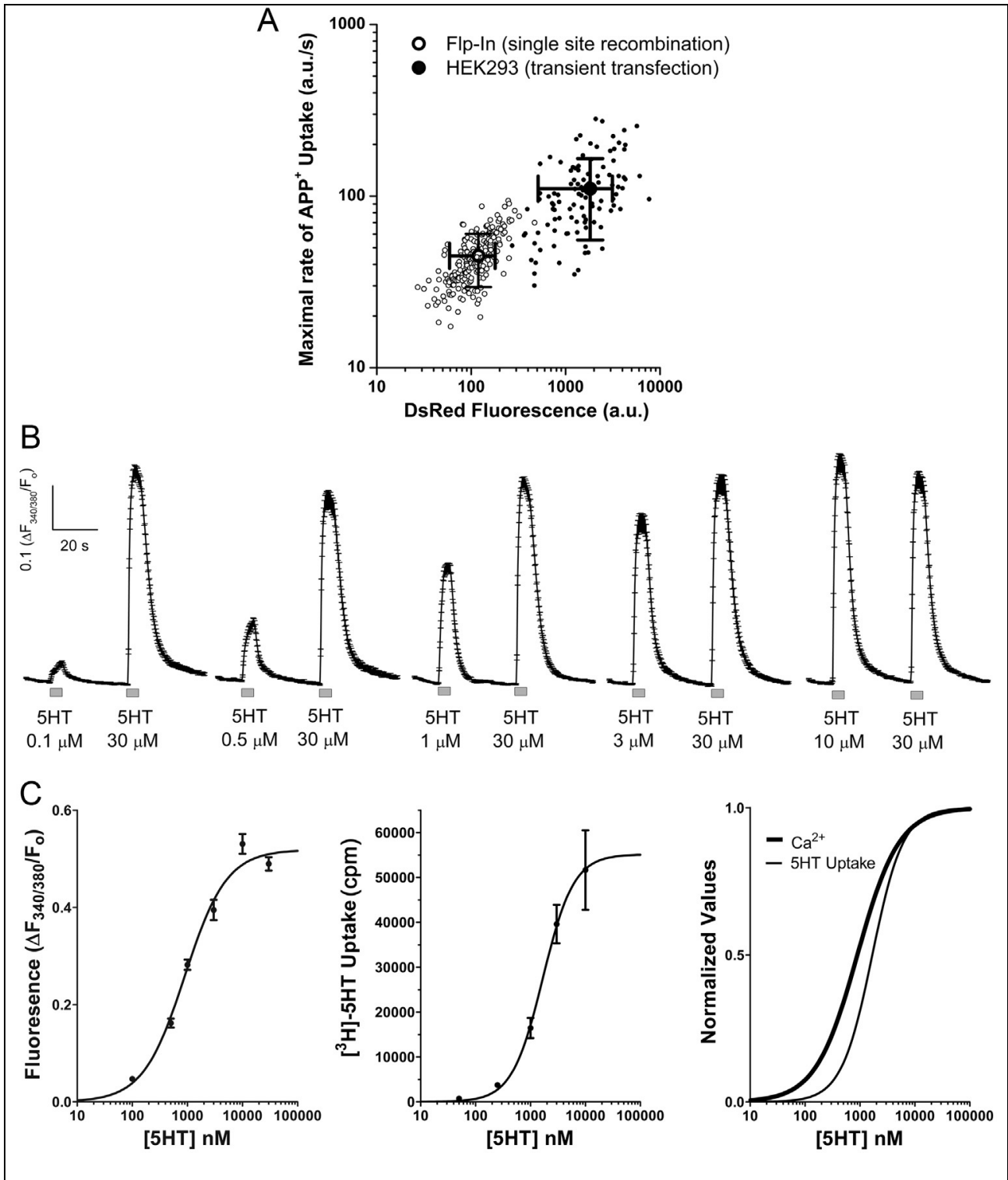
A

B

C

Figure 5.5: The electrical coupling between hSERT and CaV1.3 take place in the physiological concentration range of 5HT. (A) Flp-InTMT-RexTMcells (Flp-In, open circles) expressing the hSERT-IRES-DsRed constructs was generated as described in Material and methods, and HEK293 cells (closed circles) were subjected to transient transfection using the hSERT-IRES-DsRed plasmid. To compare the activity of hSERT among cell types, the maximal rate of APP$^+$ uptake was measured computing the maximum of the first derivative of APP$^+$ signal as function of time. In addition, the DsRed signal was measured for each cell. The maximal rate of APP$^+$ uptake (y axis) and DsRED fluorescence (x axis) is plotted for each individual cell (note that the axis are in logarithmic scale) and the values shown are the mean ± _standard deviation. The hSERT activity was 44.8*** ± _15.4 (a.u./s), and110.4 ± _55.0 (a.u./s) for Flp-In cells (n = 202) and HEK293 cells (n = 107), respectively (***p < 0.0001, t-test). The DsRed signal was 119*** ± _60 (a.u.) and 1821 ± 1310, for Flp-In cells (n = 202) and HEK293 cells (n = 107), respectively (***p < 0.0001, t-test). (B) Flp-In cells were transiently transfected with CaV1.3 as described in Material and methods, the transfected cells were identified by the EGFP fluorescence and the Ca^{2+} signal was determined using Fura-2AM. Measurements were done under constant perfusion at 35∘C and the acquisition frequency was 3 Hz. The cells were exposed to a variable concentration of 5HT followed by 30 μM 5HT to record the maximal response. The traces shown are mean ± _S.E.M. of n ≥ 57 cells for each condition. (C) The dose–response experiments shown in B were fit to Eq. (2) (Materials and methods) and yield the following fitting parameters for the 5HT-dependent Ca^{2+} signal: maximal response = 0.519 ± 0.013 ([F$_{340/380}$/Fo]), EC$_{50}$= 0.90 ± 0.08 (μM) and Hill slope = 1.15 ± 0.12 (n > 57). The dose response of [3H]-5HT uptake in Flp-In cells was fit to Eq. (2) (Material and methods) and yield the following parameters. Maximal response = 55,155 ± _5512 (cpm), EC50= 1.68 ± 0.38** (μM) and Hill slope = 1.55 ± 0.43 (n = 5, **p < 0.01 vs. EC$_{50}$ of Ca^{2+} experiments, t-test). The fitted curves of the Ca^{2+} signal and [^{3}H]-5HT uptake experiments were normalized and superimposed for better comparison.

6. Chapter six- results: Electrical coupling between calcium channels and monoamine transports can discriminate substrates and blockers of the transporters

6.1 A. Developing calcium protocol for substrates and blockers

Cells expressing hDAT were transfected 3 days before the experiment with Ca_V (all subunits). Calcium visualization was done using epifluorescence microscopy after loading cells with Fura 2 (for details see Materials and Methods). Using this Ca^{2+} assay, it is possible to detect substrates or blockers of monoamine transporters. Examples of substrate and blocker protocols are shown in Figure 6.1 where hDAT-expressing cells undergo exposure to the control (hDAT cells are exposed to 10µM DA) for 5 second (first peak signal) under constant perfusion. The second peak represents perfusion of the cells with different concentrations of the studied substrate (in our example N-Methyl 4-MA) for 5 sec [94]. Both the control and the studied drug were washed with IS for 30 second (Figure 6.1 A). Since blockers do not produce Ca^{2+} signal, concentration-dependence signal is acquire by blocking the Ca^{2+} signal evoked by the control compound DA for hDAT cells or 5HT for hSERT not shown (Figure 6.1 B).
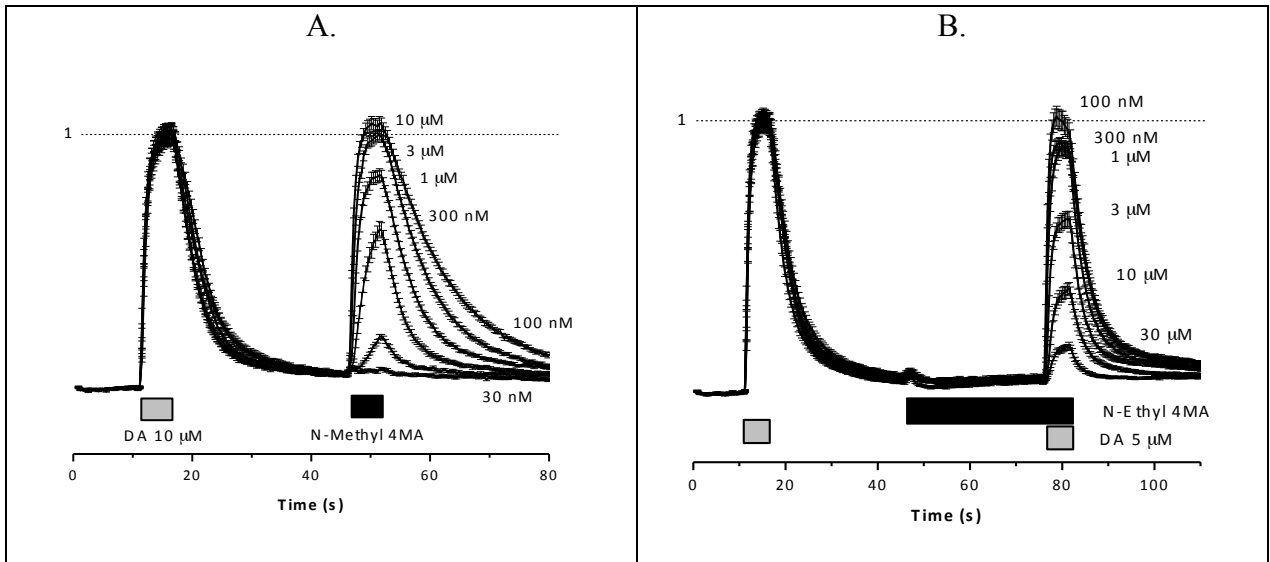
Figure 6.1. Identification of substrate (A) or blocker (B) of monoamine transporters using Ca²⁺ imaging. Cells co-expressing hDAT and Ca$_V$1.2 show Ca²⁺ signals when exposed to 10uM DA (first Ca²⁺ peak) and concentration-dependent increase of Ca²⁺ signal when exposed to substrate, N-Methyl 4-MA (second Ca²⁺ peak, top figure). For blockers, second Ca²⁺ peak represent concentration-dependent blockade using N-Ethyl 4-MA of the Ca²⁺ signal produced by control (5µM DA).

Calcium signal induced after application of the substrate is an indirect measurement of substrate-induced current of monoamine transporter. To directly test this current, oocytes were transfected with hDAT cRNA; recordings were done at room temperature using TEVC under constant perfusion. Two drugs tested previously in HEK cells (Figure 6.1) were used, N-Methyl 4-MA and N-Ethyl 4-MA, which are shown in Figure 6.2. 10µM N-Methyl 4-MA induces 30nA inward current that is correlated with the data in HEK293 cells where 10uM N-Methyl 4-MA induces the opening of the calcium channel and increase in intracellular calcium. N-Ethyl 4-MA, on the other hand, induces outward current at -60mV, which indicates blockage of endogenous leak current hDAT.
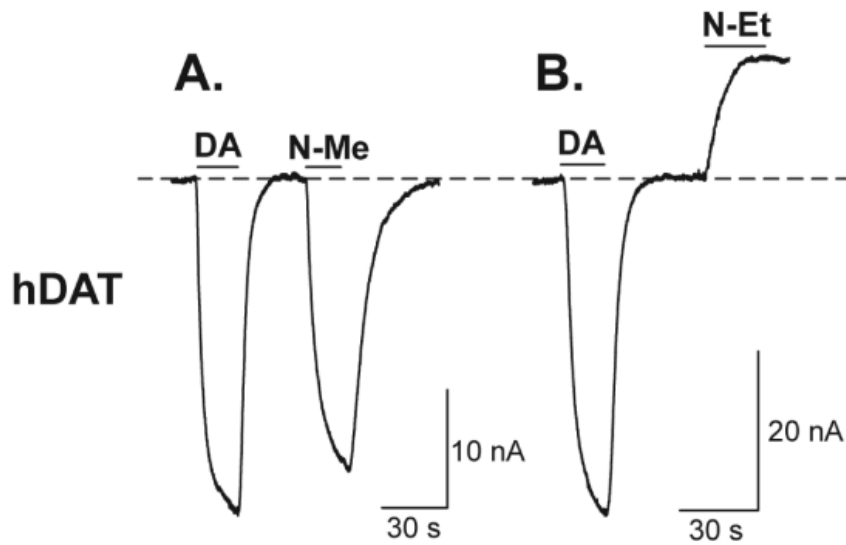
Figure 6.2. Effect of N-Methyl and N-Ethyl 4-MA on membrane currents in oocytes injected with hDAT cRNA. Modified from [94].

6.2 Finding the least amount of subunits required to have functional calcium channels

As was mentioned earlier (see introduction), beta subunit is important in the expression of the calcium channel. To find the least amount of subunits required for functional calcium channel and electrical coupling with transporters hDAT cells were transfected with varied amounts of subunits. Cells were subsequently transfected with $\alpha_{1C} + \beta_3$, $\alpha_{1C} + \alpha_2\delta$, or α_{1C} alone. The calcium signals shown in Figure 6.3 represent response to $10\mu M$ S(+)Amph and $135mM$ K$^+$. Cells expressing only pore domain α_{1C} show signals very similar to cells expressing additional subunits.
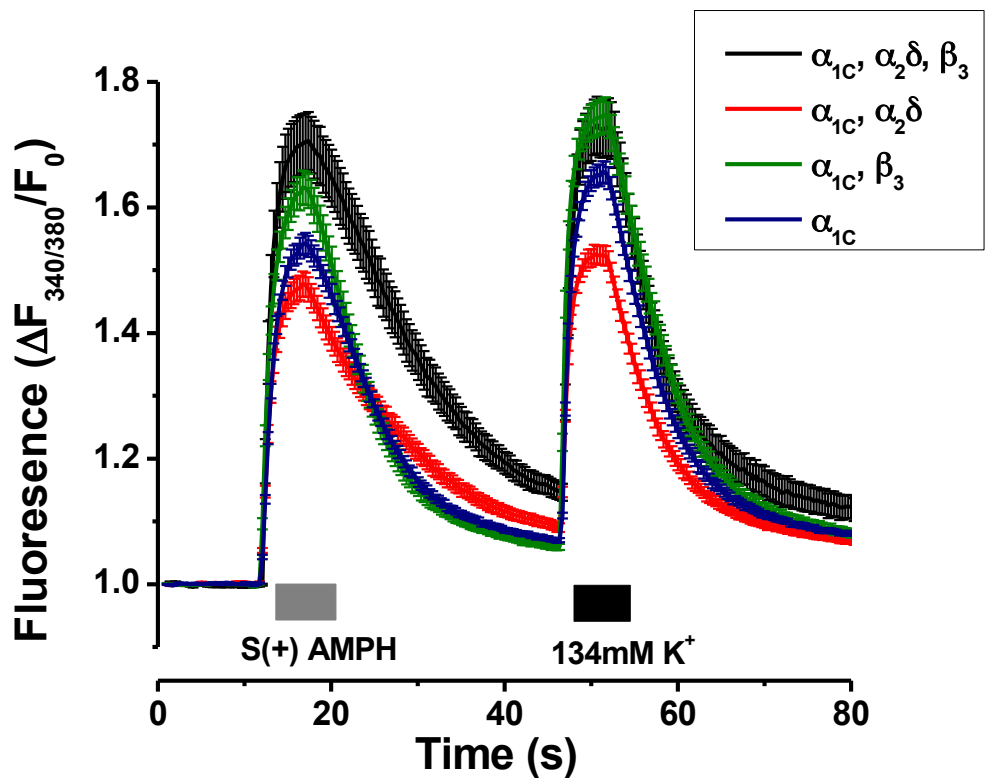
Figure 6.3: Ca^{2+} signals in hDAT-expressing cells transfected with Ca$_V$1.2 (α_{1C}) and auxiliary subunits.

Dose-response experiments for S(+)Amph were conducted in cells transfected with the α_{1C} alone or α_{1C}, β, $\alpha_2\delta$ (Figure 6.4). Cells co-expressing hDAT and Ca$_V$1.2 with all auxiliary subunits produce Ca^{2+} signals with EC$_{50}$, almost identical to cells expressing only α_{1C} subunit (see also table), EC$_{50}$ ± SEM of n $\geq$ 100.
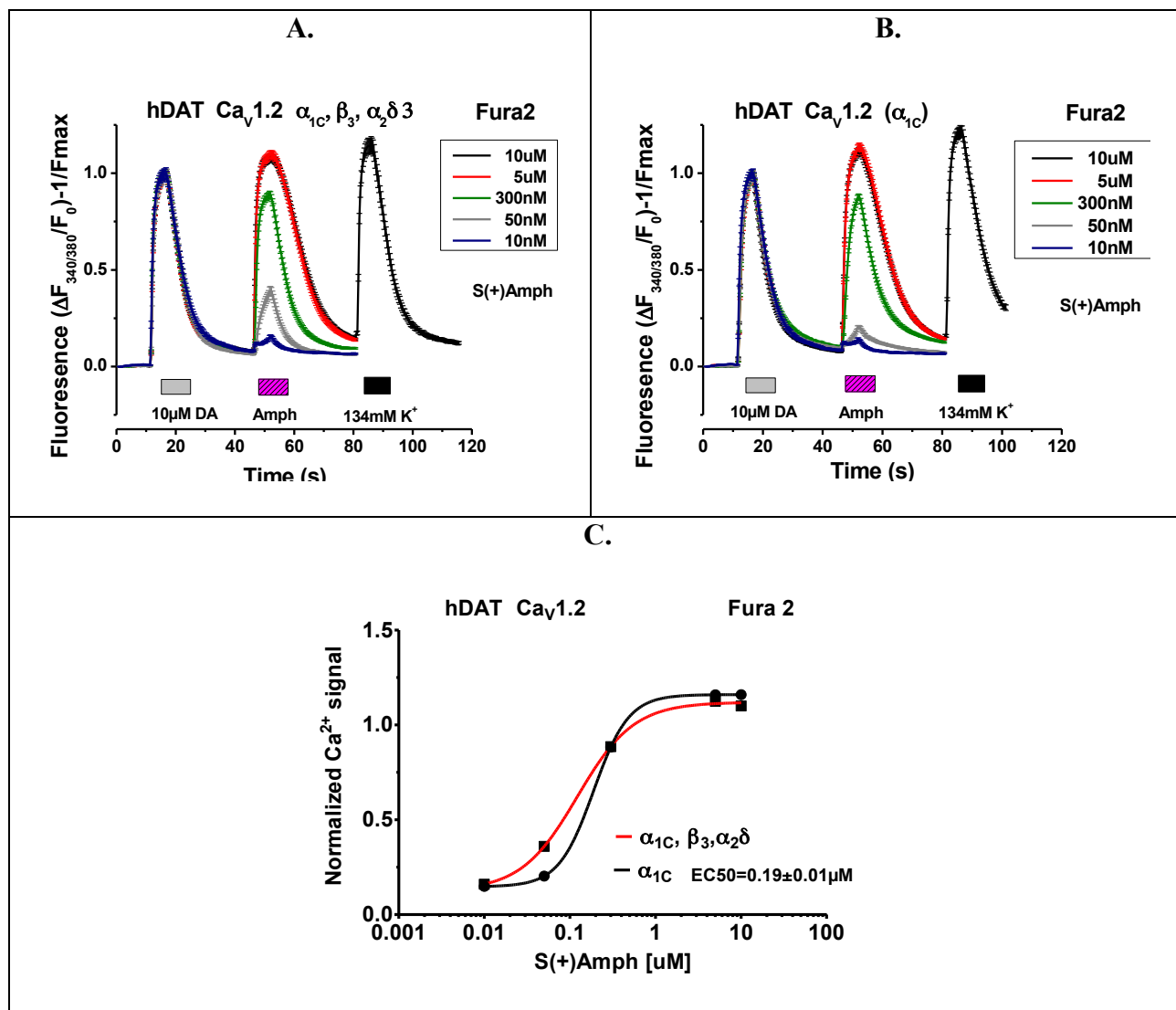
Figure 6.4: Ca^{2+} signals in hDAT-expressing cells transfected with Ca$_V$1.2 and varied auxiliary subunits. (A) Normalized Ca^{2+} signals in hDAT-expressing cells transfected with Ca$_V$1.2 and all auxiliary subunits (α_{1C}, β, $\alpha_2\delta$) using Fura-2. (B) Normalized Ca^{2+} signals in hDAT-expressing cells transfected with Ca$_V$1.2 α_{1C} (no auxiliary subunits). (C) Dose response of S(+)Amph normalized to control (10µM DA). EC$_{50}$=0.12µM for cells transfected with Ca$_V$1.2 and all auxiliary subunits (α_{1C}, β, $\alpha_2\delta$) while EC$_{50}$=0.19µM with cells transfected with α_{1C} (no auxiliary subunits).

Ca^{2+} signals acquired in hSERT expressing cells are shown in Figure 6.5. Dose-response experiments for N-Methyl 4MA were conducted in cells transfected with all subunits (α_{1C}, β, $\alpha_2\delta$), α_{1C} alone, and α_{1C} and β (Figure 6.4 B, C, E). Cells expressing hSERT should be transfected with at least the β auxiliary subunit to evoke calcium signals that are similar in size to signals evoked by cells expressing all auxiliary subunits (Figure 6.5 E).
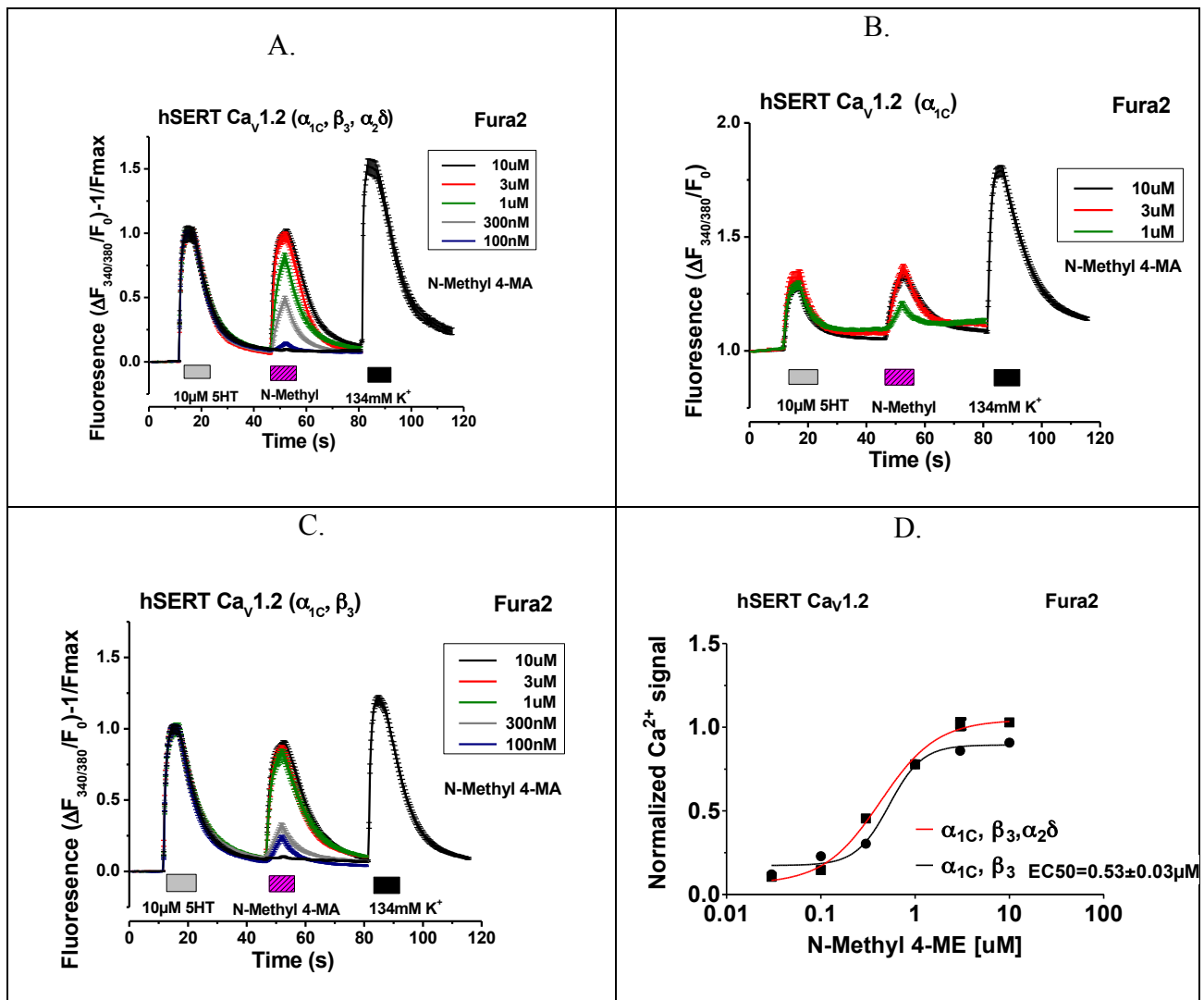
Figure 6.5: Normalized Ca^{2+} signals in hSERT-expressing cells transfected with Ca$_V$1.2 and varied auxiliary subunits (α_{1C}, β, $\alpha_2\delta$) using Fura-2. (A) Cells transfected with Ca$_V$1.2 and all subunits α_{1C}, β_3, $\alpha_2\delta$. (B) Cells transfected with Ca$_V$1.2 α_{1C} (no auxiliary subunits). (C) Cells transfected with Ca$_V$1.2: α_{1C} and β_3. (B) Dose response of N-Methyl 4MA normalized to control (10μM 5HT) in cells expressing all auxiliary subunits (α_{1C}, β_3, $\alpha_2\delta$) (red) and α_{1C} and β (black).

6.3 Determination of dynamic rage, sensitivity and kinetics of calcium sensors (Fluo4 and GCaMP's)

6.3.1 Molecular characteristics of genetically encoded Ca^{2+} sensors

GCaMPs are a new class of genetically encoded indicators of intracellular calcium. These high-sensitive proteins have been widely used in determining rapid neuronal calcium dynamics [95]. They consist of circular permuted green fluorescence protein (cpEGFP) that is attached to calcium-binding calmodulin (CaM) and CaM-interacting M13 a peptide sequence from myosin light chain kinase. In a normal condition, (low Ca^{2+} state) (Figure 6.6) chromophore is in a poor fluorescent and absorbance state due to the water pathway that enables protonation of the chromophore. In the presence of Ca^{2+}, CaM undergoes hinge motion that allows binding of M13, thus rearranging the structure in a way that removes the solvent pathway, causing rapid re-protonation of the chromophore and fluorescence [96].

Figure 6.6: Crystal structure of Ca^{2+}-free (left) and Ca^{2+}-saturated (right) GCaMP. Picture taken from [97]
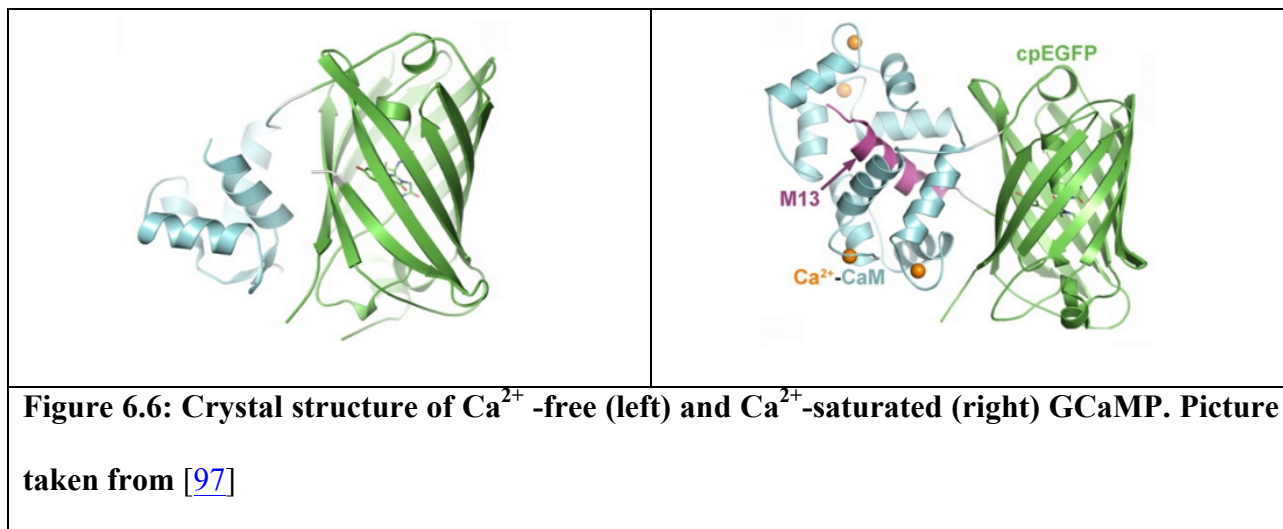
Since the first introduction, GCaMP underwent many optimizations using mutagenesis. Mutations usually took place on the interface between cpGFP and CaM and yielded different sensitivity variants with more sensitive sensors having slower kinetics. Here, two ultrasensitive GCaMP6 sensors - GCaMP6s with slow kinetics and GCaMP6f that was considered the fastest genetically encoded calcium indicators in neurons were tested [95]. We also wanted to test GCaMP-CAAX membrane tethered version of GCaMP6s since we would expect that membrane-targeted sensor should have higher sensitivity due to its closest proximity to calcium channels.

6.3.2 Efficiency of the calcium dyes

Three GCaMP including GCaMP6s, GCaMP6f, GCaMP6s-CAAX were tested. They were compared to Fluo-4, well-established Ca^{2+} dye used to measure intracellular calcium (Figure 6.6). All experiments were done in the same conditions. To test Fluo-4, cells expressing hDAT were transfected with $Ca_V1.2$ α_{1C} and before the experiment 50µl of Fluo-4 were added to the cells and incubated for 15min at 37°C. After that the solution with Fluo-4 was exchanged for IS and cells settled for 25min. The experiment was then performed. Since GCaMPs are genetically encoded, they were co-transfected with α_{1C} in hDAT-expressing cells. Before the experiments, IS was exchanged with DMEM media and cells settled for 25minues. Cells underwent exposure to 10µM DA, 5 µM Amph and 134mM K^+. GCamP6s is the brightest among the Ca^{2+} sensors, yielding a very large fluorescent signal ~5 fold over the baseline in average (Figure 6.7).
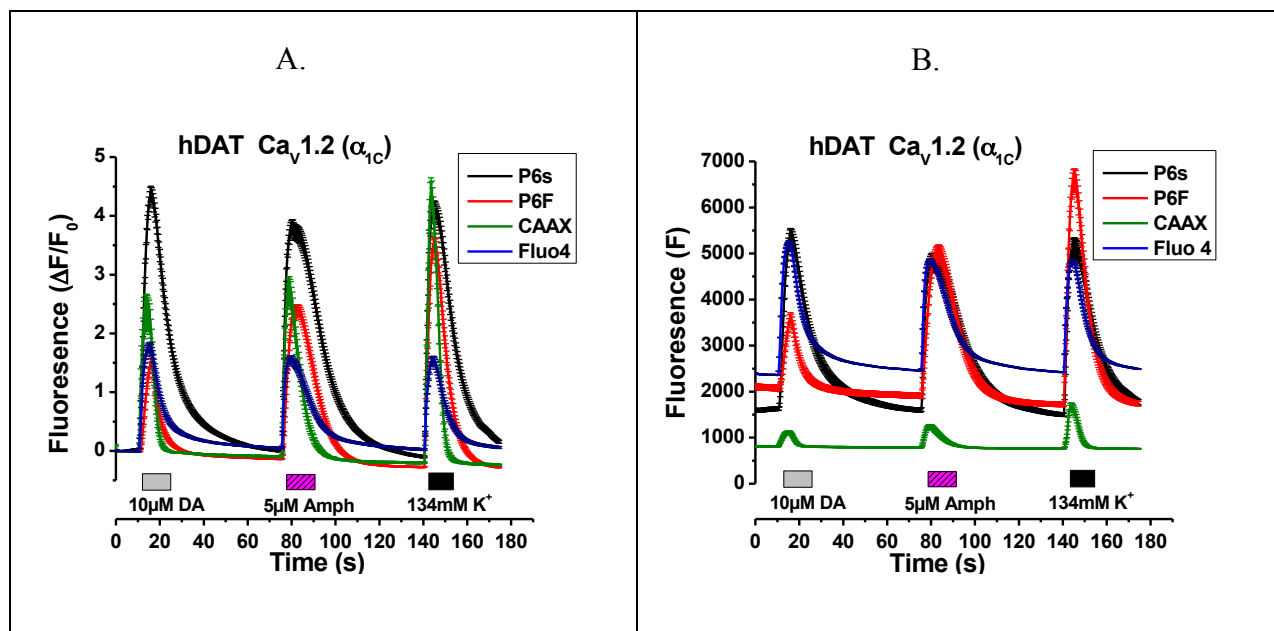
Fig. 6.7 Comparison of Ca^{2+} signals using single wavelength Ca^{2+} sensors (A) ΔF Fluorescence, (B) raw data. Either 10 μM dopamine or 5 μM S(+)Amphetamine induces Ca^{2+} signals in hDAT cells co-expressing Ca$_V$1.2 (no auxiliary subunits were included in the transfection mix).

Since GCaMP6's sensor yields robust Ca^{2+} signals after exposure to monoamine substrates and can be used in drug-profiling purposes we wanted to analyze how monoamine transporters affinities of drugs vary using this biosensor. To achieve that, we examined drugs previously tested using Fura-2. hDAT-expressing cells transfected with only pore α_{1C} subunit underwent exposure to different concentrations of Amph, yielding EC$_{50}$=0.31±0.02 μM (Figure 6.8). hSERT-expressing cells were transfected with α_{1C} and β subunits yielding EC$_{50}$=0.44±0.03 μM.

Figure 6.8: Ca²⁺ signals using GCamp6s. (A) Ca^{2+} signals in hDAT-expressing cells transfected with CaV and α_{1C}. (B) Dose response curve with EC50=0.31±0.02 μM (C) Ca^{2+} signals in hSERT-expressing cells transfected with CaV α_{1C} and β. (D) Dose response curve with EC50=0.44±0.03 μM.
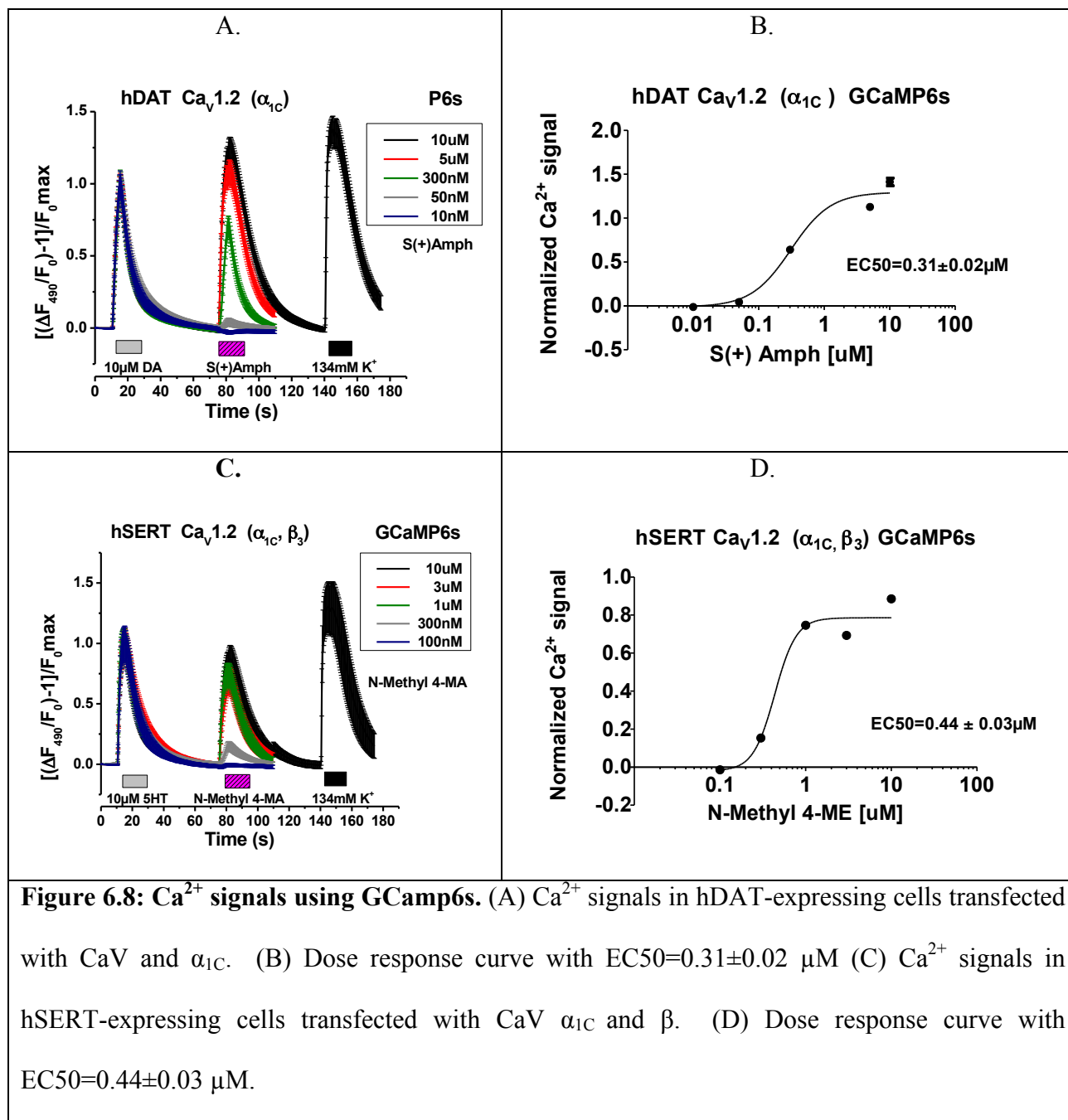
To induce calcium signals in hSERT-expressing cells using Fura-2, we had to transfect cells with α_{1C} and β auxiliary subunit (Figure 6.4). Interestingly, hSERT cells expressing only α_{1C} and GCaMP6 induced calcium signals when challenged with N-Methyl 4MA, although with lower potency (EC_{50}=1.1±0.1μM) (Figure 6.9), than hSERT expressing α_{1C} and β (EC50=0.4μM).
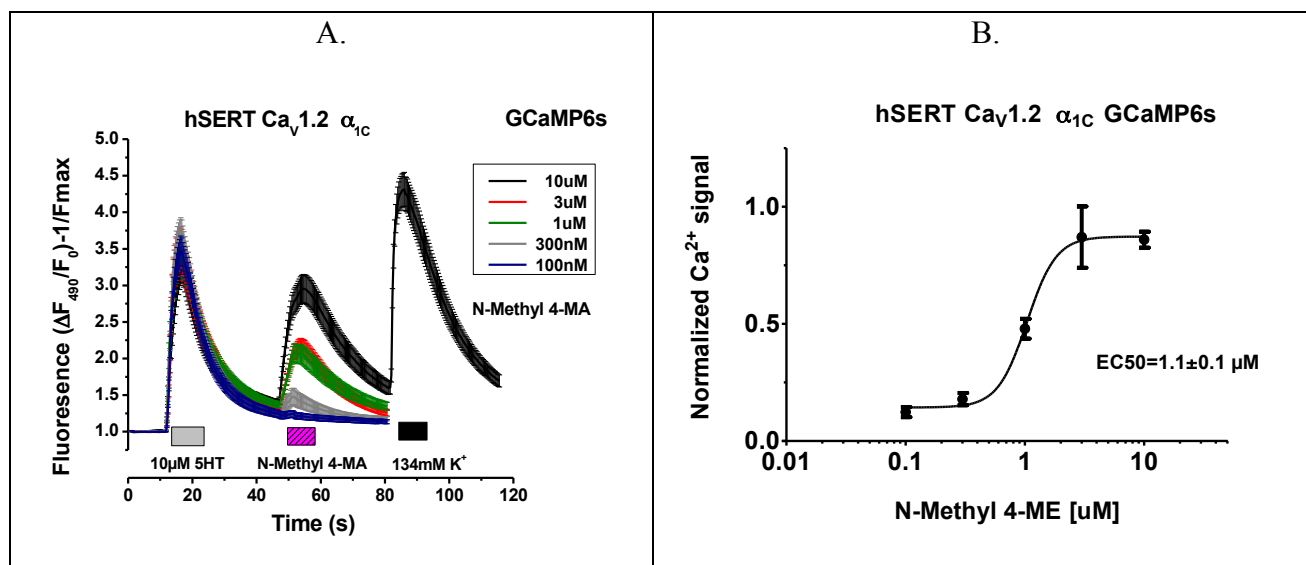
Figure 6.9: Ca^{2+} signals using GCamp6s in hSERT expressing cells transfected with α_{1C}. (A) Ca^{2+} signals in hSERT-expressing cells transfected with CaV and α_{1C}. (B) Dose response curve with EC50=1.1±0.1 μM.

	hDAT	hSERT	hDAT	hSERT
	Fura 2		P6s	
α_{1C}, β, $\alpha_2\delta$	0.12±0.01	0.43±0.03		
α_{1C}	0.19±0.01	-	0.31±0.02	1.1±0.1
α_{1C}, β		0.53±0.03		0.44±0.03

Figure 6.10: EC50 of Amph/4-Methyl 4-MA in Ca^{2+} signals in hDAT/hSERT -expressing cells transfected with varied auxiliary subunits. All data are presented in μM.

6.4   Flex Station as calcium mobilization assay technique in first approach for HTS

6.4.1   Ca^{2+} signals determined using either Fluo4 or GCamP6s in Flex Station plate reader.

To minimize the time of drug-profiling using Flex Station as Ca^{2+} mobilization assay, in which 96-well imaging plates were transfected either with hDAT or with hSERT-expressing cells. Cells were either loaded with Fluo-4 or transfected with calcium sensors GCaMP6s as indicated. The application of S(+)Amph (red traces) produced robust increase in fluorescence. Cells expressing GCaMP6s generated a much higher fluorescence signal when exposed to this substrate compared to cells loaded with Fluo 4 (Figure 6.11). GCaMP6s generated robust increase in fluorescence in hSERT-expressing cells (Figure 6.12) when cells were exposed to S(+)MDMA (green trace). Signal was completely blocked during application of hSERT blocker Fluoxetine (gray trace).
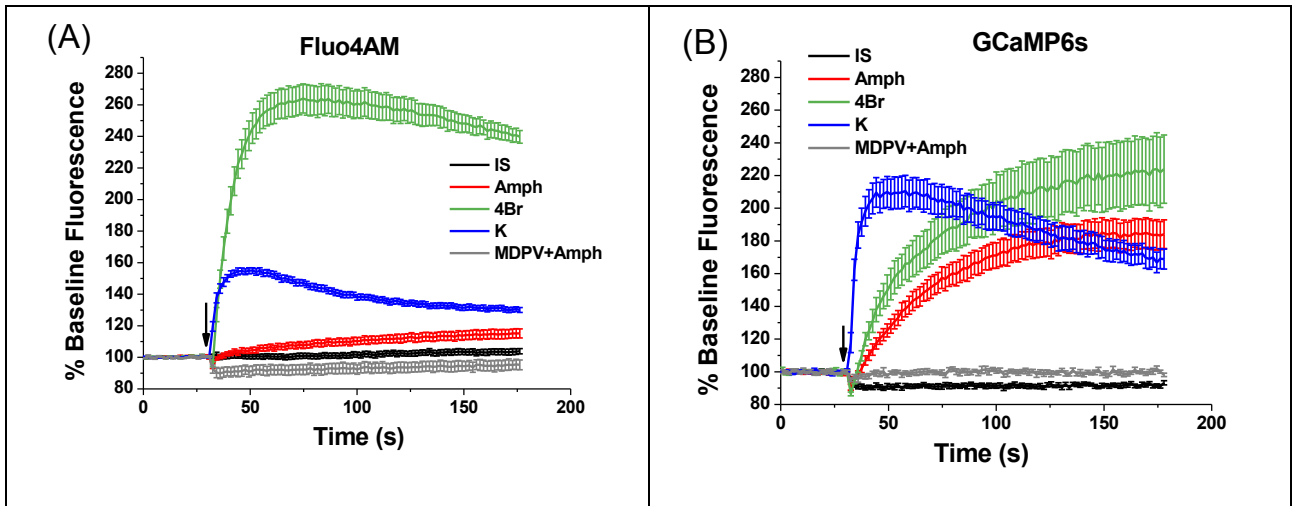
Figure 6.11: Substrates and blockers of the dopamine transporter are identified using the Flex Station 3 plate reader and the Ca^{2+} sensors Fluo-4AM (left) or GCaMP6s (right) Cells that permanently express hDAT were co-transfected with Ca$_V$1.2 (no auxiliary subunits) and GCamp6s coding plasmids, and were plated in a 96 well-imaging plates. Time-lapse of the fluorescent signal was acquired in a Flex Station 3; the injection of drugs in each well is indicated by the arrow. Control responses include IS (control imaging solution, black traces), 4Br-A23187 (Ca^{2+} ionophore, green traces), 90mM K$^+$ solutions (blue traces). The signal induced by the hDAT substrate S(+)AMPH (red trace) was blocked by pre-incubating the cells with MDPV (hDAT blocker, gray trace). Traces are plotted as mean ± SEM of n=6.
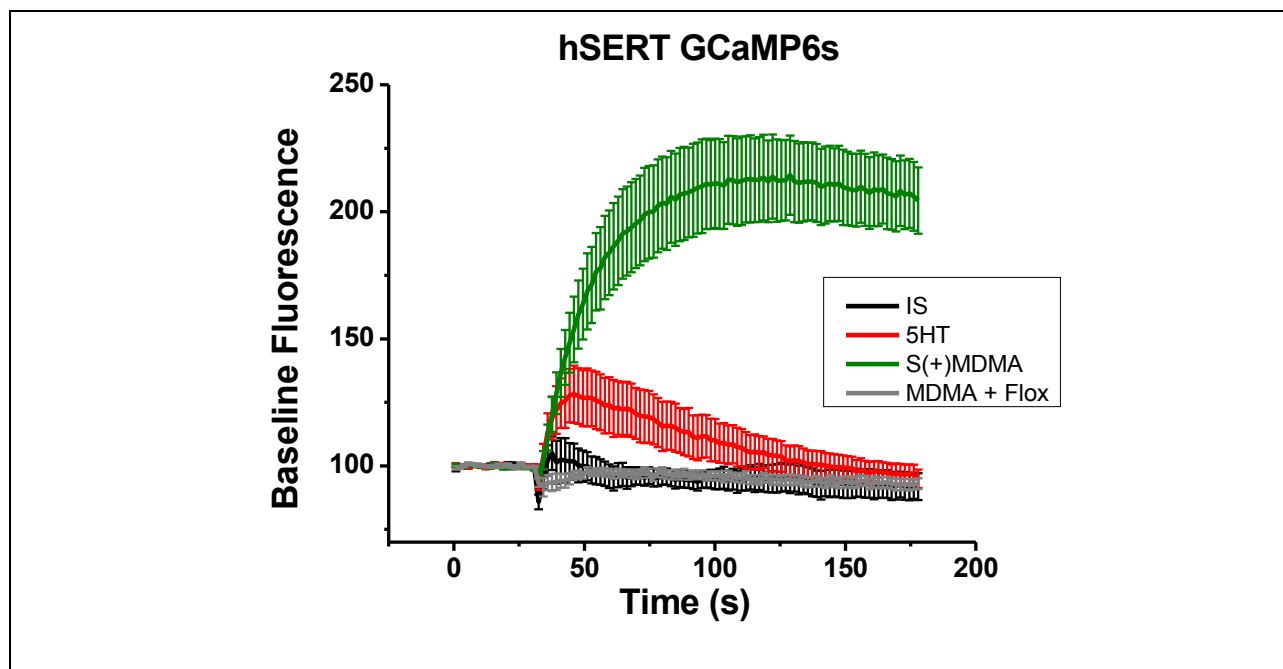
Figure 6.12: Substrates and blockers of the serotonin transporter are identified using Flex Station 3 plate reader. Cells that permanently express hSERT were co-transfected with $Ca_V1.2$ (α_{1C} and β) and GCamp6s coding plasmids, and were plated in a 96 well-imaging plate. Time-lapse of the fluorescent signal was acquired in a Flex Station 3; Control responses include IS (control imaging solution, black traces), The signal induced by the hSERT substrate S(+)MDMA (green trace) was blocked by pre-incubating the cells with Fluoxetine (hSERT blocker, grey trace). Traces are plotted as mean ± SEM of n=6.

6.4.2 Potencies of the drugs using FlexStation and epifluorescence microscopy technique

We wanted to characterize how different are the apparent potencies of drugs when calcium determinations are carried out using FlexStation or epifluorescence microscopy. An amphetamine analog (RAD-081) was tested using hDAT-expressing cells transfected with all Ca_V subunits using both assays. Dose-response curves are shown in Figure 6.13. Epifluorescence is a much more controlled assay where calcium response from the drug can be normalized to its own control

and single cell analysis is possible. In FlexStation such control is impossible to obtain since drugs are injected just once on the well and signals are collected from each well as a whole. EC_{50} acquired in FlexStation is about 5-fold higher than using epifluorescence microscopy.
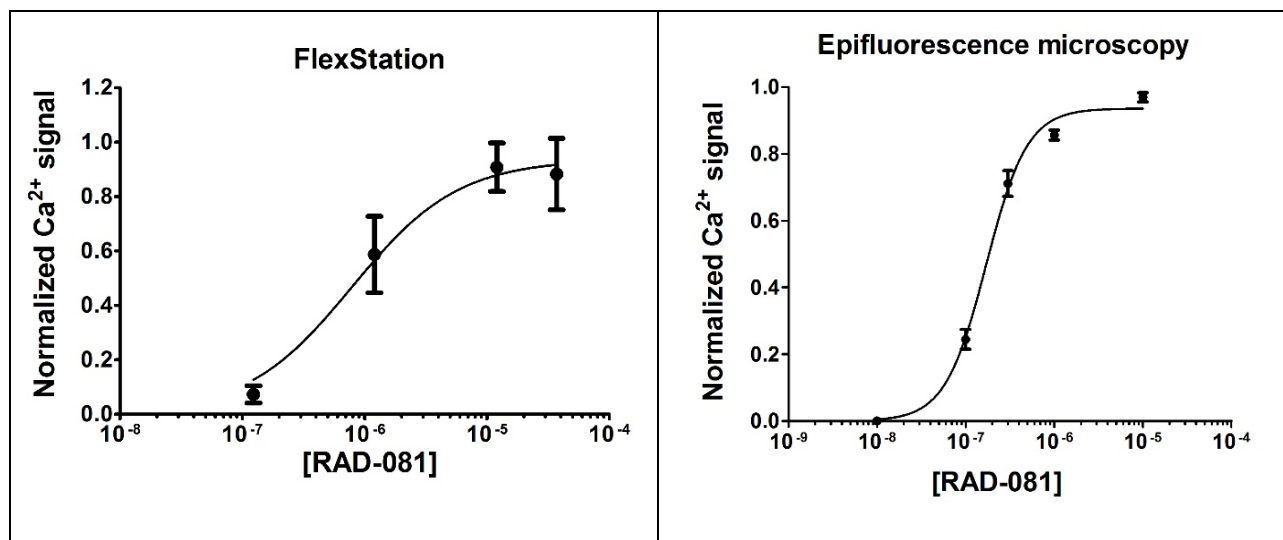
Figure 6.13: Dose-response curves of RAD-081 using FlexStation (left) and epifluorescence (right) measurement. hDAT cells were transfected with $Ca_V1.2$ (all subunits). Dose responses curves of RAD-081 were in FlexStation calcium mobilization assay and in epifluorescence microscope yielding EC_{50}=0.79 µM and 0.17µM, respectively.

Since the FlexStation calcium mobilization system is sensitive enough to acquire dose-response curves of compounds (substrates), we also wanted to extend our study to blockers of monoamine transporters. N-Ethyl 4-MA is blocker of intermediate potency on hDAT [94]. 10 µM N-Ethyl 4-MA strongly shifted the DA dose-response curve to the right (Figure 6.14B), this result clearly show that this method can be used to identify hDAT blockers.

A.

B.
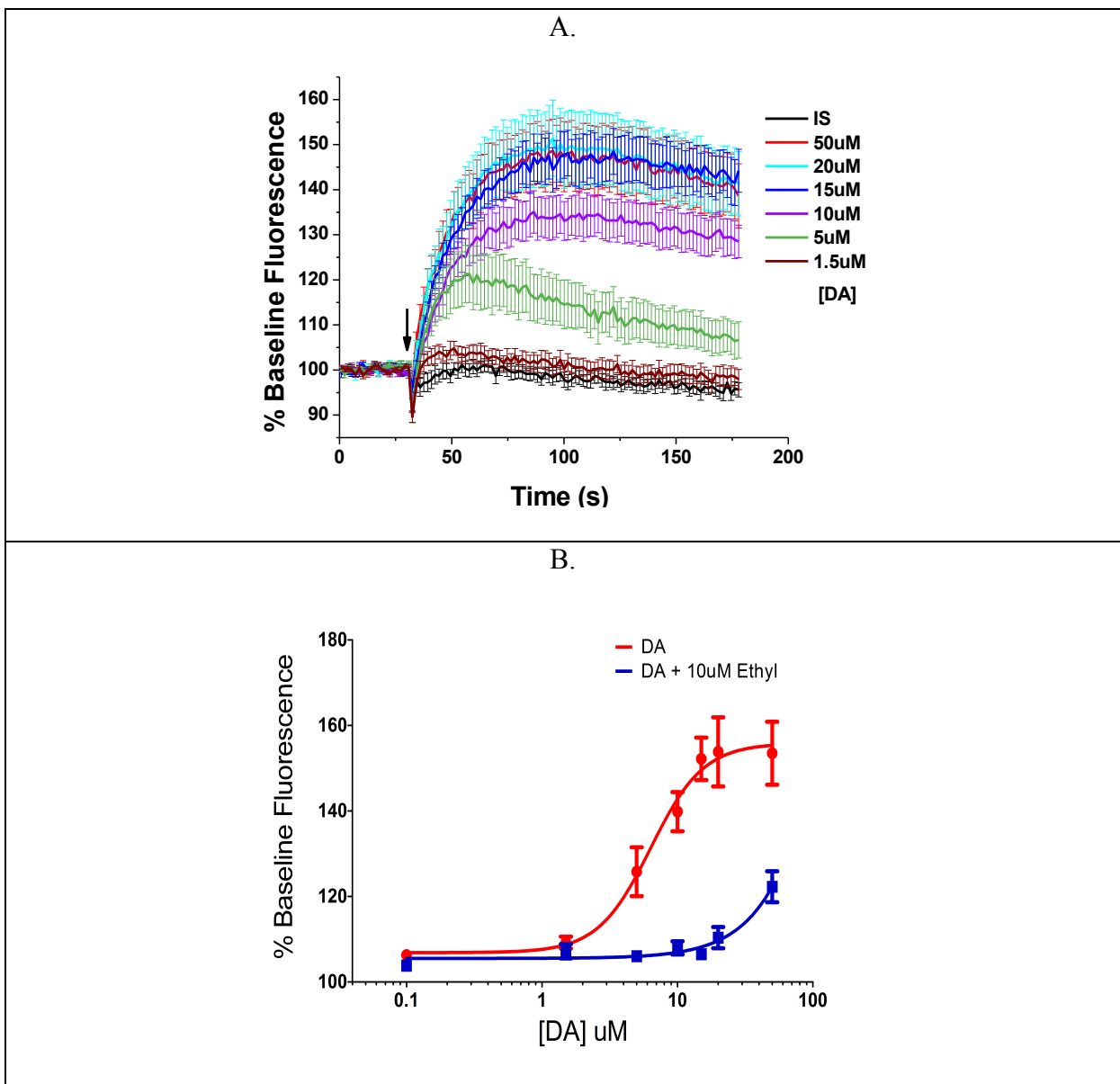
Figure 6.14: Identification of an hDAT blocker using Flex Station 3 plate reader. Cells that permanently express hDAT were co-transfected with $Ca_V1.2$ (no auxiliary subunits) and GCamp6s coding plasmids, and were plated in a 96 well-imaging plate. Time-lapse of the fluorescent signal was acquired in a Flex Station 3; the arrow indicates injection of drugs in each well. (A) DA dose dependence yield $EC_{50}=6.3\mu M \pm1.4$ (B) The red trace represents the signal of 12 control wells (DA alone). The blue trace shows 12 wells where DA (variable concentration) was injected in combination of $10\mu M$ *N*-Ethyl-4-MA. The traces shown are mean ± SEM of n=12.

6.5   Drugs screening using Flexstation

We tested 20 newly synthetized, non-scheduled phenylethylamines (listed below) that were provided by Dr. Richard Glennon (Medicinal Chemistry at VCU). Phenylethylamines are a large family of organic small molecules structurally related to catecholamines [98, 99]. Many of these compounds are active on monoamine transporters either as substrates or blockers.

1	RK-621	MW=227.73	5.1mg
2	RK-622	MW=333.21	5.7 mg
3	UMB-30	MW= 199.72	5.7mg
4	UMB-148	MW=297.90	6.3 mg
5	UMB-168	MW=287.48	5.4mg
6	UMB-178	MW=371.00	6.0mg
7	UMB-172	MW=453.53	5.2mg
8	UMB-201	MW=628.72	5.0mg
9	UMB-223	MW=615.00	6.1mg
10	UMB-208	MW=496.53	6.8mg
11	FTS-096	MW=185.65	5.5mg
12	RK-654	MW=307.86	5.3mg
13	UMB-198	MW=297.12	5.0mg
14	UMB-202	MW=306.31	5.4mg
15	UMB-209	MW=215.68	6.1mg
16	UMB-210	MW=215.68	6.5mg
17	UMB-321	MW=332.35	5.3mg
18	UMB-325	MW=332.35	5.5mg
19	UMB-328	MW=201.69	5.8mg
20	UMB-331	MW=327.37	5.2mg

The first approach was to test these drugs in FlexStation. FlexStation is a multi-well fluorometer plate reader with fully automated liquid transfer machinery to inject solution-containing drugs from compounds plate to each well of cells-containing plate. The emitted fluorescence light is directed to the photomultiplier where light emission intensity is digitalized and recorded. This machine can record time lapses with an acquisition frequency of ~1 Hz. FlexStation is operating using an 8-channel pipettor that transfers reagents into consecutive columns. In each column we run two controls – IS (row B) and either 20µM DA or 90mM K^+ (row A). Each drug was tested in two columns, where rows C-E in 1st column measured lower concentration of the drug ~10µM, and rows C-E in 2nd column measured high concentration of the drug ~50µM. If the tested drug is a substrate, it will increase the intracellular Ca^{2+} concentration and will produce a fluorescent signal. If the tested drug is a blocker, there will be no signal. Rows F-H measured the same concentration of the drug as C-D in each column, respectively but in the presence of 20µM DA. Using this approach, we can distinguish if a potential blocker does in fact interact with monoamine transporter. If the signal of drug + DA is smaller than DA alone, we can assume that the drug competed with DA, thus interacted with transporter (Figure 6.15). In wells F-H also test if the test drug is blocker but at higher concentration, this will detect weak blockers.

	1	2	3	4	5	6	7	8	9	10	11	12
A	DA	K	DA	K	DA	K	DA	K	DA	K	DA	K
B	IS	IS	IS	IS	IS	IS	IS	IS	IS	IS	IS	IS
C	10uM	50 uM										
D	10uM	50 uM										
E	10uM	50 uM										
F	10 +DA	50 +DA										
G	10 +DA	50 +DA										
H	10 +DA	50 +DA										

Figure 6.15: Schematic representation of compound plate with indicated drug-solutions. Each color (two columns) represents test of a one drug. Row A – 20μM DA (odd numbers column) or 90mM K^+ (even numbers column) control solution, row B – IS control solution, row C-D 10μM of tested drug (odd numbers column) and 50μM (even numbers column), row F-H 10μM drug +20μM DA (odd numbers column) and 50μM drug +20μM DA (even numbers column).

Summary of FlexStation data analysis is represented in Figure 6.16. Bar graphs represent Ca^{2+} fluorescence data normalized to DA signal. Each color denotes one drug. The 1st column of each graph is a signal acquired from the injection of 10μM drug, the 2nd column 10μM drug + 20μM DA, 3rd 50μM drug, 4th 50μM drug + 20μM DA. For drugs 7-20 all concentrations were increased by 20%.

Drugs that induce signals in column 1st and 3rd are potential substrates. Only Drug #3 and drug#11 induced calcium signals, whereas drug#3 was more potent than drug#11. All the rest of the tested drugs were potential blockers with different efficacies. To validate the outcomes we tested these compounds using epifluorescence microscopy as a secondary screening tool.
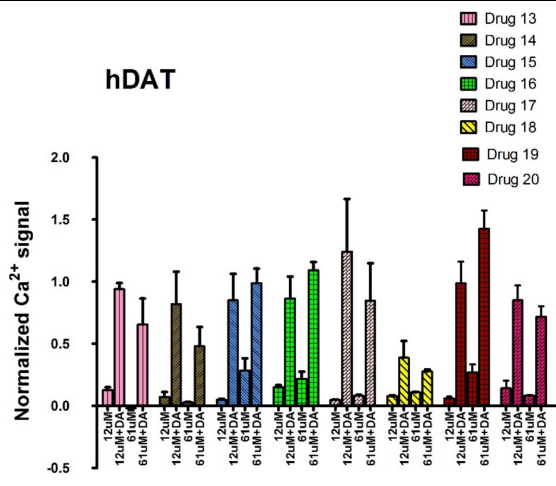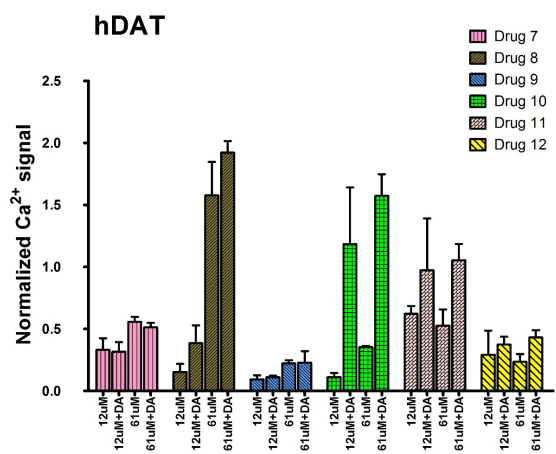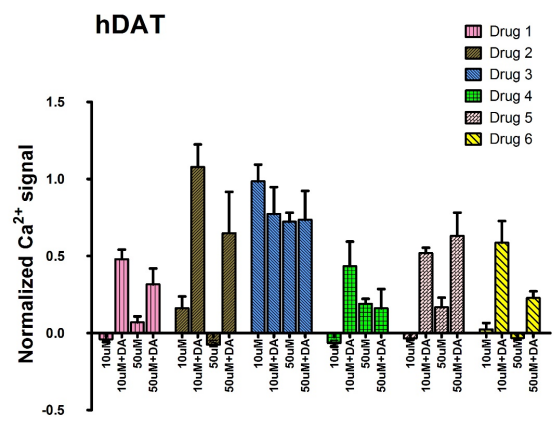
Figure 6.16: Normalized Ca²⁺ fluorescence signal induced by tested dugs in hDAT-expressing cells using GCaMP6s in Flex Station. Mean ± SEM signals were normalized to 20µM DA.

6.6   Secondary drug test in epifluorescence microscope

Protocol for validating drugs using epifluorescence microscopy is shown in Figure 6.17
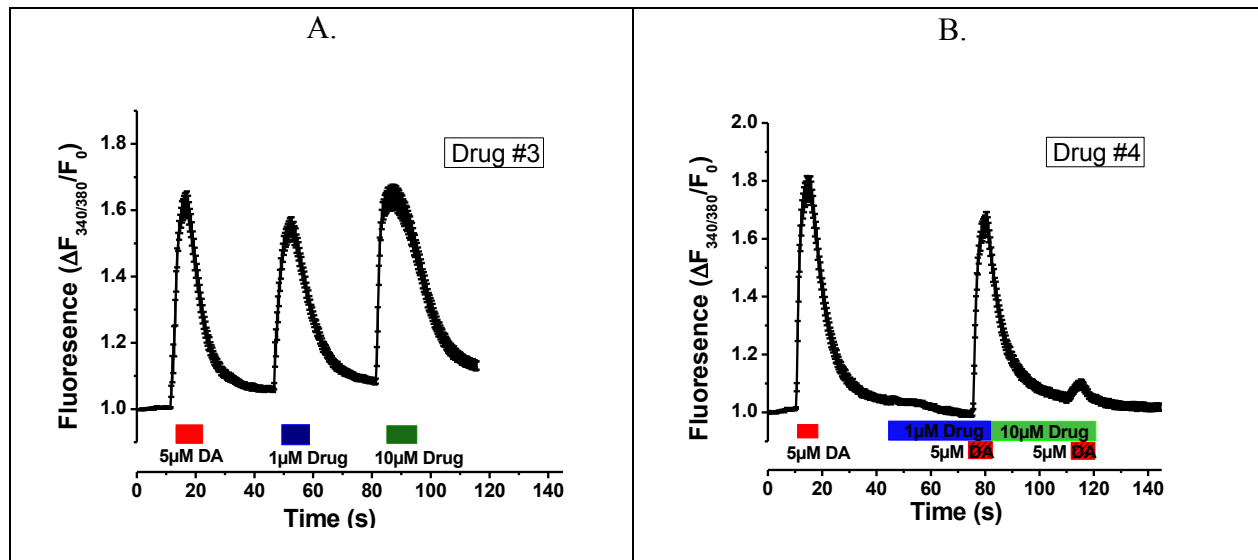
Figure 6.17: Substrate protocol (A) and blocker protocol (B) of monoamine transporters using Ca^{2+} imaging. Cells co-expressing hDAT and Ca$_V$1.2 were loaded with Fura2 and the Ca signals were determined by epifluorescence microscopy. Potential substrates were exposed to control 5µM DA (first Ca^{2+} peak) during 5 sec and subsequent concentrations of the tested drug: 1µM and 10µM with 30 sec wash between were applied as depicted in the figure timeline. For blockers, cells were exposed to pulses of 5µM DA (5sec) in the absence or presence of 1µM and 10µM of the drug as indicated in the figure timeline.

6.6.1 Study the effect of 20 new phenylalkylamines on hSERT and hDAT

hDAT and hSERT- expressing cells underwent blocker or substrate protocol shown in Figure 6.17. We analyzed potential substrate data by dividing the peak signal of the tested drugs at 1μM or 10μM concentration by the control signal (5μM DA for hDAT cells and 5μM 5HT for hSERT cells). Summary of the finding are shown in Figure 6.18. All the bars represent the normalized Ca^{2+} signals. In case of substrates, Ca^{2+} signals were induced by the drugs and to differentiate them from blockers they are arbitrarily represented as bars of negative values in Figure 6.18. The larger the bar the better efficacy of the drug. In case of blockers (shown as positive values), Ca^{2+} signal was induced by the control compound (either DA or 5HT) in combination with tested drug. Bars' values closer to 1 represent drugs that did not undergo competition with DA (or very weak competitors), thus smaller the bar the better the blocker.
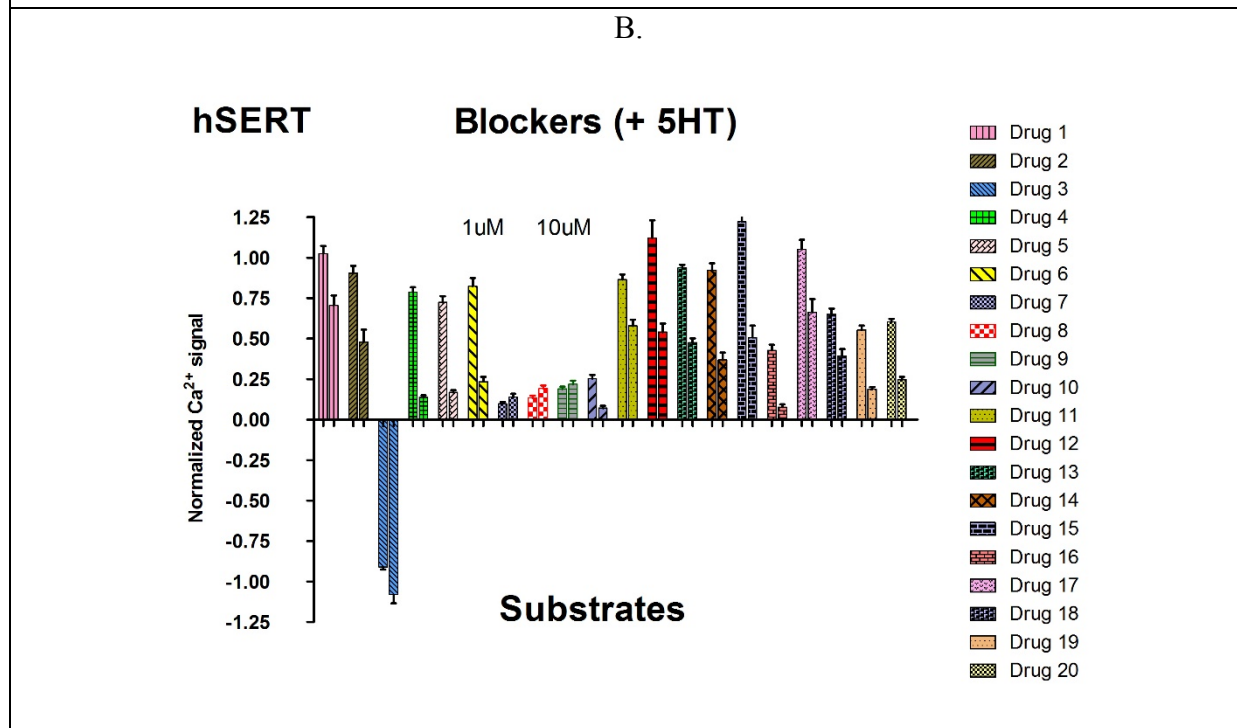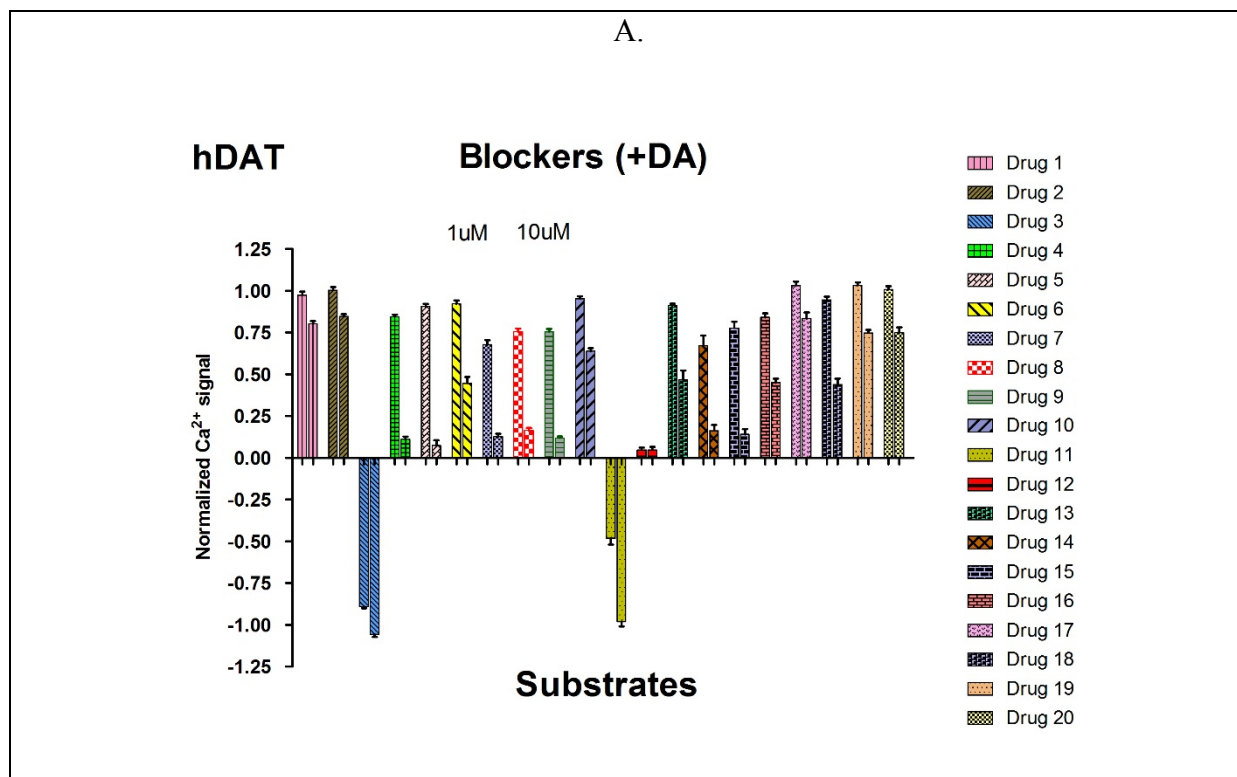
Figure 6.18: Normalized Ca²⁺ signals in hDAT (A) and hSERT (B) expressing cells. Each color represents effect of one drug, first and second bar correspond to signal induced by 1μM and 10μM respectively. For substrates, bars represent Ca²⁺ signals achieved after applying drug (depicted arbitrarily as negative values). For blockers bars represents the remaining Ca²⁺ signals of a control substrate (DA and 5HT for hDAT and hSERT expressing cells, respectively) in the presence of the test drug (depicted as positive values) mean ± SEM, n ≥6.

To make better comparison of the drugs from Figure 6.18, Figure 6.19 represents the same data but in terms of potencies of the drugs. Weak blockers and weak substrates shows values close to zero, (e.g. Drug #2 on hDAT), while strong blockers or substrate are represented by values close to one (e.g. Drug #7 on hSERT or Drug #11 on hDAT).

		hDAT		hSERT	
		1uM	10uM	1uM	10uM
1	RK-621	0.03	0.2	0.03	0.3
2	RK-622	0	0.15	0.1	0.52
3	UMB-30	0.89	1.06	0.91	1.08
4	UMB-148	0.16	0.89	0.21	0.86
5	UMB-168	0.09	0.93	0.28	0.83
6	UMB-178	0.08	0.55	0.18	0.77
7	UMB-172	0.32	0.87	0.9	0.86
8	UMB-201	0.25	0.84	0.87	0.81
9	UMB-223	0.25	0.88	0.81	0.78
10	UMB-208	0.05	0.36	0.75	0.93
11	FTS-096	0.48	0.98	0.14	0.42
12	RK-654	0.95	0.95	0.12	0.46
13	UMB-198	0.09	0.53	0.06	0.52
14	UMB-202	0.33	0.84	0.08	0.63
15	UMB-209	0.22	0.86	0.22	0.49
16	UMB-210	0.16	0.55	0.57	0.92
17	UMB-321	0.03	0.17	0.05	0.34
18	UMB-325	0.06	0.56	0.35	0.61
19	UMB-328	0.03	0.25	0.45	0.81
20	UMB-331	0.01	0.25	0.4	0.75
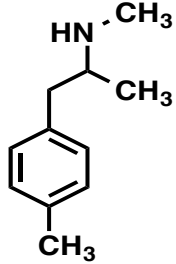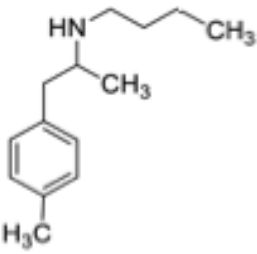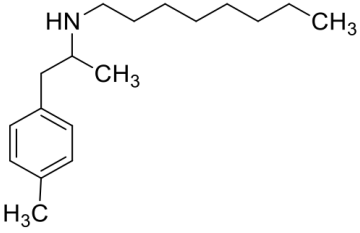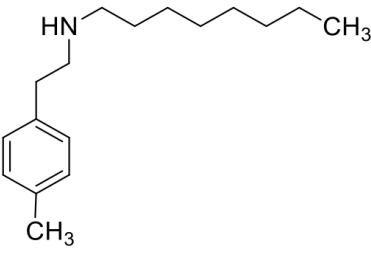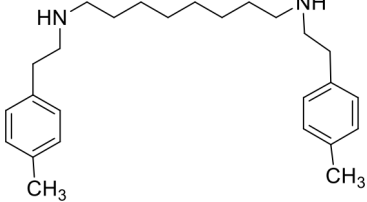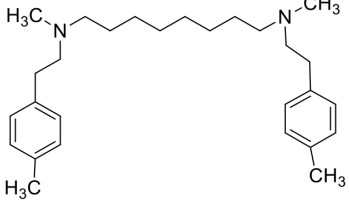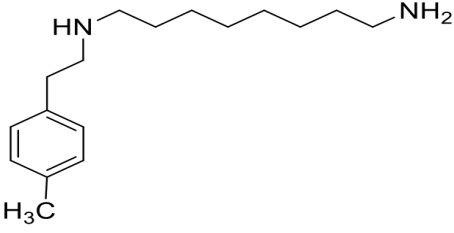
Substrate	Blocker: At 10uM blocks completely (or almost completely) 5uM DA signal	Blocker: At 1uM blocks completely (or almost completely) 5uM DA signal	Weak Blocker

Figure 6.19: Values indicate normalized potencies of the tested drugs.

Structure of the few drugs that we found the most interesting, are shown below:

3. UMB-030 (N-methyl 4-MA)	N-butyl 4-MA
4.UMB148 (N-octyl 4-MA)	5. UMB 168 (N-octyl 4-Methyl PEA)
7. UMB 172	9.UMB-223

10. UMB 208

There are few characteristics of these drugs. N-methyl 4-MA is a DAT substrate with a $EC_{50} \sim 200nM$ range [94]. Increasing the length of the N-alkyl chain only by one methyl group (N-ethyl) makes the drug a blocker with IC_{50} about 4uM in the Ca^{2+} assay. Subsequent addition of another methyl group (N-propyl) increases the IC_{50} value 4 times. N-butyl further decreases potency 3.3 times. Following this pattern, we could extrapolate that additional lengthening the chain would decrease the affinity 12 fold for N-octyl 4-MA to about 720uM. Surprisingly N-octyl 4-MA (Drug #4) affinity on DAT is in range of 1-10μM, where 10μM completely blocks the signal. This inverted U shape behavior suggests that additional binding moieties are potentiating the bind of the elongated compounds. For hSERT-expressing cells increasing the length of the N-alkyl from N-methyl to N-propyl decreases the substrate EC_{50} from about 500nM to 2μMwhile N-butyl 4MA was very weak on SERT [94]. Increasing the length of chain to 8 (Drug #4) make the drug a SERT blocker with IC_{50} ranging from 1-10μM, where 1uM blocks the signal in 20% and 10μM by 100%. The only difference between Drug #4 and Drug #5 is additional methyl group in alpha carbon position of N-octyl 4-MA. This modification does not change affinities on hDAT nor hSERT. Adding an amine group at the end of the N-alkyl chain of Drug #5 yields Drug #10. This drug shows decreased affinity on hDAT making it a very weak blocker. On the contrary, the same amine group (Drug #10) profoundly increased affinity on hSERT almost 3 times in comparison with Drug #5 (1μM of Drug #5 blocks 30% of the signal, while Drug#10 blocks 75% of the signal at 1μM).

Bivalent compounds (such as Drug #7 or Drug #9) derived from monovalent drug (Drug #10) increase affinity on hDAT about 2 times (when comparing blockage of the signal at 10μM). On hSERT, bivalent compounds (Drug #7 and Drug #9) block the signal in 90% already at 1μM, and are stronger than the monovalent counterpart (Drug #10) that blocks 75% at 1μM.

7. Chapter seven- discussion

HYPOTHESIS 1: Monoamine transporters substrates indirectly activates voltage gated Ca^{2+} channels

Most if not all transporters forming the SLC6 gene family show substrate-induced inward ionic currents when challenged near rest. In particular, for monoamine neurotransmitter transporters, such as the electoneutral serotonin transporter or the electrogenic dopamine and norepinephrine transporters, the charge measured during substrate flux exceeds by several fold what is predicted by their transport rate and stoichiometry [70, 74, 100-102]. Single channel events have been described in monoamine neurotransmitter transporters, mimicking bona fide ion channels. The study of the 5HT-induced current I_{5HT} of the serotonin transporter at the single channel level reveals that Na^{+} is the main carrier [101]; conversely, though Cl^{-} is not the main carrier it can influence the channel opening rate [101]. Single channel recording in dopaminergic neurons from *C. elegans* showed that Cl^{-} is permeated through the dopamine transporter [74], moreover dopamine transporter currents carried by Cl^{-} ions are implicated in increasing excitability in midbrain dopaminergic neurons [76]. We measured an increase of Na^{+} permeability induced by 5HT in agreement with Petersen and DeFelice for *Drosophila* SERT [92], or by S(+)MDMA in cells expressing hSERT (Fig. 4.2). Similar increase in Na^{+} was reported previously in cells expressing the dopamine transporter exposed to amphetamine [103]. Interestingly, when hSERT-expressing cells are exposed to S(+)MDMA, the Na^{+} reaches higher levels than when exposed to 5HT (Fig. 4.2). The set point of Na^{+} at rest is given by the equilibrium between Na^{+} influx and efflux as described in the boundary theorem discussed for Ca^{2+} but which also applies to Na^{+} [104]. Since there is no evidence of changes in Na^{+} efflux when cells are exposed to hSERT substrates, we studied I_{5HT} and $I_{MDMA,}$ which is a measure of

67

Na$^+$ influx. Long I$_{5HT}$ and I$_{MDMA}$ recordings (50 s) showed that the initial amplitudes of both currents are identical (Fig. 5.2D), but I$_{5HT}$ undergoes inactivation that is less pronounced in I$_{MDMA}$ (Fig. 5.2D). It is possible that the progressive accumulation of the transported 5HT in the cytosol may decrease I$_{5HT}$ over time [105]; in addition, the concomitant increase of internal Na$^+$ may result in hSERT-mediated 5HT efflux [106, 107], decreasing the hSERT-mediated Na$^+$ influx. This could explains the weaker increase of intracellular Na$^+$ concentration induced by 5HT when compared to S(+)MDMA. The return of the signal to baseline during hSERT substrate wash out is much slower for S(+)MDMA than for 5HT (Fig. 5.2D). This kinetic difference could be explained by a slower repolarization for S(+)MDMA than for 5HT after wash as a result of a persistent current in the absence of substrate described for amphetamine and amphetamine analogs as previously reported by Dr. DeFelice's group [108-110].

Monoamine neurotransmitter transporters coexist with Ca^{2+} channels, a variety of Cl$^-$ and K$^+$ channels, receptors, and other transporters in excitable cells. Since the relative proportions of monoamine transporters to other current inducing membrane proteins are likely to be highly variable among cell types, it is impossible to predict if the substrate-induced current will be sufficient to significantly depolarize native cells. For instance K$^+$ conductance activated by autoreceptors (GIRK channels) [111] [112], TASK channels [113] and Ca^{2+} -activated K$^+$ conductance [114] would oppose and neutralize the depolarization evoked by monoamine transporters current. Case specific studies are required to establish resting membrane potential changes upon monoamine transporter activation. Nevertheless, dopamine-, amphetamine- and methamphetamine-induced DAT current increases action potential firing frequency in dopaminergic neurons from the midbrain [76] [78], demonstrating that the depolarization evoked by DAT activation modulates excitability in native cells. In addition, it has been shown that dopamine induces cytosolic Ca^{2+} signals in cultured neurons from midbrain, cortex and hippocampus and using pharmacological tools the authors suggest that monoamine

transporter-mediated depolarization could activate voltage-gated Ca^{2+} channels [79].

In the present work, we hypothesize that the depolarization evoked by hSERT activation is sufficient to activate voltage-gated Ca^{2+} channels. As a proof of concept, we tested this hypothesis in a controlled environment such as the one provided by the heterologous expression systems described in this study. In particular, we focused our study in the lower-threshold L-type Ca^{2+} channels, $Ca_V1.3$, because it is expressed in serotonergic and dopaminergic neurons and has been shown to modulate some aspects of their function. SERT is expressed broadly through the cell bodies and along neurite extensions in cultured serotonergic neurons. In addition, SERT is expressed in both serotonergic fibers and cells bodies of the raphe nucleus in the brain [115] [116]. $Ca_V1.3$ is also present in the dorsal raphe nucleus and is involved in the AMPA-mediated dendritic serotonin release in serotonergic neurons [117], which is implicated in depression [118, 119]; thus altogether these data suggest that SERT and $Ca_V1.3$ may co-localize in the soma and dendrites of serotonergic neurons. In dopaminergic neurons, by means of its voltage dependence characteristics, $Ca_V1.3$ drives pace making and bursts of electrical activity [120]. In addition, $Ca_V1.3$ activity is implicated in selective death of dopaminergic neurons in the substantia nigra in Parkinson's disease [121]. $Ca_V1.3$ has ∼30 mV left shift in the peak current–voltage curve compared to the high-voltage-activated Ca^{2+} channel, $Ca_V2.2$ (Fig. 5.3). The threshold of activation that we measured for CaV1.3 is about −50 mV when 5mM external Ca^{2+} is used as the charge carrier (Fig. 5.3), similar to that found by others [93] [122]. When we co-expressed either $Ca_V1.3$ or $Ca_V2.2$ with hSERT in HEK239T cells, both 5HT and S(+)MDMA evoked clear activation of $Ca_V1.3$ (Fig. 5.4 C) but not of $Ca_V2.2$ (Fig. 5.4 B) despite that, both types of cells showed convincing Ca^{2+} signals induced by strong K^+-depolarization (Fig. 5.4 B and C).

Since over-expression of hSERT due to transient transfection could undermine the physiological relevance of our findings, the expression of hSERT was reduced using the Flp-In expression system, which inserts a single copy of hSERT cDNA into the cell's genome, by

targeted recombination. This procedure decreased hSERT activity by 60% when compared to transiently transfected HEK cells (Fig. 5.5 A). Despite the significant reduction in hSERT expression, the Flp-In cells showed robust coupling between hSERT activity and $Ca_V1.3$ opening. Moreover, concentrations as low as 100 nM are sufficient to induce Ca^{2+} signals implying that a relatively low number of transporters would depolarize the membrane sufficiently to activate $Ca_V1.3$ channels (Fig. 5.5 B and C). Accordingly, 5HT showed comparable potency for inducing its own transport and for activating $Ca_V1.3$-mediated Ca^{2+} signals, implying that the electrical coupling between hSERT and Ca_V channels can coexist with 5HT transport in a physiological range of 5HT concentrations.

As mentioned above, one consequence of $Ca_V1.3$ activation is the increase of action potential firing in excitable cells such as dopaminergic neurons [120]. Although the participation of $Ca_V1.3$ has not been previously implicated, it was suggested that substrate-induced currents mediated by DAT produce bursts of electrical activity in midbrain dopaminergic neurons [76] and Ca^{2+} currents may be implicated in DA release mechanisms. Therefore, the electrical coupling between a monoamine transporter and $Ca_V1.3$ described in the present study supports the hypothesis that monoamine transporter-mediated modulation of cell excitability requires $Ca_V1.3$ activation. Further research effort is needed to assess this new hypothesis, which is beyond the scope of the present study. The trans-activation of Ca^{2+} channels by the monoamine trans-porters demonstrated in our models illustrates a new mechanism by which endogenous substrates (neurotransmitters) or artificial substrates (amphetamine-related agents) could modulate excitability and signaling mechanisms directed by the rise of intra-cellular Ca^{2+} in excitable cells.

HYPOTHESIS 2: Electrical coupling between Ca^{2+} channels and monoamine transports can discriminate substrates and blockers of the transporters

The Ca^{2+} assay described here can generate dose-response curves of drugs that interact with monoamine transporters [94, 123] [89]. This new method is based on the electrical properties of monoamine transporters; the inward current induced by substrates of transporters can depolarize the plasma membrane and activate voltage-gated channels. The indirect opening of Ca^{2+} channels induced by substrates of monoamine transporters generate tight-coupled Ca^{2+} signals that can be used to identify unclassified substrates. Although blockers do not generate inward current and produce no Ca^{2+} signal, they still can be identified by inhibiting a Ca^{2+} signal induced by a known substrate (Fig. 6.1).

Neurotransmitter uptake and release studies in synaptosomes, is a well-accepted technique to identify and discriminate between substrates and blockers of monoamine transporters [51]. When the same set of drugs were tested using the new Ca^{2+} assay and compared to the outcomes using synaptosomes, the results of both techniques were highly correlated. The EC_{50} for several substrates on DAT, NET and SERT showed a coefficient correlation R=0.96 among these techniques [94]. Similarly, IC_{50} testing several blockers on the three transporters yield a perfect correlation, R=1.00.

Although the study of the release potential of test drugs using the synaptosomes method is used to distinguish between substrates and blockers of MATs, one problematic aspect of these experiments is that some potent uptake inhibitors can produce low-efficacy efflux of radiolabeled pre-loaded drugs (e.g. $[^3H]MPP^+$) [124]. Still it is not clear whether drugs that produce partial release that were discovered using the synaptosome are actually substrates of transporters. When partial releasers were evaluated in the Ca^{2+} assay and TEVC, these compounds do not generate inward current, suggesting that partial releasers are actually blockers. One possible explanation

71

for these discrepancies is that partial releasers may induce slower transitions of the transporters that may not be fast enough to generate inward current. This is possible taking into account that the synaptosome experiments are performed in a time scale in the tens of minutes, whereas the electrophysiological determinations are done in few seconds. These results clearly suggest that substrates and blockers of MATs are not part of binary states, and can be rather depicted as a continuum where it is possible to find compounds with intermediate behavior.

Since synaptosomes are isolated from brain tissue, the type of transporter studied is restricted to the origin of this tissue, in most cases the experiments are performed in rat synaptosomes. Studies show that species from which monoamine transporters come from can change interaction of drugs and transporters. Most prominent examples are different effects of cocaine on drosophila and human dopamine transporters [125] and higher sensitivity of inhibitors on human SERT than on chicken SERT [126]. The Ca^{2+} method described here has the advantage that transporters from any origin can be used. In all the experiments performed here, we used the human variant of the transporters. In addition, mutations of transporters can also be expressed to study interactions between drugs and specific transporters' residues. Additionally, Ca^{2+} assay can provide drug profiling on all three monoamine transporter tasks that, although is possible to perform using synaptosomes, is largely restricted in TEVC technique when hDAT, hNET and hSERT are meant to be expressed in Xenopus laevis oocytes. While only hSERT can be expressed efficiently in oocytes, hDAT shows expression variability and hNET is not expressed at all [127]. Thus, the Ca^{2+} technique described here provides a reliable mechanism to study the electrophysiological signature of drugs on the three transporters.

In summary, Ca^{2+} assay can help overcome some obstacles found in synaptosome and TEVC assays and can be used either as substitution of these techniques or as source of additional information about the electrophysiological signature of tested drugs and it constitutes a new quantitative analysis of substrate/blocker drug profiles on monoamine transporters.

Our next proposed approach was to strategize rapid evaluation of drug-effect profiles at monoamine transporters. Monoamine transporters are primary targets for drugs of abuse and also drugs used in treatment of mental diseases. Often, the correlation between these two groups lies in the affinity and selectivity of the drug on the transporters. Current methods to evaluate the activity profile of drugs on monoamine transporters are too slow to efficiently proliferate drug development. Synaptosome release assay, although helpful in distinguishing blockers and substrates, has low screening throughput, is laborious and time consuming, also since it uses the neuronal membrane it requires usage of agents that block effects of tested drugs on other targets. Another approach, such as TEVC in frog oocytes-expressing MATs, although measuring direct effect of drugs on monoamine transporters is not appropriate for rapid screening. Other technique suitable for high throughput screening, for instance the competition of high affinity radiolabeled MAT blockers has some limitations. It can oversight the identification of relevant substrates that normally have lower affinity than blockers on transporters. Newer approaches use fluorescent substrates able to mimic neurotransmitter interactions with transporters that are being uptaken into the cells resulting in increase of intracellular fluorescence. One of the techniques employ fluorescent substrate ASP^+ (4-(4-(dimethylamino)styrl)-N-methylpyridinium) that was developed later for microplate-based high-throughput screening for hSERT function [128]. Measuring ASP^+ uptake as fluorescence non-isotopic tool to characterize monoamine transporter occurs being a practicable and reliable approach since data shows very similar results to those done by traditional radiometric uptake assays [129]. Studies show also novel fluorescence-based neurotransmitter transporter uptake assay kit that allows for examining transport activity of DAT, NET and SERT and characterizes compounds in a high-throughput [130]. Unlike the radiolabeling-based method, fluorescence substrates allow for real-time monitoring, direct visual assessment of preparation in 96/384/1536-wells as well as temperature- controlled fluorescence plate reader that also

73

allows for automated liquid dispensation. The use of fluorescent substrates, even though can identify and characterize the potency of drugs on monoamine transporters, can only test for uptake competitors where substrate/blocker discrimination is not possible [130]. In general terms, a big limitation of all competition HTS assays is that they cannot discriminate if test compounds are blockers or substrates of transporters, they can only identify monoamine transporters ligands. The new Ca^{2+} assay described here, is a fluorescence-based technique that is amendable for HTS and it can easily discriminate substrates from blockers of monoamine transporters in a matter of seconds. Initially our fist approach was to use epifluorescence microscopy in combination with a temperature-controlled automatic perfusion system to profile drugs with high precision. In an effort to further improve this approach, we implemented several optimization steps, plus the use of FlexStation 3 plate reader to increase the rate of drug testing and as preliminary approach toward optimization for HTS.

To distinguish whether FlexStation is faster than epifluorescence microscopy we are providing the approximate time required for performing experiments in each assay (see the table below). When comparing the time required to perform one-session experiment (from preparing the plate to analysis) FlexStation assay is 2.8 times faster than epifluorescence microscope (569min/202min). When comparing the number of wells from which data were acquired during that time, FlexStation assay allows for examining 2.6 more wells than epifluorescence microscope (96well/36wells). Overall, taking to account all the steps, assessing one well in FlexStation takes approximately 2 minutes (202min/96wells), while in epifluorescence microscope almost 16 minutes (569min/36wells), so using the FlexStation technique improves time efficiency 8 times.

Time	Epifluorescence microscope	FlexStation
Preparation of the plate – coating	Coating <u>36 wells</u> with Matrigel – 5min + 20 min incubation = 25min	Coating <u>96 wells</u> with Collagen – 5 min + 25 min incubation in RT, suction of the solution and drying: 15min min, wash with PBS, drying 15min = 1h
Plating the cells	4min	7min
Preparation for the experiment	Loading the cells with Fura 2 + IS, each column has to be done separately, waiting 25 min at 37ºC = 30min	Changing solution from DMEM to IS = 5min
Preparation of the drugs solutions	30min	30min
Acquiring data	36 wells- 6h manual handling	96wells- 40min, FlexStation work
Analysis	Picking the cells' ROI + analysis using temple – 2h	Analysis using temple – 1h
Total time	25+4+30+30+6*60+2*60 = 569min~9.5h (this is for 36 wells)	60+7+5+30+40+60 = 202min~3.4h (this is for 96 wells)

When the same monoamine transporter ligands are tested using the epifluorescence microscope or the FlexStation, the potencies to generate Ca^{2+} signals differ significantly among techniques. A good example is the amphetamine analog RAD-081 that showed EC_{50} of 0.17μM and 0.79μM when tested using epifluorescence microscopy or the FlexStation, respectively. Similarly, dopamine yielded EC_{50} of 0.92 μM (microscopy) [123] compared to 6.4μM (Flex Station). In general, potencies to generate Ca^{2+} signals differ between both techniques about 5 to 10 times. One important aspect that could account for this difference is the diffusion time of the test drug to encounter the cells. We should consider that in epifluorescence microscopy cells undergo constant perfusion, and the perfusion outlet is placed very near cells; thus passive diffusion of drug particles to encounter cells is not a limiting step. In the FlexStation, the drugs are not subjected to perfusion or agitation, the only external forces that drive particle motion are: the injection of 80μl of concentrated sample to the well containing in 50μl of physiological solution, and the passive diffusion of the drug into the solution to equilibrate the final concentration in the well. The difference in speed of how cells encounter particles of the test drug between these two techniques is evident from the kinetics to generate Ca^{2+} signals (dose response acquire in epifluorescence microscope show much steeper curve as shown in Fig. 6.8 A, in comparison to the FlexStation date in Fig. 6.9 B). Of course, the depolarization of the plasma membrane, that is what drives the opening of the Ca^{2+} channel, is proportional to the number of transporters activated by the substrate in each moment. Thus, it is expected that the diffusional effect in FlexStation will decrease the depolarization induced by a theoretical concentration of drug because drug particles take more time to encounter the cells compared to perfused cells. This would explain the right shift in the apparent EC_{50} in FlexStation compared to the fluorescent microscopy assays.

The other possible explanation for the differences in apparent potencies in FlexStation vs. epifluorescence microscopy is related to how the signals are acquired in both techniques. In

FlexStation the Ca^{2+} signal is obtained from the whole well by a photomultiplier, while in the epifluorescence microscope Ca^{2+} increase is acquired by an Electron-Multiplying Charge-Coupled Device (EMCCD) camera that gives 2D information where the response of each individual cell can be analyzed. In the case of the epifluorescence microscopy, only cells that were transfected and responded to a control (e.g. DA in the case of cells expressing hDAT) were picked for analysis. Quality standards are taken into consideration for each individual cell analyzed, such as low resting Ca^{2+} level and the absence of Ca^{2+} waves or cell detachments during the experiment. This way, it can be assured that the Ca^{2+} signals included in the analysis are a result of the experiment and not an experimental artifact. In FlexStation, such a control cannot be achieved, since the Ca^{2+} signal is measured in a well as a whole. It is possible, that in some wells over-crowdedness and cell detachments may produce Ca^{2+} oscillations that may add to the overall signal and contributing in some extent to the variability of the data.

Another factor that may explain the shift of the EC_{50} between these two methods is differences in the limit of detection of the detectors. Although unlikely, if the photomultiplier has less sensitivity than the EMCCD camera to detect the fluorescence signal, responses at lower concentrations will be penalized in the FlexStation, explaining the right shift in the EC_{50} values.

One of the important features of the Ca^{2+} assay described in this work is that it can discriminate between substrates and blockers of monoamine transporters. When the outcomes of this technique using both approaches (FlexStation and the fluorescence microscope) were compared, in almost all cases drugs that showed an interaction on the transporter in the FlexStation (as either substrate or blocker) corresponded to the effect observed in the fluorescence microscope (Fig. 6.15 and 6.18). Some drugs like Drug #8 UMB-201 show some differences, in epifluorescence microscopy, this drug show features of a moderate blocker that blocks 85% of a DA signal at 10µM concentration. On the other hand, FlexStation data show that this drug is a substrate at 61µM. In this case, a closer look at the protocol in each of the techniques has to be

taken into consideration. FlexStation measures Ca^{2+} signal for a much longer time than epifluorescence microscope. In the epifluorescence microscope the exposure of the drug takes place within 5sec for substrates and 30 sec for blockers, while in FlexStation cells undergo exposure of a drug for about 2min. To test the possibility that this drug could induce Ca^{2+} signals, further studies involving long exposure of this drug to the cells must be conducted in epifluorescence microscopy. Overall, although FlexStation has some disadvantages, it can definitely be used as a first approach to distinguish between substrates and blockers of monoamine transporters.

In an effort to optimize the output of the signal in the FlexStation several Ca^{2+} sensors were evaluated by comparing three parameters: (1) the dynamic range of the signal, defined as the maximal fluorescence minus the basal fluorescence upon stimulation with saturating concentration of positive standard, (e.g. amphetamine for hDAT-expressing cells); (2) sensitivity, defined as the maximal slope in the dose response curve; (3) signal to noise ratio, defined as the dynamic range divided by the standard deviation of the reading. A standard Ca^{2+} sensor, Fluo-4 was compared to the ultrabright genetically encoded Ca^{2+}-sensing fluorescent proteins. Ca^{2+} dyes with different affinities for Ca^{2+} have been used broadly for studying intracellular Ca^{2+} signals in excitable cells. Neuronal Ca^{2+} signals that are characterized by a sometimes fast Ca^{2+} dynamic and low amplitude [131] require ultrasensitive and fast Ca^{2+} indicators. Fluorescence studies done in rat hippocampal neurons provide insight into sensitivity, dynamic rage and kinetics of GCaMPs. Using mutagenesis, improved versions of GCaMPs have been described along the years.

As we saw in Fig. 6.6 GCaMP6s (K_d=144nM with dynamic range (F_{max}/F_{min})=63.2±3.1 and K_{off}=1.12 s^{-1}) has robust Ca^{2+} signal and the widest dynamic range among all the dyes that were tested. The potency of a known substrate to generate Ca^{2+} signals using GCamP6s or Fura-2 as Ca^{2+} indicators was very similar, thus, GCamP6s can be used as a surrogate of Fura-2

to test potency of drugs on transporters. One disadvantage of GCamP6s is that, because its high affinity to Ca^{2+}, the signal can be easily saturated and the efficacy of drugs could not be resolved properly.

For the type of studies that predict low vs. high efficacy of the drugs, GCaMPf (K_d=375nM, dynamic range F_{max}/F_{min} = 52, K_{off}=3.9 s^{-1}) [95] can be used. It has fast kinetics, which produce robust Ca^{2+} signals but due to the fast binding and unbinding properties has a lower saturation range. Since the higher affinity dye GCaMP6s will saturates more easily than the lower affinity dye GCaMP6f, choosing between these two dyes might work to resolve efficacies of compounds that produce different levels of depolarization, which was shown on the example of DA and Amph signals in Fig. 6.6. What is also worth mentioning, GCaMPCAAX – the brightest version of GCaMP but tethered to the membrane, shows a very low dynamic range (Fig. 6.6). One possibility is that these proteins might be expressed in the lower amount due to more complex protein sorting mechanisms to the plasma membrane.

Detection of drugs that interact with monoamine transporters using Ca^{2+} channels is novel methodology and can be used in drug discovery. Although the primary reason to develop our method was to study the pharmacology of monoamine transporters, it is possible to use this methodology to study any membrane protein that induces an inward current. One example can be serotonin-gated 5-HT$_3$ receptor, present in the central and peripheral nervous system. This ligand-gating ion channel regulates mood and appetite, and drugs that interact with this receptor are used for treatment of depression [132]. Most importantly, 5-HT$_3$ agonists play a crucial role in suppressing vomiting side effects induced by chemotherapy and radiotherapy, thus discovering selective agonist for 5-HT$_3$ has been a great interest in cancer drug discovery research [133]. Activation of 5-HT$_3$ enhances the release of few neurotransmitters such as dopamine, cholecystokinin and GABA [134]. It was shown that this cation-selective channel [135] causes neuronal depolarization and excitatory response in neurons [136] since current is carried

mostly by sodium and potassium ions [137]. Application of 3μM 5-HT, tested in isolated rat nodose ganglion neurons, induced inward current that ranged from 40-60pA [138].

Another membrane protein, which pharmacology could be explored using our method is Organic Anion Transporter (OAT). This transporter plays a crucial role in renal function [139] . It was shown that OAT plays a role in hepatic uptake of 5-HT, while xenobiotics can alter 5-HT elimination [140]. Electrophysiological studies show that Para Aminohippuric Acid (PAH), a typical substrate of OAT [141], induces an inward current. The most common method to evaluate substrates for these transporters is using radiolabeled PAH competition assay. However, these studies cannot prove if the tested compound is translocated. One of the first methods to test translocation of substrates was electrophysiological study [142] where substrate-induced currents were conducted to distinguish structure/function relationship of the OAT. Increase of membrane conductance in flounder Renal Organic Anion Transporter (fROAT) expressing oocytes were proportional to net charges translocated though fROAT. Current clamp experiment performed in oocytes expressing fROAT showed a small depolarization of 4mV induced by 100uM PAH from a resting potential of -40mV. Holding potential at -60mV in voltage clamp investigation showed inward current of 23nA after applying PAH [142]. Even such small currents can be detected in our Ca^{2+} epifluorescence microscopy method, since currents of comparable amplitude are recorded in oocytes expressing monoamine transporters. Ca^{2+} assay would be a great tool in expanding the pharmacology of mentioned protein where their activity is linked to membrane depolarization.

New Psychoactive Substances (NPS) are substances that imitate already existing drugs of abuse, such as MDMA or cannabis. [143] They are manufactured as new "legal" substances and can be purchased online hence earning name "legal high". They are divided into 4 categories: stimulants, cannabinoids, hallucinogens and depressants. In Europe, the European Monitoring Center of Drugs and Drug Addiction monitor over 560 NPS compounds; stimulant and

synthetic cannabinoids are the most popular and cause the highest clinical encounter. Legislations regarding NPS differ in each country. In the UK, it is now illegal to sell of distribute them while possession is not. The only information about the effect on NPS comes from case reports and case series. One example of NPS is 4-Methylamphetamine (4-MA) stimulant and appetite suppressant [144] that also causes fatal intoxication [145]. From a pharmacological point of view, it is a nonselective transporter substrate with affinities equal 44nM, 22nM and 53nM on DAT, NET and SERT respectively [146]. Recent studies investigated the effect of 4-MA analogs where amine group was substituted with longer (up to 4 carbon) side chain [94]: N-methyl, N-ethyl, N-propyl and N-butyl. The studies showed few interesting findings regarding increasing the length of the N-alkyl chain first – it decreases inhibitory potencies on monoamine transporters, second – loss substrate activity on DAT (N-alkyl chain greater than N-methyl group) and NET (N-alkyl chain greater than N-ethyl group) causing loss of rewarding effect of these compounds. The compound with the longest studied chain N-butyl was a very weak substrate at SERT and a very weak blocker at DAT according to TEVC data. In Ca^{2+} assay (hSERT) N-butyl 4-MA behaved also as a weak substrate with a potency too small to be clearly determined, while on hDAT the IC_{50} was about 60µM [94]. What can be concluded from these findings is that increasing the N-alkyl side chain on 4-MA weakens the effect on DAT and SERT. Surprisingly one of the compound that we tested, Drug #4 (N-octyl 4-MA) (Fig. 6.19) with 8-carbon length, showed resuscitated blocker activity on DAT and SERT with IC50~5uM (where 10µM drug blocks 100% of the signal). Furthermore, additional bivalent drug (Drug #7) derived from monovalent drug (Drug#10) increases affinity on DAT about 5 times when comparing blockage of the signal at 10uM. One of the explanations might be simultaneous binding to multiple sites on monoamine transporters.

It has been shown that designing bivalent compounds produces selective opioid, serotonin and muscarinic receptor ligands with one order of magnitude higher affinity compared to its monovalent parent ligand [147] [148] [149]. This phenomenon cannot simply be explained by increasing concentrations of monovalent ligand but rather can be understood in the thermodynamic energy landscape of the ligand-protein interaction. In this system cooperative binding of the ligand that is tethered to the additional ligand lower the entropy of the ligand/protein complex. [150] Also, in relation to monoamine transporters creating bivalent pentamethyl spacer-linker yield 2300-fold higher inhibition activity [151]. Another study showed that two phenyltropane moieties with 6-8 carbon linker are a potent inhibitor of DAT [152]. Furthermore, two substrate-like phenylalkylamine linked by an aliphatic spacer achieved up to 82-fold gain in inhibition of [^{3}H] CFT binding compared with monovalent equivalent. Modeling and docking studies of the most potent bivalent ligands confirmed two discrete substrate-binding domains [153]. To test the possibility that our tested drug indeed binds to two binding sites, or that one site plays a role of allosteric modulator, further studies involving mutagenesis have to be conducted.

REFERENCES

1.	World Health Organization., *Neuroscience of psychoactive substance use and dependence*. 2004, Geneva: World Health Organization. xx, 264 p.

2.	Vetulani, J., *Drug addiction. Part I. Psychoactive substances in the past and presence.* Pol J Pharmacol, 2001. **53**(3): p. 201-14.

3.	Merlin, M.D. *Archaeological evidence for the tradition of psychoactive plant use in the old world*. 2003 [cited 19-06-2017 17:13 UTC.

4.	Michelot, D. and L.M. Melendez-Howell, *Amanita muscaria: chemistry, biology, toxicology, and ethnomycology*. Mycol Res, 2003. **107**(Pt 2): p. 131-46.

5.	Nutt, D., et al., *Development of a rational scale to assess the harm of drugs of potential misuse.* Lancet, 2007. **369**(9566): p. 1047-53.

6.	Pattinson, K.T., *Opioids and the control of respiration.* Br J Anaesth, 2008. **100**(6): p. 747-58.

7.	Paparelli, A., et al., *Drug-induced psychosis: how to avoid star gazing in schizophrenia research by looking at more obvious sources of light.* Front Behav Neurosci, 2011. **5**: p. 1.

8.	UNODC, *Global illicit drug trends 2003*. 2003, New York: United Nations.

9.	Favrod-Coune, T. and B. Broers, *The Health Effect of Psychostimulants: A Literature Review.* Pharmaceuticals (Basel), 2010. **3**(7): p. 2333-2361.

10.	Koob, G.F. and N.D. Volkow, *Neurocircuitry of addiction.* Neuropsychopharmacology, 2010. **35**(1): p. 217-38.

11.	Tzschentke, T.M. and W.J. Schmidt, *Functional relationship among medial prefrontal cortex, nucleus accumbens, and ventral tegmental area in locomotion and reward.* Crit Rev Neurobiol, 2000. **14**(2): p. 131-42.

12.	Bidwell, L.C., F.J. McClernon, and S.H. Kollins, *Cognitive enhancers for the treatment*

of ADHD. Pharmacol Biochem Behav, 2011. **99**(2): p. 262-74.

13.   Ikemoto, S., *Brain reward circuitry beyond the mesolimbic dopamine system: a neurobiological theory.* Neurosci Biobehav Rev, 2010. **35**(2): p. 129-50.

14.   Koob, G.F. and M. Le Moal, *Plasticity of reward neurocircuitry and the 'dark side' of drug addiction.* Nat Neurosci, 2005. **8**(11): p. 1442-4.

15.   Chinta, S.J. and J.K. Andersen, *Dopaminergic neurons.* Int J Biochem Cell Biol, 2005. **37**(5): p. 942-6.

16.   Fleckenstein, A.E., et al., *New insights into the mechanism of action of amphetamines.* Annu Rev Pharmacol Toxicol, 2007. **47**: p. 681-98.

17.   Howell, L.L. and H.L. Kimmel, *Monoamine transporters and psychostimulant addiction.* Biochem Pharmacol, 2008. **75**(1): p. 196-217.

18.   Volkow, N.D., G.F. Koob, and A.T. McLellan, *Neurobiologic Advances from the Brain Disease Model of Addiction.* N Engl J Med, 2016. **374**(4): p. 363-71.

19.   Mohammad-Zadeh, L.F., L. Moses, and S.M. Gwaltney-Brant, *Serotonin: a review.* J Vet Pharmacol Ther, 2008. **31**(3): p. 187-99.

20.   Jacobs, B.L. and E.C. Azmitia, *Structure and function of the brain serotonin system.* Physiol Rev, 1992. **72**(1): p. 165-229.

21.   Sara, S.J., *Locus Coeruleus in time with the making of memories.* Curr Opin Neurobiol, 2015. **35**: p. 87-94.

22.   Rothman, R.B. and M.H. Baumann, *Monoamine transporters and psychostimulant drugs.* Eur J Pharmacol, 2003. **479**(1-3): p. 23-40.

23.   Kristensen, A.S., et al., *SLC6 neurotransmitter transporters: structure, function, and regulation.* Pharmacol Rev, 2011. **63**(3): p. 585-640.

24.   Hertting, G. and J. Axelrod, *Fate of tritiated noradrenaline at the sympathetic nerve-endings.* Nature, 1961. **192**: p. 172-3.

25. Iversen, L.L., *Role of transmitter uptake mechanisms in synaptic neurotransmission.* Br J Pharmacol, 1971. **41**(4): p. 571-91.

26. Kim, H.J., et al., *Imaging and quantitation of dopamine transporters with iodine-123-IPT in normal and Parkinson's disease subjects.* J Nucl Med, 1997. **38**(11): p. 1703-11.

27. Malison, R.T., et al., *[123I]beta-CIT SPECT imaging of striatal dopamine transporter binding in Tourette's disorder.* Am J Psychiatry, 1995. **152**(9): p. 1359-61.

28. Laasonen-Balk, T., et al., *Striatal dopamine transporter density in major depression.* Psychopharmacology (Berl), 1999. **144**(3): p. 282-5.

29. Dougherty, D.D., et al., *Dopamine transporter density in patients with attention deficit hyperactivity disorder.* Lancet, 1999. **354**(9196): p. 2132-3.

30. Ciccarone, D., *Stimulant abuse: pharmacology, cocaine, methamphetamine, treatment, attempts at pharmacotherapy.* Prim Care, 2011. **38**(1): p. 41-58, v-vi.

31. Robertson, S.D., H.J. Matthies, and A. Galli, *A closer look at amphetamine-induced reverse transport and trafficking of the dopamine and norepinephrine transporters.* Mol Neurobiol, 2009. **39**(2): p. 73-80.

32. Rudnick, G. and J. Clark, *From synapse to vesicle: the reuptake and storage of biogenic amine neurotransmitters.* Biochim Biophys Acta, 1993. **1144**(3): p. 249-63.

33. Torres, G.E., R.R. Gainetdinov, and M.G. Caron, *Plasma membrane monoamine transporters: structure, regulation and function.* Nat Rev Neurosci, 2003. **4**(1): p. 13-25.

34. Gillman, P.K., *Tricyclic antidepressant pharmacology and therapeutic drug interactions updated.* Br J Pharmacol, 2007. **151**(6): p. 737-48.

35. Mandrioli, R., et al., *Selective serotonin reuptake inhibitors (SSRIs): therapeutic drug monitoring and pharmacological interactions.* Curr Med Chem, 2012. **19**(12): p. 1846-63.

36. Benfield, P., R.C. Heel, and S.P. Lewis, *Fluoxetine. A review of its pharmacodynamic and*

pharmacokinetic properties, and therapeutic efficacy in depressive illness. Drugs, 1986. **32**(6): p. 481-508.

37.   Matthews, P.R., *Efficacy of antidepressants: similar but different.* Int J Neuropsychopharmacol, 2011. **14**(10): p. 1433-4; author reply 1435-7.

38.   Brambilla, P., et al., *Side-effect profile of fluoxetine in comparison with other SSRIs, tricyclic and newer antidepressants: a meta-analysis of clinical trial data.* Pharmacopsychiatry, 2005. **38**(2): p. 69-77.

39.   Fuchs, T., et al., *Neurofeedback treatment for attention-deficit/hyperactivity disorder in children: a comparison with methylphenidate.* Appl Psychophysiol Biofeedback, 2003. **28**(1): p. 1-12.

40.   Lakhan, S.E. and A. Kirchgessner, *Prescription stimulants in individuals with and without attention deficit hyperactivity disorder: misuse, cognitive impact, and adverse effects.* Brain Behav, 2012. **2**(5): p. 661-77.

41.   Bachi, K., et al., *Vascular disease in cocaine addiction.* Atherosclerosis, 2017. **262**: p. 154-162.

42.   Sordo, L., et al., *Cocaine use and risk of stroke: a systematic review.* Drug Alcohol Depend, 2014. **142**: p. 1-13.

43.   Cadet, J.L., et al., *Neurotoxicity of substituted amphetamines: molecular and cellular mechanisms.* Neurotox Res, 2007. **11**(3-4): p. 183-202.

44.   Brown, J.M. and B.K. Yamamoto, *Effects of amphetamines on mitochondrial function: role of free radicals and oxidative stress.* Pharmacol Ther, 2003. **99**(1): p. 45-53.

45.   Fleckenstein, A.E., et al., *Interaction between hyperthermia and oxygen radical formation in the 5-hydroxytryptaminergic response to a single methamphetamine administration.* J Pharmacol Exp Ther, 1997. **283**(1): p. 281-5.

46.   Silva, A.P., et al., *Brain injury associated with widely abused amphetamines:*

neuroinflammation, neurogenesis and blood-brain barrier. Curr Drug Abuse Rev, 2010. **3**(4): p. 239-54.

47.   Hotchkiss, A.J., M.E. Morgan, and J.W. Gibb, *The long-term effects of multiple doses of methamphetamine on neostriatal tryptophan hydroxylase, tyrosine hydroxylase, choline acetyltransferase and glutamate decarboxylase activities.* Life Sci, 1979. **25**(16): p. 1373-8.

48.   Villemagne, V., et al., *Brain dopamine neurotoxicity in baboons treated with doses of methamphetamine comparable to those recreationally abused by humans: evidence from [11C]WIN-35,428 positron emission tomography studies and direct in vitro determinations.* J Neurosci, 1998. **18**(1): p. 419-27.

49.   Frey, K., M. Kilbourn, and T. Robinson, *Reduced striatal vesicular monoamine transporters after neurotoxic but not after behaviorally-sensitizing doses of methamphetamine.* Eur J Pharmacol, 1997. **334**(2-3): p. 273-9.

50.   Axt, K.J. and M.E. Molliver, *Immunocytochemical evidence for methamphetamine-induced serotonergic axon loss in the rat brain.* Synapse, 1991. **9**(4): p. 302-13.

51.   Baumann, M.H., et al., *The designer methcathinone analogs, mephedrone and methylone, are substrates for monoamine transporters in brain tissue.* Neuropsychopharmacology, 2012. **37**(5): p. 1192-203.

52.   Glatz, A.C., et al., *Inhibition of cocaine self-administration by fluoxetine or D-fenfluramine combined with phentermine.* Pharmacol Biochem Behav, 2002. **71**(1-2): p. 197-204.

53.   Glowa, J.R., et al., *Phentermine/fenfluramine decreases cocaine self-administration in rhesus monkeys.* Neuroreport, 1997. **8**(6): p. 1347-51.

54.   Rothman, R.B., et al., *Amphetamine-type central nervous system stimulants release norepinephrine more potently than they release dopamine and serotonin.* Synapse, 2001. **39**(1): p. 32-41.

55.   Munzar, P., R. Nosal, and S.R. Goldberg, *Potentiation of the discriminative-*

stimulus effects of methamphetamine by the histamine H3 receptor antagonist thioperamide in rats. Eur J Pharmacol, 1998. **363**(2-3): p. 93-101.

56.   Ricaurte, G.A., et al., *Amphetamine treatment similar to that used in the treatment of adult attention-deficit/hyperactivity disorder damages dopaminergic nerve endings in the striatum of adult nonhuman primates.* J Pharmacol Exp Ther, 2005. **315**(1): p. 91-8.

57.   Rothman, R.B., et al., *Neurochemical neutralization of methamphetamine with high-affinity nonselective inhibitors of biogenic amine transporters: a pharmacological strategy for treating stimulant abuse.* Synapse, 2000. **35**(3): p. 222-7.

58.   Gu, X.H., et al., *Design, synthesis, and monoamine transporter binding site affinities of methoxy derivatives of indatraline.* J Med Chem, 2000. **43**(25): p. 4868-76.

59.   Rothman, R.B., et al., *Aminorex, fenfluramine, and chlorphentermine are serotonin transporter substrates. Implications for primary pulmonary hypertension.* Circulation, 1999. **100**(8): p. 869-75.

60.   Kitayama, S., et al., *Dopamine transporter site-directed mutations differentially alter substrate transport and cocaine binding.* Proc Natl Acad Sci U S A, 1992. **89**(16): p. 7782-5.

61.   Xu, C., L.L. Coffey, and M.E. Reith, *Binding domains for blockers and substrates on the dopamine transporter in rat striatal membranes studied by protection against N-ethylmaleimide-induced reduction of [3H]WIN 35,428 binding.* Naunyn Schmiedebergs Arch Pharmacol, 1997. **355**(1): p. 64-73.

62.   Whittaker, V.P., I.A. Michaelson, and R.J. Kirkland, *The separation of synaptic vesicles from nerve-ending particles ('synaptosomes').* Biochem J, 1964. **90**(2): p. 293-303.

63.   Han, D.D. and H.H. Gu, *Comparison of the monoamine transporters from human and mouse in their sensitivities to psychostimulant drugs.* BMC Pharmacol, 2006. **6**: p. 6.

64.   Carlezon, W.A., Jr. and E.H. Chartoff, *Intracranial self-stimulation (ICSS) in rodents to study the neurobiology of motivation.* Nat Protoc, 2007. **2**(11): p. 2987-95.

65.   Negus, S.S. and L.L. Miller, *Intracranial self-stimulation to evaluate abuse potential of drugs.* Pharmacol Rev, 2014. **66**(3): p. 869-917.

66.   Bonano, J.S., et al., *Abuse-related and abuse-limiting effects of methcathinone and the synthetic "bath salts" cathinone analogs methylenedioxypyrovalerone (MDPV), methylone and mephedrone on intracranial self-stimulation in rats.* Psychopharmacology (Berl), 2014. **231**(1): p. 199-207.

67.   Bauer, C.T., et al., *Use of intracranial self-stimulation to evaluate abuse-related and abuse-limiting effects of monoamine releasers in rats.* Br J Pharmacol, 2013. **168**(4): p. 850-62.

68.   Amara, S.G. and M.J. Kuhar, *Neurotransmitter transporters: recent progress.* Annu Rev Neurosci, 1993. **16**: p. 73-93.

69.   Gu, H.H., S. Wall, and G. Rudnick, *Ion coupling stoichiometry for the norepinephrine transporter in membrane vesicles from stably transfected cells.* J Biol Chem, 1996. **271**(12): p. 6911-6.

70.   Mager, S., et al., *Conducting states of a mammalian serotonin transporter.* Neuron, 1994. **12**(4): p. 845-59.

71.   Galli, A., et al., *Sodium-dependent norepinephrine-induced currents in norepinephrine-transporter-transfected HEK-293 cells blocked by cocaine and antidepressants.* J Exp Biol, 1995. **198**(Pt 10): p. 2197-212.

72.   Sonders, M.S., et al., *Multiple ionic conductances of the human dopamine transporter: the actions of dopamine and psychostimulants.* J Neurosci, 1997. **17**(3): p. 960-74.

73.   Galli, A., R.D. Blakely, and L.J. DeFelice, *Norepinephrine transporters have channel modes of conduction.* Proc Natl Acad Sci U S A, 1996. **93**(16): p. 8671-6.

74.   Carvelli, L., et al., *Dopamine transporters depolarize neurons by a channel mechanism.* Proc Natl Acad Sci U S A, 2004. **101**(45): p. 16046-51.

75.   Adams, S.V. and L.J. DeFelice, *Flux coupling in the human serotonin transporter.* Biophys J, 2002. **83**(6): p. 3268-82.

76.   Ingram, S.L., B.M. Prasad, and S.G. Amara, *Dopamine transporter-mediated conductances increase excitability of midbrain dopamine neurons.* Nat Neurosci, 2002. **5**(10): p. 971-8.

77.   Lacey, M.G., N.B. Mercuri, and R.A. North, *Actions of cocaine on rat dopaminergic neurones in vitro.* Br J Pharmacol, 1990. **99**(4): p. 731-5.

78.   Branch, S.Y. and M.J. Beckstead, *Methamphetamine produces bidirectional, concentration-dependent effects on dopamine neuron excitability and dopamine-mediated synaptic currents.* J Neurophysiol, 2012. **108**(3): p. 802-9.

79.   Vaarmann, A., et al., *Novel pathway for an old neurotransmitter: dopamine-induced neuronal calcium signalling via receptor-independent mechanisms.* Cell Calcium, 2010. **48**(2-3): p. 176-82.

80.   Wu, J., J.J. Dougherty, and R.A. Nichols, *Dopamine receptor regulation of Ca2+ levels in individual isolated nerve terminals from rat striatum: comparison of presynaptic D1-like and D2-like receptors.* J Neurochem, 2006. **98**(2): p. 481-94.

81.   Morel, N., et al., *The action of calcium channel blockers on recombinant L-type calcium channel alpha1-subunits.* Br J Pharmacol, 1998. **125**(5): p. 1005-12.

82.   Dolphin, A.C., *A short history of voltage-gated calcium channels.* Br J Pharmacol, 2006. **147 Suppl 1**: p. S56-62.

83.   Bichet, D., et al., *The I-II loop of the Ca2+ channel alpha1 subunit contains an endoplasmic reticulum retention signal antagonized by the beta subunit.* Neuron, 2000. **25**(1): p. 177-90.

84.   Buraei, Z. and J. Yang, *Structure and function of the beta subunit of voltage-gated Ca(2)(+) channels.* Biochim Biophys Acta, 2013. **1828**(7): p. 1530-40.

85.   Colecraft, H.M., et al., *Novel functional properties of Ca(2+) channel beta subunits revealed by their expression in adult rat heart cells.* J Physiol, 2002. **541**(Pt 2): p. 435-52.

86.   Lipscombe, D., *L-type calcium channels: highs and new lows.* Circ Res, 2002. **90**(9): p. 933-5.

87.   Catterall, W.A., *Voltage-gated calcium channels.* Cold Spring Harb Perspect Biol, 2011. **3**(8): p. a003947.

88.   Catterall, W.A. and A.P. Few, *Calcium channel regulation and presynaptic plasticity.* Neuron, 2008. **59**(6): p. 882-901.

89.   Ruchala, I., et al., *Electrical coupling between the human serotonin transporter and voltage-gated Ca(2+) channels.* Cell Calcium, 2014. **56**(1): p. 25-33.

90.   Solis, E., Jr., et al., *4-(4-(dimethylamino)phenyl)-1-methylpyridinium (APP+) is a fluorescent substrate for the human serotonin transporter.* J Biol Chem, 2012. **287**(12): p. 8852-63.

91.   Eltit, J.M., et al., *Reduced gain of excitation-contraction coupling in triadin-null myotubes is mediated by the disruption of FKBP12/RyR1 interaction.* Cell Calcium, 2011. **49**(2): p. 128-35.

92.   Petersen, C.I. and L.J. DeFelice, *Ionic interactions in the Drosophila serotonin transporter identify it as a serotonin channel.* Nat Neurosci, 1999. **2**(7): p. 605-10.

93.   Helton, T.D., W. Xu, and D. Lipscombe, *Neuronal L-type calcium channels open quickly and are inhibited slowly.* J Neurosci, 2005. **25**(44): p. 10247-51.

94.   Solis, E., et al., *N-Alkylated Analogs of 4-Methylamphetamine (4-MA) Differentially Affect Monoamine Transporters and Abuse Liability.* Neuropsychopharmacology, 2017.

95.   Chen, T.W., et al., *Ultrasensitive fluorescent proteins for imaging neuronal activity.* Nature, 2013. **499**(7458): p. 295-300.

96.   Wang, Q., et al., *Structural basis for calcium sensing by GCaMP2.* Structure, 2008. **16**(12): p. 1817-27.

97.   Akerboom, J., et al., *Crystal structures of the GCaMP calcium sensor reveal the mechanism of fluorescence signal change and aid rational design.* J Biol Chem, 2009. **284**(10): p. 6455-64.

98.   Glennon, R.A., *Phenylalkylamine stimulants, hallucinogens, and designer drugs.* NIDA Res Monogr, 1990. **105**: p. 154-60.

99.   Liechti, M., *Novel psychoactive substances (designer drugs): overview and pharmacology of modulators of monoamine signaling.* Swiss Med Wkly, 2015. **145**: p. w14043.

100.   Sonders, M.S. and S.G. Amara, *Channels in transporters.* Curr Opin Neurobiol, 1996. **6**(3): p. 294-302.

101.   Lin, F., H.A. Lester, and S. Mager, *Single-channel currents produced by the serotonin transporter and analysis of a mutation affecting ion permeation.* Biophys J, 1996. **71**(6): p. 3126-35.

102.   DeFelice, L.J. and T. Goswami, *Transporters as channels.* Annu Rev Physiol, 2007. **69**: p. 87-112.

103.   Khoshbouei, H., et al., *Amphetamine-induced dopamine efflux. A voltage-sensitive and intracellular Na+-dependent mechanism.* J Biol Chem, 2003. **278**(14): p. 12070-7.

104.   Rios, E., *The cell boundary theorem: a simple law of the control of cytosolic calcium concentration.* J Physiol Sci, 2010. **60**(1): p. 81-4.

105.   Adams, S.V. and L.J. DeFelice, *Ionic currents in the human serotonin transporter reveal inconsistencies in the alternating access hypothesis.* Biophys J, 2003. **85**(3): p. 1548-59.

106.   Nelson, P.J. and G. Rudnick, *Coupling between platelet 5-hydroxytryptamine and potassium transport.* J Biol Chem, 1979. **254**(20): p. 10084-9.

107.   Rudnick, G. and S.C. Wall, *The molecular mechanism of "ecstasy" [3,4-methylenedioxy-methamphetamine (MDMA)]: serotonin transporters are targets for MDMA-induced serotonin release.* Proc Natl Acad Sci U S A, 1992. **89**(5):   p. 1817-21.

108.   Rodriguez-Menchaca, A.A., et al., *S(+)amphetamine induces a persistent leak in the human dopamine transporter: molecular stent hypothesis.* Br J Pharmacol, 2012. **165**(8): p. 2749-57.

109.   Cameron, K., et al., *Mephedrone and methylenedioxypyrovalerone (MDPV), major constituents of "bath salts," produce opposite effects at the human dopamine transporter.* Psychopharmacology (Berl), 2013. **227**(3): p. 493-9.

110.   Cameron, K.N., et al., *Bath salts components mephedrone and methylenedioxypyrovalerone (MDPV) act synergistically at the human dopamine transporter.* Br J Pharmacol, 2013. **168**(7): p. 1750-7.

111.   Johnson, S.W. and R.A. North, *Two types of neurone in the rat ventral tegmental area and their synaptic inputs.* J Physiol, 1992. **450**: p. 455-68.

112.   Beckstead, M.J., et al., *Vesicular dopamine release elicits an inhibitory postsynaptic current in midbrain dopamine neurons.* Neuron, 2004. **42**(6): p. 939-46.

113.   Washburn, C.P., et al., *Serotonergic raphe neurons express TASK channel transcripts and a TASK-like pH- and halothane-sensitive K+ conductance.* J Neurosci, 2002. **22**(4): p. 1256-65.

114.   Deignan, J., et al., *SK2 and SK3 expression differentially affect firing frequency and precision in dopamine neurons.* Neuroscience, 2012. **217**: p. 67-76.

115.   Lau, T., et al., *Antidepressant-induced internalization of the serotonin transporter in serotonergic neurons.* FASEB J, 2008. **22**(6): p. 1702-14.

116.   Sukiasyan, N., H. Hultborn, and M. Zhang, *Distribution of calcium channel Ca(V)1.3 immunoreactivity in the rat spinal cord and brain stem.* Neuroscience, 2009. **159**(1): p. 217-35.

117.   Colgan, L.A., et al., *Action potential-independent and pharmacologically unique vesicular serotonin release from dendrites.* J Neurosci, 2012. **32**(45): p. 15737-46.

118.   Busquet, P., et al., *CaV1.3 L-type Ca2+ channels modulate depression-like behaviour in*

mice independent of deaf phenotype. Int J Neuropsychopharmacol, 2010. **13**(4): p. 499-513.

119. Casamassima, F., et al., *L-type calcium channels and psychiatric disorders: A brief review.* Am J Med Genet B Neuropsychiatr Genet, 2010. **153B**(8): p. 1373-90.

120. Putzier, I., et al., *Cav1.3 channel voltage dependence, not Ca2+ selectivity, drives pacemaker activity and amplifies bursts in nigral dopamine neurons.* J Neurosci, 2009. **29**(49): p. 15414-9.

121. Chan, C.S., et al., *'Rejuvenation' protects neurons in mouse models of Parkinson's disease.* Nature, 2007. **447**(7148): p. 1081-6.

122. Lipscombe, D., T.D. Helton, and W. Xu, *L-type calcium channels: the low down.* J Neurophysiol, 2004. **92**(5): p. 2633-41.

123. Cameron, K.N., et al., *Amphetamine activates calcium channels through dopamine transporter-mediated depolarization.* Cell Calcium, 2015.

124. Scholze, P., et al., *Transporter-mediated release: a superfusion study on human embryonic kidney cells stably expressing the human serotonin transporter.* J Pharmacol Exp Ther, 2000. **293**(3): p. 870-8.

125. Porzgen, P., et al., *The antidepressant-sensitive dopamine transporter in Drosophila melanogaster: a primordial carrier for catecholamines.* Mol Pharmacol, 2001. **59**(1): p. 83-95.

126. Larsen, M.B., B. Elfving, and O. Wiborg, *The chicken serotonin transporter discriminates between serotonin-selective reuptake inhibitors. A species-scanning mutagenesis study.* J Biol Chem, 2004. **279**(40): p. 42147-56.

127. Blakely, R.D., M.B. Robinson, and S.G. Amara, *Expression of neurotransmitter transport from rat brain mRNA in Xenopus laevis oocytes.* Proc Natl Acad Sci U S A, 1988. **85**(24): p. 9846-50.

128. Fowler, A., et al., *A nonradioactive high-throughput/high-content assay for measurement of the human serotonin reuptake transporter function in vitro.* J Biomol Screen, 2006.

94

11(8): p. 1027-34.

129.   Mason, J.N., et al., *Novel fluorescence-based approaches for the study of biogenic amine transporter localization, activity, and regulation.* J Neurosci Methods, 2005. **143**(1): p. 3-25.

130.   Jorgensen, S., et al., *Validation of a fluorescence-based high-throughput assay for the measurement of neurotransmitter transporter uptake activity.* J Neurosci Methods, 2008. **169**(1): p. 168-76.

131.   Sabatini, B.L., T.G. Oertner, and K. Svoboda, *The life cycle of Ca(2+) ions in dendritic spines.* Neuron, 2002. **33**(3): p. 439-52.

132.   Schmid, E.L., et al., *Screening ligands for membrane protein receptors by total internal reflection fluorescence: the 5-HT3 serotonin receptor.* Anal Chem, 1998. **70**(7): p. 1331-8.

133.   Thompson, A.J. and S.C. Lummis, *The 5-HT3 receptor as a therapeutic target.* Expert Opin Ther Targets, 2007. **11**(4): p. 527-40.

134.   Katsurabayashi, S., et al., *A distinct distribution of functional presynaptic 5-HT receptor subtypes on GABAergic nerve terminals projecting to single hippocampal CA1 pyramidal neurons.* Neuropharmacology, 2003. **44**(8): p. 1022-30.

135.   Derkach, V., A. Surprenant, and R.A. North, *5-HT3 receptors are membrane ion channels.* Nature, 1989. **339**(6227): p. 706-9.

136.   Barnes, N.M., et al., *The 5-HT3 receptor--the relationship between structure and function.* Neuropharmacology, 2009. **56**(1): p. 273-84.

137.   Thompson, A.J. and S.C. Lummis, *5-HT3 receptors.* Curr Pharm Des, 2006. **12**(28): p. 3615-30.

138.   Fan, P., *Effects of antidepressants on the inward current mediated by 5-HT3 receptors in rat nodose ganglion neurones.* Br J Pharmacol, 1994. **112**(3): p. 741-4.

139.   Koepsell, H., *The SLC22 family with transporters of organic cations, anions and zwitterions.* Mol Aspects Med, 2013. **34**(2-3): p.   413-35.

140.   Boxberger, K.H., B. Hagenbuch, and J.N. Lampe, *Common drugs inhibit human organic cation transporter 1 (OCT1)-mediated neurotransmitter uptake.* Drug Metab Dispos, 2014. **42**(6): p. 990-5.

141.   Shimada, H., B. Moewes, and G. Burckhardt, *Indirect coupling to Na+ of p-aminohippuric acid uptake into rat renal basolateral membrane vesicles.* Am J Physiol, 1987. **253**(5 Pt 2): p. F795-801.

142.   Burckhardt, B.C., N.A. Wolff, and G. Burckhardt, *Electrophysiologic characterization of an organic anion transporter cloned from winter flounder kidney (fROAT).* J Am Soc Nephrol, 2000. **11**(1): p. 9-17.

143.   Tracy, D.K., D.M. Wood, and D. Baumeister, *Novel psychoactive substances: types, mechanisms of action, and effects.* BMJ, 2017. **356**: p. i6848.

144.   Gelvin, E.P. and G.T. Mc, *2-Amino-1-(p-methylphenyl)-propane (aptrol) as an anorexigenic agent in weight reduction.* N Y State J Med, 1952. **52**(2): p. 223-6.

145.   Blanckaert, P., et al., *4-Methyl-amphetamine: a health threat for recreational amphetamine users.* J Psychopharmacol, 2013. **27**(9): p. 817-22.

146.   Wee, S., et al., *Relationship between the serotonergic activity and reinforcing effects of a series of amphetamine analogs.* J Pharmacol Exp Ther, 2005. **313**(2): p. 848-54.

147.   Daniels, D.J., et al., *Opioid-induced tolerance and dependence in mice is modulated by the distance between pharmacophores in a bivalent ligand series.* Proc Natl Acad Sci U S A, 2005. **102**(52): p. 19208-13.

148.   Christopoulos, A., et al., *Synthesis and pharmacological evaluation of dimeric muscarinic acetylcholine receptor agonists.* J Pharmacol Exp Ther, 2001. **298**(3): p. 1260-8.

149.   Steinfeld, T., et al., *A novel multivalent ligand that bridges the allosteric and orthosteric binding sites of the M2 muscarinic receptor.* Mol Pharmacol, 2007. **72**(2): p. 291-302.

150.   Portoghese, P.S., *Bivalent ligands and the message-address concept in the design of*

selective opioid receptor antagonists. Trends Pharmacol Sci, 1989. **10**(6): p. 230-5.

151.   Amir P. Tamiz , J.Z., Mei Zhang , Cheng Z. Wang , Kenneth M. Johnson , and Alan P. Kozikowski, *Application of the Bivalent Ligand Approach to the Design of Novel Dimeric Serotonin Reuptake Inhibitors.* 2000.

152.   Fandrick, K., et al., *Bivalent biogenic amine reuptake inhibitors.* Bioorg Med Chem Lett, 2003. **13**(13): p. 2151-4.

153.   Schmitt, K.C., et al., *Bivalent phenethylamines as novel dopamine transporter inhibitors: evidence for multiple substrate-binding sites in a single transporter.* J Neurochem, 2010. **112**(6): p. 1605-18.

Curriculum vitae
Iwona Ruchala
ruchalai@vcu.edu

Education

School of Medicine, Virginia Commonwealth University   *Richmond, VA*
Department of Physiology and Biophysics   8/2012- 7/2017
Doctor of Philosophy (PhD)

Virginia Commonwealth University   *Richmond, VA*
Department of Physics   8/2009-6/2011
Master of Science (MS) Applied Physics
Dissertation Title: *The Effect of Ambient on Photoluminescence from GaN*

University of Wroclaw   *Wroclaw (Poland)*
Department of Physics and Astronomy   10/2003-5/2008
Bachelor of Science (BS) Theoretical Physics

Research/Projects

Novel methodology for drugs screening
Developing novel method for rapid characterization of drug-effect profiles on monoamine transporters that can be beneficial for discovery of new psychotherapeutics for treatment of mental illnesses (ADHD, depression, PTSD, addiction), to characterize mechanisms of emerging drugs of abuse and to discover new molecules useful as neuroscience research tools.

Electrical coupling between monoamine transporters and calcium channels
Introducing new mechanism by which endogenous neurotransmitters (dopamine, serotonin) or exogenous substrates (Amphetamine, Ecstasy) can modulate calcium-driven signals. Monoamine transporters' substrates can indirectly activate low-voltage gated calcium channels (CaV1.2 and CaV1.3).

Studies of the effect of ambient on photoluminescence (PL) from Gallium nitride (GaN)
Determining PL intensity that is four times higher in vacuum than it is in the air. Increase in PL intensity can be explained only by changes in the nonradiative recombination rate at the surface (recombination mechanism). In vacuum and acid vapor, some surface species are desorbed or passivated, resulting in a decreased nonradiative recombination rate and increased PL intensity.

Teaching Experience

Virginia Commonwealth University   1/2012-6/2012 Richmond, VA
Physics Adjunct Faculty
Supervising and teaching physics laboratories for General Physics courses, grading exams and homework

Virginia Commonwealth University   8/2009-6/2011 Richmond, VA
Teaching Assistant
Teaching physics laboratories for General Physics courses- physics for life-science majors, grading,
proctoring

Publications

"N-Alkylated analogs of 4-methylamphetamine (4-MA) differentially affect monoamine transporters and
abuse liability" Ernesto Solis, Jr., John S. Partilla**, Iwona Ruchala**, Farhana Sakloth, Kathryn L. Schwienteck, Louis J. De Felice, Jose M. Eltit, Richard A. Glennon, S. Stevens Negus, Michael H. Baumann. Neuropsychopharmacology (2017)

"Retigabine holds KV7 channels open and stabilizes the resting potential" Aaron Corbin-Leftwich, Sayeed M. Mossadeq, Junghoon Ha, **Iwona Ruchala**, Audrey Han Ngoc Le and Carlos A. Villalba-Galea. J. Gen. Physiol. (2016) Vol. 147 No. 3 229–241

"Amphetamine activates calcium channels through dopamine transporter-mediated depolarization" Krasnodara N. Cameron, Ernesto Solis Jr., **Iwona Ruchala**, Louis J. De Felice, Jose M. Eltit. Cell Calcium 58 (2015) 457–466

"Electrical coupling between the human serotonin transporter and voltage-gated Ca2+channels" **Iwona Ruchala**, Vanessa Cabra, Ernesto Solis Jr., Richard A. Glennon, Louis J. De Felice, Jose M. Eltit. Cell Calcium 56 (2014) 25–33

Abstracts/Posters

"Voltage-gated calcium channels as detecting tools of psychoactive drugs" **Iwona Ruchala**, *Alan Harris, Louis J. De Felice, Jose M. Eltit. Biophysical Society meeting, New Orleans, LA, February 2017*

"Expanding psycho-pharmacotherapies using novel biosensors" **Iwona Ruchala**, *Jose M. Eltit.*
Society for Laboratory Automation and Screening SLAS2017 International Conference and Exhibition in Washington, DC, February 2017

"Voltage-gated Ca^{2+} channels as a tool for the quick detection of psychoactive drugs"
Iwona Ruchala, *Alan Harris , Jose M. Eltit. International Conference on Calcium Signaling from store to channels, Chapel Hill, NC, August 2016*

"Integrated strategy for drug discovery with monoamine transporter ligands: application to structure-activity studies with 4-methylamphetamine analogs" *Farhana Sakloth, Jose M. Eltit, Ernesto Solis Jr. E, John S. Partilla,* **Iwona Ruchala**, *Schwienteck K, Michael H. Baumann, Louis J. De Felice, Richard A. Glennon, Steve Negus. Symposium on Drug Discovery for the Brain, Richmond, VA, May 2016*

"Monoamine transporters produce Ca^{2+} signals through L-type Ca^{2+} channel activation"
Krasnodara Cameron, Ernesto Solis Jr., **Iwona Ruchala**, *Louis J. De Felice, Jose M. Eltit. Biophysical Society meeting. Baltimore, MD, January 2015; article in Biophysical Journal*

108(2):462a-463a, January 2015

"Electrical coupling between the human serotonin transporter and voltage-gated Ca^{2+} channels" **Iwona Ruchala**, *Vanessa Cabra, Ernesto Solis Jr. , Richard A. Glennon, Louis J. De Felice, Jose M. Eltit. Ion channels and transporters conference, Erice, Italy, May 2014*

"Surface Characterization of Ga-doped ZnO layers" Joy D. McNamara, Josephus Ferguson, Michael Foussekis, **Iwona Ruchala**, *Michael A. Reshchikov, Alison A. Baski, H. Liu, Vitaliy Avrutin, Hadis Morkoç. Symposium MM on Transparent Conducting Oxides and Applications / Fall Meeting of the Materials-Research-Society (MRS), Mat. Res. Soc. Symp. Proc., 1315, 77-82 (2011).*

Volunteering work

Volunteering at Women Building Bio; the XX Factor   9/2017 Fairfax, VA
Representing Virginia Bio at bio industry statewide conference highlighting and building on the contributions of women to the biosciences in Virginia.

Community Work at Bethlehem Farm   5/11   -5/20/2009
Alderson, WV

Skills

Mammalian cell culture • Isolation and culture midbrain neurons • Live-cell imaging - Epifluorescence • Immunocytochemistry • Atomic Force Microscopy • Photoluminescence Equipment High Resolution Microscopy • Molecular Biology - Standard DNA techniques (DNA purification, subcloning) - RNA isolation - Transfection of mammalian cells - Transduction of neuronal lines using retroviruses - protein overexpression, purification, quantification, Western blots • Whole-cell voltage-clamp and current-clamp • Automated cell-based assay (FlexStation) • Computer software - Excel, Origin, PowerPoint, GraphPad Prism